ROLE OF TYROSINE RECEPTOR KINASE B IN THE DEVELOPMENT AND FUNCTION OF THE CENTRAL NERVOUS SYSTEM

APPROVED BY SUPERVISORY COMMITTEE

Luis F. Parada Ph.D., Mentor

James A. Bibb Ph.D., Committee Chair

Jane E. Johnson Ph.D.

Joachim Herz M.D.

To Mom and Dad

ROLE OF TYROSINE RECEPTOR KINASE B IN THE DEVELOPMENT AND FUNCTION OF THE CENTRAL NERVOUS SYSTEM

by

YUN LI

DISSERTATION

Presented to the Faculty of the Graduate School of Biomedical Sciences

The University of Texas Southwestern Medical Center at Dallas

In Partial Fulfillment of the Requirements

For the Degree of

DOCTOR OF PHILOSOPHY

The University of Texas Southwestern Medical Center at Dallas

Dallas, Texas

August, 2008

ACKNOWLEDGEMENTS

First and foremost I would like to thank my mentor Dr. Luis Parada for giving me the opportunity to work and learn along his side. His passion for science is an inspiration to everyone who knows him, but even more so to his students like me. I am truly grateful to Luis for his guidance, his unflagging support, and for believing in me during my most difficult struggles.

I would like to give my thanks to my committee members Drs. Jane Johnson, James Bibb and Joachim Herz for their insightfulness and the tremendous support they have given me over the years.

I also want to express my sincere gratitude to all the members of the Parada lab, past and present. I was lucky to be in a lab with their camaraderie and friendship. I was particularly fortunate to start my graduate study when Drs. Bryan Luikart and Mark Lush were in the lab and Steve Kernie was only a stone's throw away. They have been an invaluable source of mentorship. I collaborated with Mark on his NF1 project on barrel cortex formation; Bryan and Steve have also contributed data and ideas to various aspects of the TrkB projects. It has been a great pleasure working with them.

I am indebted to my collaborators here at UT Southwestern and elsewhere for their help in moving my work forward. I am grateful to Drs. Susan McConnell, Kenneth Campbell, Albee Messing, Jamey Marth, Dieter Riethmacher, Louis Reichardt, Serge Nef, Yuan Zhu, Chang-Hyuk Kwon for providing reagents; Drs. Eric Nestler, Shari Birnbaum , Rhonda Bassel-Duby, Dustin Corgan for their collaboration on behavioral experiments. I wish to thank my colleagues Drs. Daishi Yui, Lu Zhou, Lei Lei, Jian Chen, Sheila Alcantara, Darko Bosnakovski, Joshua Koch, JingSheng Yan for their help on

experiments, and Linda McClellan, Shawna Kennedy, Steven McKinnon for technical assistance. I thank Dr. David Ginty for the stimulating discussions. I have had the pleasure to work with Lori Loomis, Jihan Osborne, Alvin Chandra and Andrew Tyler during their rotations, and I greatly appreciate the hard work they put forth.

Most of all I would like to thank my family for their love and support. My mother MeiZhen Xiong and father ZhongHua Li have always sought to give me and my sister the best education and upbringing they could. I am eternally grateful to them and wish I have made them proud. My sister Nan Li and brother-in-law Gang Liu have given me constant encouragements over the years. It would have been impossible to complete this journey without the caring words from all of them.

ROLE OF TYROSINE RECEPTOR KINASE B IN THE DEVELOPMENT AND FUNCTION OF THE CENTRAL NERVOUS SYSTEM

Publication No._____

Yun Li, Ph.D.

The University of Texas Southwestern Medical Center at Dallas, 2008

Supervising Professor: Luis F. Parada, Ph.D

Abstract

Tyrosine Receptor Kinase B (TrkB) was initially identified as the high-affinity receptor for Brain-Derived Neurotrophic Factor (BDNF) in regulating the survival of sympathetic and sensory neurons. In the CNS, however, BDNF-TrkB interaction has been shown to regulate the diverse aspects of development, physiology and pathology. In the current studies we focus on the roles of TrkB and its downstream signaling pathways in the progression and amelioration of CNS diseases. Though the nature of the diseases diverges, they share a common molecular regulatory mechanism. First we report that TrkB is required cell-autonomously to regulate the generation of new neurons. Mice lacking TrkB in hippocampal neural progenitor cells had impaired proliferation and

neurogenesis, and are behaviorally insensitive to antidepressive treatments. Specific deletion of NF1, an antagonist of Ras, in adult neural progenitor cells enabled rapid proliferative and behavioral responses to sub-chronic antidepressants, and led to spontaneous antidepressive-like behaviors in the long run. Thus, our findings demonstrate impairment of the neural precursor niche as an etiological factor for refractory responses to antidepressive regimen, and the activation of adult neurogenesis as an approach to modulate depression and anxiety-like behaviors.

In the second half, we report that ablation of *bdnf* from the cortex and the substantia nigra leads to depletion of BDNF in the striatum. Mice lacking BDNF-TrkB signaling in the corticostriatal and nigrostriatal circuits displayed severe motor deficits and striatal degeneration reminiscent of the Huntington's disease. In contrast, specific ablation of TrkB from the striatal medium spiny neurons resulted in late-onset neuronal loss and spine degeneration, without causing obvious movement abnormalities. Thus, our results establish an essential role for TrkB in regulating the normal maturation and maintenance of striatal medium spiny neurons.

TABLE OF CONTENTS

PRIOR PUBLICATIONS

Lush, M.E.*, **Li, Y.***, Kwon, C.H., Chen, J., and Parada, L.F. (2008) Neurofibromin is required for barrel formation in the mouse somatosensory cortex. J Neurosci. 28 (7): 1580-1587. (*co-first author)

Li, Y., Luikart, B.W., Birnbaum, S., Chen, J., Kwon, C.H., Kernie, S.G., Bassel-Duby, R., and Parada, L.F. (2008) TrkB regulates hippocampal neurogenesis and governs sensitivity to antidepressive treatment. Neuron 59(3): 399-412.

LIST OF FIGURES

LIST OF TABLES

LIST OF APPENDICES

LIST OF ABBREVIATIONS

AD	Antidepressant
ANOVA	Analysis of Variance
BDNF	Brain-Derived Neurotrophic Factor
BF1	Brain Factor 1 (also known as FoxG1)
β-Gal	β-Galactosidase
BrdU	5-bromo-2-deoxyuridine
CaMKII	Calmodulin-dependent protein Kinase II
CNS	Central Nervous System
CREB	cAMP response element binding
DARPP32	Dopamine- and cyclic AMP- regulated phosphoprotein, 32 kDa
DG	Dentate Gyrus
DLX	Dixtalless
DTA	Diphtheria Toxin, Subunit A
EGF	Epidermal Growth Factor
ELISA	Enzyme-Linked Immunosorbent Assay
ER	Estrogen Receptor
bFGF	basic Fibroblast Growth Factor
ERK	Extracellular signal-regulated kinase
FACS	Fluorescent-Activated Cell Sorting
Flx	Fluoxetine
FST	Forced-Swim Test
GFAP	Glial Fibrillary Acidic Protein

GFP	Green Fluorescent Protein
GLM	Generalized Linear Models
HD	Huntington's Disease
Imi	Imipramine
MAPK	Mitogen-Activated Protein Kinase
MSN	Medium Spiny Neuron
NF1	Neurofibromatosis type 1
NGF	Nerve Growth Factor
NPC	Neural Progenitor Cell
NSC	Neural Stem Cell
NSFT	Novelty-Suppressed Feeding Test
NT3/4	Neurotrophin 3/4
pH3	Phosphorylated Histone H3
PI3K	Phosphatidylinositol-3-Kinase
PLCγ	Phospholipase C γ
PNS	Peripheral Nervous System
RasGAP	Ras GTPase Activating Protein
Sal	Saline
SGZ	Sub-Granular Zone
SVZ	Sub-Ventricular Zone
Syn	Synapsin
TH	Tyrosine Hydroxylase
TRK	Tyrosine Receptor Kinase

TST	Tail-Suspension Test
TUNEL	TdT-mediated dUTP Nick End Labeling
VTA	Ventral Tegmental Area
WT	Wild Type
X-Gal	5-bromo-4-chloro-3-indolyl-β-D-galactopyranoside

CHAPTER 1

INTRODUCTION

1.1 Neurotrophins

Neurotrophins are a class of small proteins whose first identified member is nerve growth factor (NGF) (Levi-Montalcini, 1966). In the mammalian brain, four neurotrophins have been characterized. NGF, Brain-Derived Neurotrophic Factor (BDNF), Neurotrophin 3 (NT3), and Neurotrophin 4/5 (NT4/5) arise from the same ancestral gene, and remain closely related in sequence and structure (Lewin and Barde, 1996). All neurotrophins share similar biochemical characteristics. They are secretory proteins that are first synthesized as glycosylated precursors (pro-neurotrophins) and then post-translationally converted to mature neurotrophins. Whether the cleavage of pro-neurotrophins occurs intracellularly (Matsumoto et al., 2008), or extracellularly following activity-dependent release of pro-neurotrophins (Lu et al., 2005) remains controversial. Mice lacking each of the neurotrophins have been generated, of which germline knockout of NGF, BDNF and NT3 were proven to be neonatal lethal, while NT4 knockout mice could survive to adulthood.

As the central concept of the neurotrophic hypothesis, targets of innervation secrete limited amounts of survival factors that function to balance the size of the target tissue and the number of the innervating neurons. In the PNS, it has been shown that the survival of sympathetic and sensory neurons is dependent on the availability of neurotrophins produced in their target organs (Korsching, 1993; Zweifel et al., 2005). From these sources, neurotrophins are captured in the axon terminals by receptor-mediated endocytosis and are retrogradely transported into the cell bodies where they act to promote survival and differentiation. More recently, it has been shown that

neurotrophins are not only transported bi-directionally, they also act in the autocrine and paracrine fashion. In addition, various cell types have been identified to express neurotrophins, both neuronal and non-neuronal. These findings coincide with a growing body of work implicating neurotrophins in such diverse functions including survival, proliferation, cell-fate determination, migration, axonal/dendritic growth, synaptogenesis and plasticity.

1.2 Neurotrophin Receptors

The actions of neurotrophins are mediated by two principle trans-membrane receptor systems. All four ligands bind to the low-affinity neurotrophin receptor p75, a distant member of the tumor necrosis factor receptor family. Neurotrophins also bind to high-affinity receptors that belong to the tyrosine receptor kinase (trk) family. NGF is specific for TrkA, BDNF and NT4 bind TrkB, NT3 activates TrkC but also binds TrkA and TrkB albeit at a lower efficiency. Germline knockout of each of the Trk receptors was proven to be neonatal lethal, with phenotypes strikingly similar to knockout mice of their respective ligands (Snider, 1994). Therefore, the Trk receptors largely determine the specificity of neurotrophin effects.

Neurotrophins generally function as noncovalently associated homodimers. Direct binding to the Trk triggers dimerization of these receptors, which results in activation of the tyrosine kinases present in their intracellular domains. Phosphorylation of the tyrosine residues within the autoregulatory loop of the kinase

domain further activates the receptors. Phosphorylation of the additional tyrosine residues creates docking sites for adaptor proteins containing the src-homology-2 (SH-2) motif or the phosphotyrosine-binding motif. These adaptor proteins connect Trk to intracellular signaling pathways, including Ras/ERK (extracellular signal-regulated kinase), phospholipase C (PLCγ), phosphatidylinositol-3-kinase (PI3K), NFκB and atypical protein kinase C pathways. In particular, phosphorylations of the Y490 and Y785 sites (of human TrkA sequence) recruit Shc and PLCγ, thus propagate signaling transduction towards the ERK/PI3K and PLCγ pathways.

1.3 BDNF and TrkB in development and disease of the CNS

In studies on neurotrophin functions within the CNS, particular attention has been focused on BDNF because of its importance in modulating synaptic plasticity. Both BDNF and TrkB are widely expressed in the developing and adult nervous system. Expression of BDNF is controlled by eight distinct promoters. Of particular interest, expressions from promoter I, II, IV and VI have all been shown to be activity-dependent. BDNF transcriptions from these promoters are controlled by CREB (Tao et al., 1998), CaRF (Tao et al., 2002), MeCP2 (Chen et al., 2003), among others. These activity-dependent transcriptions enable rapid changes in BDNF mRNA and protein level in response to physiological (stress, sensory inputs and learning experience), as well as pathological (seizure and trauma) stimuli.

Human genetics studies have indicated loss of one copy of the *bdnf* gene leads

to severe developmental and functional impairments (Gray et al., 2006). The presence of a single nucleotide polymorphism in the *bdnf* gene (V66M) has been shown to affect selective hippocampal episodic memory (Egan et al., 2003). Furthermore, a *de novo* mutation at the intracellular tyrosine residue of TrkB (Y722C) has been shown to result in obesity and developmental delay (Yeo et al., 2004). More systematic loss-of-function studies in mice have also demonstrated a wide range of neurological deficits as results of BDNF or TrkB deletion in the CNS (Kernie et al., 2000; Luikart et al., 2005; Minichiello et al., 1999; Monteggia et al., 2007). In addition, reductions in BDNF level have been reported in human and animal models of Schizophrenia, Alzheimer's Disease, Amyotrophic Lateral Sclerosis, Huntington's Disease (HD), Rett Syndrome, Depression and Bipolar Disorder, though whether such reductions represent causes or symptoms of the disease progression remains unknown.

1.4 Statement of Purpose

The evidence that BDNF-TrkB signaling regulates development and function of the adult CNS is compelling. For example, studies on BDNF heterozygous and forebrain-specific conditional knockout mice have yielded interesting results on associating BDNF, neurogenesis and stress-induced behavior changes. However, many of these studies have relied on global reduction of BDNF and do not address signaling transductions downstream from BDNF. A survey of the literature revealed numerous inconsistency and contradicting results. Similarly, BDNF reduction has been reported in human and animal models of HD, yet whether this loss of BDNF exacerbates disease

progression, and whether loss of BDNF from the cortex or the striatum is associated with the disease remains unknown. In the current studies, we are employing a combinatorial approach that involves the analyses of conditional knockout mice with deletion of BDNF, TrkB or their downstream components. Furthermore, we have selected to conduct genetic manipulation with a panel of Cre lines that will provide the temporal and spatial precision required to study functions on the cellular and circuitry level. Chapter 2 details our effort to elucidate the role of BDNF-TrkB in the regulation of adult hippocampal neurogenesis, and its function in governing the behavioral effects of antidepressive treatments. Chapter 3 is devoted to the investigation of signaling cascades downstream from tyrosine receptor kinases, and the discovery that enhancing neurogenesis in the adult brain is sufficient to modulate depression and anxiety-like behaviors. Chapter 4 describes the finding that BDNF protein anterogradely transported from the cortex and the substantia nigra is important in the maintenance of striatal neuron morphology and functionality. Loss of BDNF or TrkB in different compartments of the corticostriatal and nigrostriatal circuits results in cellular and behavioral phenotypes reminiscent of HD.

CHAPTER 2

TRKB REGULATES NEURAL PROGENITOR CELLS AND MEDIATES DEPRESSION AND ANXIETY LIKE BEHAVIORS

2.1 Summary

Adult hippocampal neurogenesis is stimulated by chronic administration of antidepressants (ADs) and by voluntary exercise. Neural progenitor cells (NPCs) in the dentate gyrus (DG) that are capable of continuous proliferation and neuronal differentiation are the source of such structural plasticity. Here we report that mice lacking the receptor tyrosine kinase TrkB in hippocampal NPCs have impaired proliferation and neurogenesis. When exposed to chronic AD or wheel running, no increase in proliferation or neurogenesis is observed. Ablation of TrkB also renders these mice behaviorally insensitive to antidepressive treatment in depression and anxiety-like paradigms. In contrast, mice lacking TrkB only in differentiated DG neurons display typical neurogenesis and respond normally to chronic AD. Thus, our data establish an essential cell autonomous role for TrkB in regulating hippocampal neurogenesis, behavioral sensitivity to antidepressive treatments, and support the notion that impairment of the neural precursor niche is an etiological factor for refractory responses to antidepressive regimen.

2.2 Background

Depression is a significant public health problem due to both its high prevalence and its devastating impact on individuals and society. Despite much excitement generated by recent advances in the knowledge of brain development and function, the mechanisms underlying the pathogenesis of depression, as well as its amelioration by antidepressant (AD) treatment remain poorly understood (Manji et al., 2001; Nestler et al., 2002). Clinical studies demonstrate that 40% of depressed patients fail to respond to first-line ADs and 70% do not undergo full remission (Fagiolini and Kupfer, 2003; Thase and Rush, 1995). Such variable range of effectiveness underscores the heterogeneity of the illness and the urgent need for thorough delineation of the cellular and molecular process involved in the action of ADs.

As predicted by their pharmacological characteristics, most ADs appear to act by increasing the activity of serotonergic and noradrenergic circuits (Morilak and Frazer, 2004). However, these medications usually require chronic administration for weeks to months before clinically appreciable effects are achieved. This represents an extended delay compared to the rapid increase of serotonin and noradrenaline elicited by these drugs (Frazer, 1997). Therefore, gradual, yet essential changes to the brain that occur during the period of delay appear to be

required for the response to ADs. Animal studies indicate one such delayed response is the increased production of new neurons in the dentate gyrus (DG) (Malberg et al., 2000; Perera et al., 2007). Physical activity such as running, which is considered beneficial for mental health (Babyak et al., 2000; Salmon, 2001), also induces increased production of neurons (Pereira et al., 2007; van Praag et al., 1999). Similarly, electroconvulsive therapy has also been shown to robustly induce neurogenesis in the rodent DG. Though this form of treatment is often reserved for patients suffering from severe depression that have not responded to other treatment, partly due to the potential adverse side effects (such as memory loss), it has remained one of the most effective treatment for severe major depression. Animal studies have shown that upon exposure to chronic ADs, exercise or electro-shock, neural progenitor cells (NPCs) in the sub-granular zone (SGZ) of the DG undergo enhanced proliferation, which drives the increase in neurogenesis (Encinas et al., 2006; Perera et al., 2007). Although the functional significance remains to be proven, the positive association of neurogenesis with antidepressive therapies, as well as other beneficial stimulations such as diet, learning and environmental enrichment (Alvarez-Buylla, 1992; Kempermann et al., 1997; Lee et al., 2000), implicates it as a physiologically relevant phenomenon. Indeed, irradiation-mediated ablation of proliferating cells in the hippocampus compromises the ability of certain strains of rodents to display a behavioral response to ADs, suggesting that neurogenesis is an

intrinsic requirement (Airan et al., 2007; Holick et al., 2008; Santarelli et al., 2003; Wang et al., 2008a). The genetic mechanism underlying this observation remains unclear.

Coinciding with the elevation of neurogenesis, chronic AD exposure elicits a variety of molecular adaptations (Tardito et al., 2006). The mechanisms that link these molecular changes to the biological effects of ADs are only beginning to be unveiled. One of the molecules implicated is brain-derived neurotrophic factor (BDNF), whose level in the hippocampus is increased by chronic but not acute AD exposure (Nibuya et al., 1995). Infusion of BDNF into the DG produces AD-like responses in several behavioral paradigms (Shirayama et al., 2002). Mutant animals with a global reduction of BDNF have a blunted response to acute AD induced behavioral changes (Monteggia et al., 2004; Saarelainen et al., 2003). In humans, a single nucleotide polymorphism of the *bdnf* gene (val66met) that interferes with the activity-dependent secretion of BDNF protein has been associated with cognitive and structural abnormalities of the CNS (Egan et al., 2003; Pezawas et al., 2004; Szeszko et al., 2005), though consensus is lacking on its influence on susceptibility to mood disorders (Choi et al., 2006; Jiang et al., 2005; Kaufman et al., 2006; Schule et al., 2006). Interestingly, recent generation of mutant mice carrying the same polymorphism indicates a causative link between the genetic change and elevated

anxiety-like behaviors that are not normalized by AD (Chen et al., 2006). These observations, coupled with evidence that exogenous BDNF promotes proliferation of hippocampal NPCs (Bull and Bartlett, 2005; Scharfman et al., 2005), suggest an important role for BDNF in mediating the biological response to chronic AD treatments (Wang et al., 2008b). Whether BDNF acts directly on NPCs *in vivo*, and if its effects on NPCs then contribute to the overall influence of BDNF on AD response is unresolved.

In the present study, we conditionally ablated the gene encoding TrkB, the high affinity receptor for BDNF, in a regional and cell-type specific manner. We show that NPC deletion of *trkB*, both in embryos or in the adult, results in impairment of hippocampal neurogenesis and prevents behavioral improvements induced by chronic AD administration or by wheel running. In contrast, deleting *trkB* in differentiated neurons of the same brain regions does not affect neurogenesis or the behavioral responses to ADs. Our findings provide genetic evidence of a functional, cell autonomous requirement of TrkB in the neurogenic and behavioral responses to antidepressive treatments. Furthermore, our results support the notion that DG NPCs are a required component in the amelioration of depression (Zhao et al., 2008).

2.3 Results

2.3.1 TrkB is expressed by hippocampal neural progenitor cells

We, and others have previously demonstrated the presence of TrkB transcripts and protein in the hippocampus (Klein et al., 1990; Zhou et al., 1993). To determine whether transcripts are present in the neurogenic zone, we first examined TrkB expression in the postnatal and adult DG. *In situ* hybridization analysis showed prominent expression of both BDNF and TrkB in the granular layer and SGZ of the DG (Figure 2.1). In particular, TrkB mRNA, represented by silver bromide grains (black spheres), was detectable throughout the cellular layers of the DG (Figure 2.1A, right panel). To further examine whether the DG NPCs express TrkB, we utilized Nestin-GFP transgenic mice, in which GFP expression is confined to NPCs (Figure 2.1B) (Yu et al., 2005). Using fluorescent-activated cell sorting (FACS), GFP positive cells from the DG of transgenic mice at various ages were isolated and analysis of these cells by RT-PCR demonstrated the presence of NPCs markers and the absence of markers from the differentiated lineages (Figure 2.2). TrkB and BDNF mRNAs were detected in the GFP positive cells at all ages tested (postnatal day (P) 2, 15 and 60, n=3 animals for each age, Figure 2.1C). Similarly, TrkB and BDNF mRNAs were also detected in neurospheres derived from the DG of adult wild-type mice (n=3, Figure 2.1C). We further analyzed the distribution of TrkB protein in the progenitor population by co-immunostaining. Consistent with

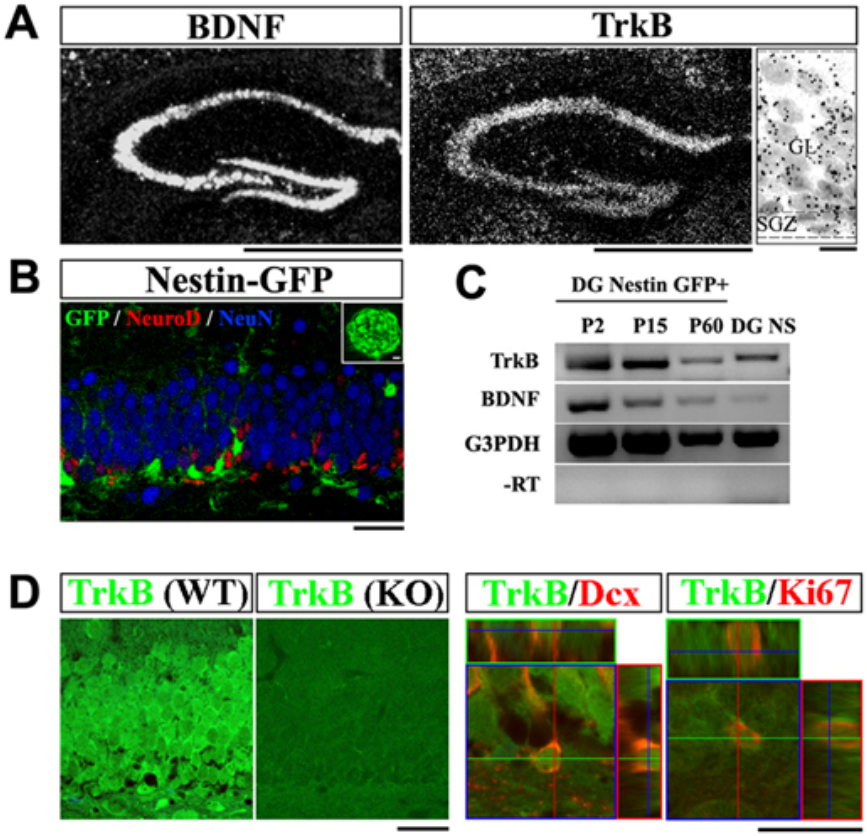

Figure 2.1. TrkB is expressed by hippocampal NPCs

(A) *In situ* hybridization analysis of TrkB and BDNF mRNA in the adult DG. In the high magnification image (right), note the distribution of silver grains (black spheres) in all cells. Scale bars, 1mm (low-magnification) and 10um (high-magnification). GL, granular layer; SGZ, sub-granular zone.

(B) Confocal image of the DG of an adult Nestin-GFP transgenic mouse, co-immunostained for GFP (green), NeuroD (red) and NeuN (blue). GFP expression was restricted to NPCs and did not co-localize with immature (NeuroD+) or mature (NeuN+) neurons. Insert showed a DG derived neurosphere that expresses GFP. Scale bars, 10um.

(C) RT-PCR detection of TrkB and BDNF transcripts in FACS sorted Nestin-GFP positive cells and DG derived neurospheres. NS, neurosphere.

(D) Immuno-staining for TrkB (green) on adult DG sections from wild-type and $TrkB^{hGFAP}$ mice (left panels). Co-staining for TrkB (green) and Ki67 (red), or Doublecortin (red) demonstrated co-localization of TrkB with proliferating (Ki67+) and differentiating (Doublecortin+) cells. Dcx, doublecortin. Scale bars, 10um and 5um. WT, wild-type.

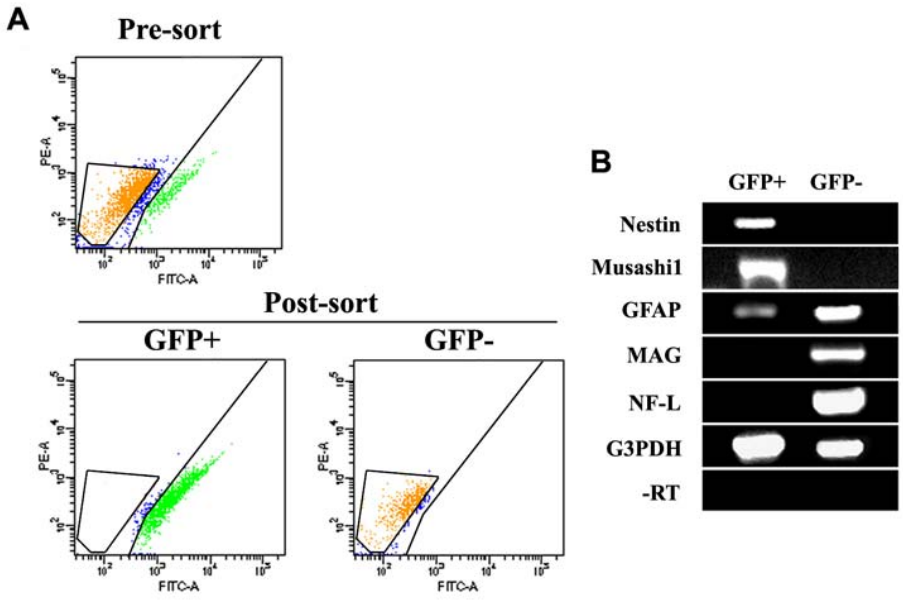

Figure 2.2. FACS isolation of Nestin-GFP positive and negative cells.
(A) Freshly dissociated DG cells were analyzed on a flow cytometer for their FITC intensity (top panel). Gated area (to the right of black line) included GFP positive population found absent in cells from non-transgenic mice. Cells were subsequently sorted based on their GFP intensity and the purity of the sorted cells post-examined (lower panels).
(B) RT-PCR detection of Nestin, musashi1 and GFAP (markers for NPCs) in FACS sorted GFP positive cells. Transcripts specific for differentiated oligodendrocytes (MAG, myelin associated glycoprotein) and neuron (NF-L, neurofilament light chain) were not detected in GFP positive cells.

its mRNA distribution, TrkB protein was detected in all layers of the adult DG; confocal microscopy revealed its presence in both proliferating progenitors that are Ki67 positive (86.2%, n=160 cells from 3 animals), and immature neurons that express Doublecortin (94.9%, n=177 cells from 3 animals) (Figure 2.1D). Taken together, our results demonstrate the presence of TrkB mRNA and protein in hippocampal NPCs.

2.3.2 hGFAP-Cre activity in hippocampal progenitor cells

Germline homozygous TrkB knockout animals die shortly after birth. To investigate the role of TrkB in postnatal stages, conditional knockout animals were generated by crossing mice harboring the *trkB* flox alleles (Luikart et al., 2005) to transgenic mice expressing the Cre recombinase either under the human GFAP (hGFAP) promoter (Zhu et al., 2005a; Zhuo et al., 2001) or the Synapsin I (Syn) promoter (Zhu et al., 2001). In both the hGFAP-Cre and the Syn-Cre transgenic animals, the pattern of Cre expression allows recombination throughout the forebrain, including cerebral cortex, hippocampus and olfactory bulb. In other regions of the brain, such as the midbrain (dopaminergic neurons) and brainstem (serotonergic neurons), Cre expression is minimal (Figure 2.4 and not shown). When interbred with Rosa26-stop-lacZ reporter mice (R26) (Soriano, 1999) and analyzed at the age of 2 months, a majority of the neurons in these regions appeared to express functional beta-galactosidase (β-gal) (Figure 2.3A and data not shown). However, when such animals were analyzed and compared at a younger age (P10), a distinct anatomical difference in the recombination patterns of the two Cre lines was observed in the DG. In the $R26^{hGFAP}$ animal most cells throughout the DG expressed β-gal (Figure 2.3A);

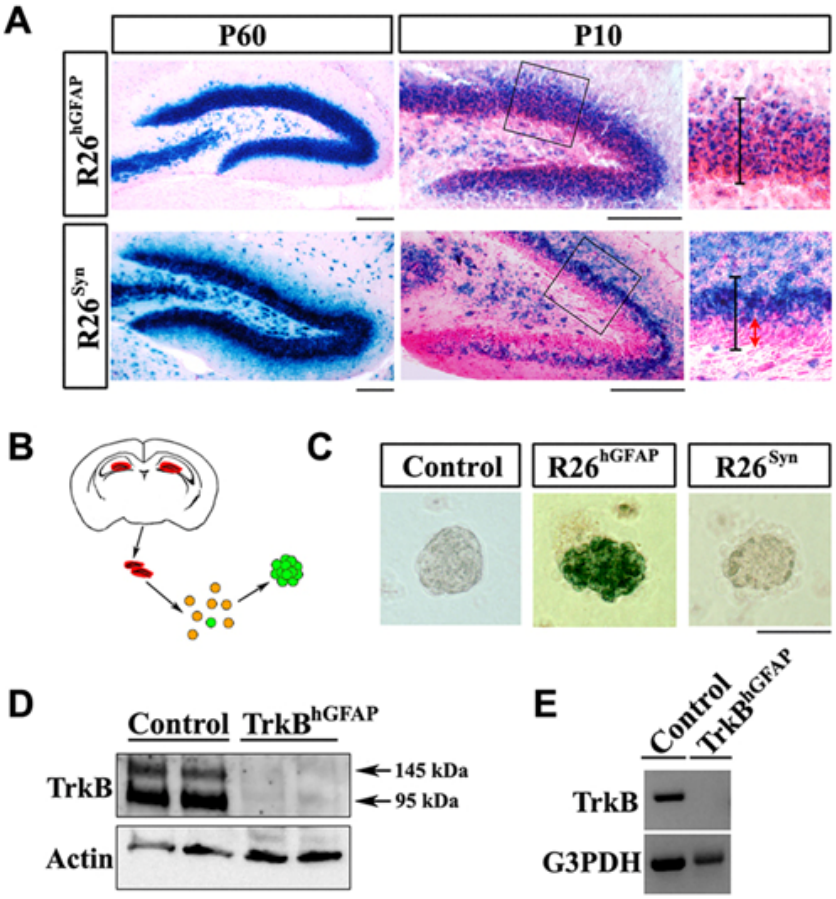

Figure 2.3. hGFAP-Cre, but not Syn-Cre, mediated recombination in hippocampal NPCs

(A) X-gal staining on DG sections of $R26^{hGFAP}$ and $R26^{Syn}$ mice at P10 and P60. Higher magnification views of the circled areas are shown in the right panels, in which black lines outline the granular layer, while the red arrow highlights the SGZ and inner granular layer where recombination was spared. Scale bars, 100um.

(B) Schematic diagram of the procedure to generate neurospheres from adult DG.

(C) X-gal staining on primary neurospheres derived from the DG of adult control, $R26^{hGFAP}$ and $R26^{Syn}$ mice. Blue staining in the neurosphere from $R26^{hGFAP}$ mice indicated the occurrence of recombination. Scale bar, 100um.

(D) Western blots of lysates from the hippocampus of control and $TrkB^{hGFAP}$ mice, probed for TrkB and actin. Note the absence of TrkB in the $TrkB^{hGFAP}$ mice.

(E) RT-PCR detection of TrkB and G3PDH transcripts in FACS sorted Nestin-GFP positive cells from the DG of Control and $TrkB^{hGFAP}$ mice. Note the absence of TrkB in the $TrkB^{hGFAP}$ mice.

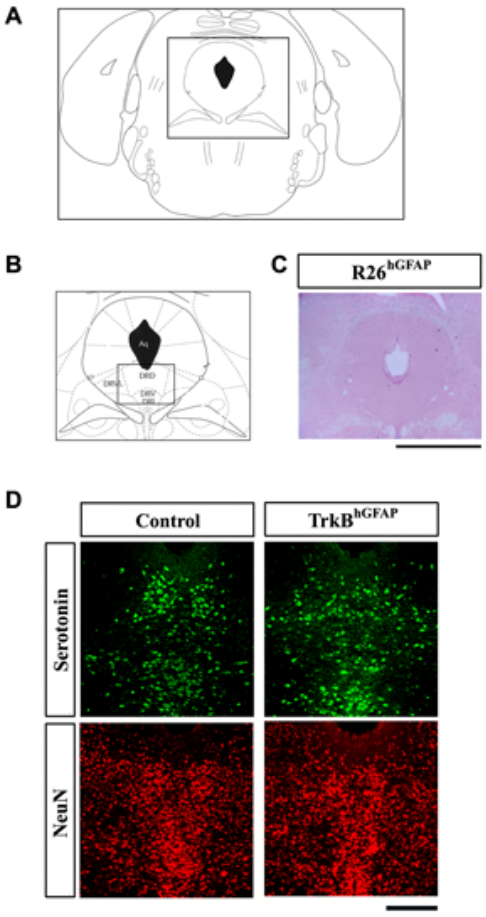

Figure 2.4. Examination of the dorsal raphe serotonergic neurons in the TrkB^{hGFAP} mice.
(A and B) Diagram of the brainstem dorsal raphe nucleus. (B) is a higher magnification view of the insert box in (A). Insert box in (B) depicts the areas shown in (D).
(C) X-gal staining on the brainstem section of R26^{hGFAP} mice. Note the absence of X-gal staining in the dorsal raphe region. Scale bar, 1mm.
(D) Co-staining for serotonin (green) and NeuN (red) on the dorsal raphe sections of control and TrkB^{hGFAP} mice. Scale bar, 100um.

whereas in the R26^{Syn} animal β-gal expression was confined to the outer layers of the DG, while the SGZ and inner granule layer, where NPCs and immature neurons reside, were essentially spared of recombination (Figure 2.3A).

We next enriched NPCs from 2-month old adult mice by culturing primary cells from the DG in neurosphere forming media (Figure 2.3B). Upon X-gal staining, only neurospheres isolated from the DG of $R26^{hGFAP}$, but not those from the $R26^{Syn}$ or control mice stained positive for β-gal activity, indicating that recombination only occurred in the hippocampal NPCs from the $R26^{hGFAP}$ mice (Figure 2.3C). Thus, the masking of X-gal staining difference in the adult DG (Figure 2.3A, left panels) was likely the result of the considerably reduced numbers of NPCs and immature neuron populations at this age compared to P10. Nonetheless, we demonstrated that in adult mice the Syn-Cre transgene could only elicit recombination in differentiated neurons, while the hGFAP-Cre affected both NPCs and neurons. The effective ablation of TrkB with the hGFAP-Cre was further demonstrated by immuno-blotting for TrkB in the hippocampus of adult mice (Figure 2.3D), and by RT-PCR detection of TrkB mRNA in FACS isolated Nestin-GFP positive DG NPCs (Figure 2.3E). Therefore by utilizing these two different Cre transgenic lines, differences between genetic ablation of the TrkB gene in the granule layer of the DG versus additional ablation in the SGZ where progenitors reside can be studied.

2.3.3 Ablation of TrkB in early postnatal NPCs impairs DG morphogenesis

The conditional knockout animals, either carrying the hGFAP-Cre ($TrkB^{hGFAP}$) or the Syn-Cre ($TrkB^{Syn}$) were viable at birth and had normal survival rates (up to 15 months recorded) (He et al., 2004; Luikart et al., 2005). The $TrkB^{hGFAP}$ mice displayed a significant reduction in the volume of the DG granular layer (Figure 2.5A and 2.5B) that first became measurable at P10. The volume reduction stabilized at around 30% after the initial postnatal weeks and persisted throughout adulthood (Figure 2.5B; measured up to P450). This abnormality was not caused by changes in cell density or cell size (Figure 2.5D; $p>0.2$ for both comparisons), but rather was a result of decrease in the number of granule neurons, evidenced by a significant reduction in the thickness of DG granular layer (Figure 2.5C; n=6 for each, $F_{2,15}=5.477$, $p=0.0164$). The number and morphology of glial cells (astrocytes and oligodendrocytes) were not appreciably affected in the $TrkB^{hGFAP}$ mice (Figure 2.6 and not shown). The reduction of volume was most prominently observed in the hippocampus and DG, and did not appear to be a secondary result of broader developmental defect, as the $TrkB^{hGFAP}$ mice had normal body and brain size at all ages examined (Figure 2.7). We also measured the volumes of other anatomical regions, such as the striatum, in 2-month old $TrkB^{hGFAP}$ mice and found normal volume (23.62 +/- 0.94 mm^3 in controls, 23.32 +/- 1.06 mm^3 in $TrkB^{hGFAP}$, n=6 for each, $p>0.2$). The $TrkB^{Syn}$ animals, contrary to the $TrkB^{hGFAP}$ mice, displayed normal development of the DG granular layer (Figure

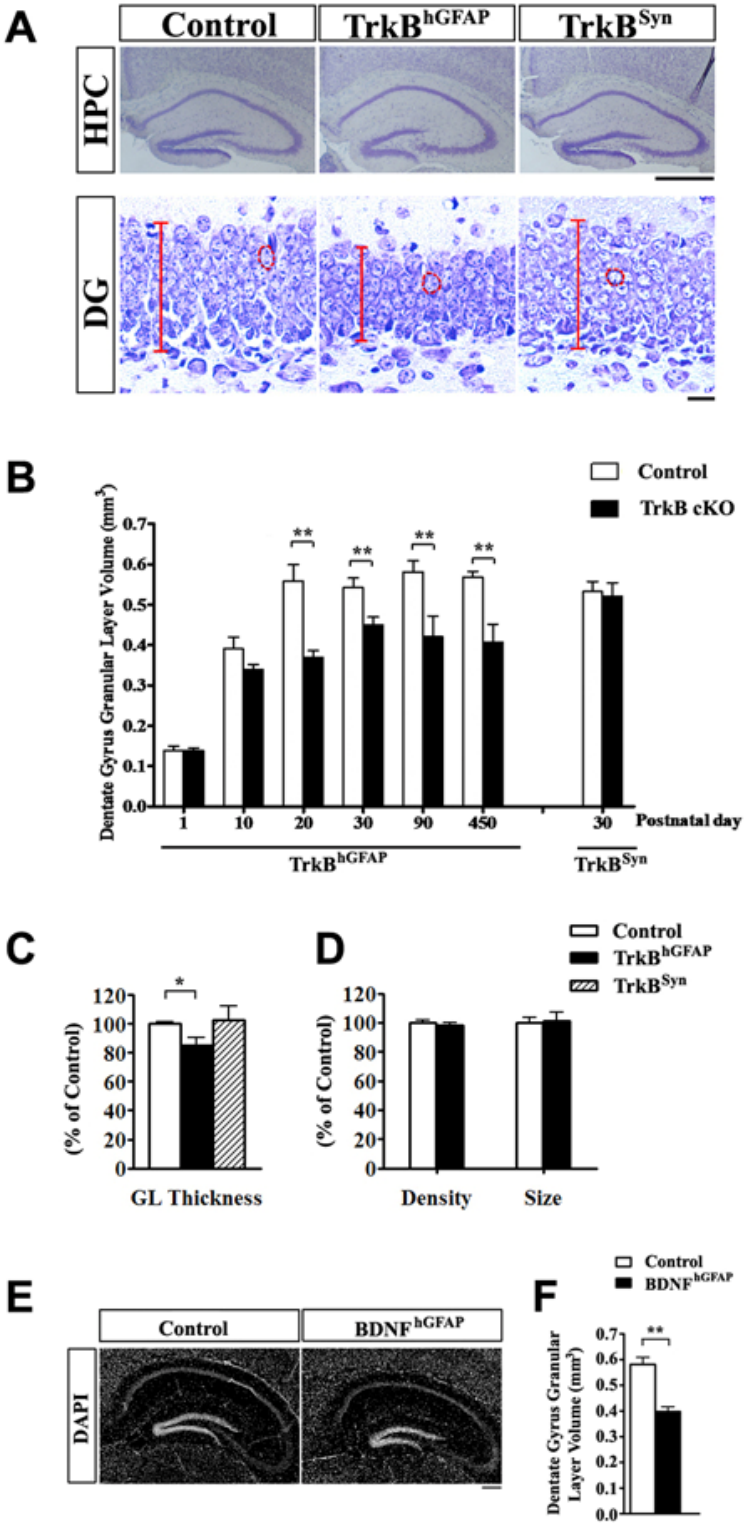

Figure 2.5. Ablation of TrkB in postnatal NPCs impaired DG morphogenesis

(A) Representative images of Nissl stained DG sections from control, TrkB^{hGFAP} and TrkB^{Syn}

mice at P15. The decreases in DG size and granular layer thickness were only observed in $TrkB^{hGFAP}$ mice. Red lines and circles highlight the length of the granular layer, and the size of single cells, respectively. Scale bars, 1mm (hippocampus) and 10um (DG).
(B) Quantitative analysis revealed that the reduction in the DG volume of $TrkB^{hGFAP}$ mice first became measurable at P10 and persisted in adulthood. Results are mean + SEM here and in subsequent figures; n>7 for each.
(C) At P15, $TrkB^{hGFAP}$, but not $TrkB^{Syn}$ mice had thinner granular layer, demonstrated a decrease in neuronal number. Data was shown as percentage of control. N=6 for each. $F_{2,15}$=5.477, p=0.0164. GL, granular layer.
(D) Comparative analysis ofw the size and density of DG granular neurons from control and $TrkB^{hGFAP}$ mice. Note the absence of difference in either category.
(E) DAPI staining of hippocampus sections from control and $BDNF^{hGFAP}$ mice at the age of 2 month. Note the decrease in DG size in the $BDNF^{hGFAP}$ mice. Scale bar, 200um.
(F) Quantitative analysis revealed a 30% reduction in DG volume in the $BDNF^{hGFAP}$ mice at the age of 2 months. N=8-10 for each.
* p<0.05; ** p<0.01

2.5A to 2.5C). These observations demonstrate that TrkB expression in the SGZ is required for the normal structural development of the DG. The phenotypic difference between the $TrkB^{hGFAP}$ and $TrkB^{Syn}$ mice suggests a cell autonomous function of TrkB in the DG NPCs. We have previously reported that conditional deletion of BDNF using the hGFAP-Cre ($BDNF^{hGFAP}$ mice) resulted in 80% reduction of BDNF protein level in the hippocampus (Monteggia et al., 2007), we note that these mice also displayed significantly reduced DG granular layer volume, indicating a ligand-receptor coincidence (Figure 2.5E and 2.5F, n=8-10 for each genotype, p<0.005).

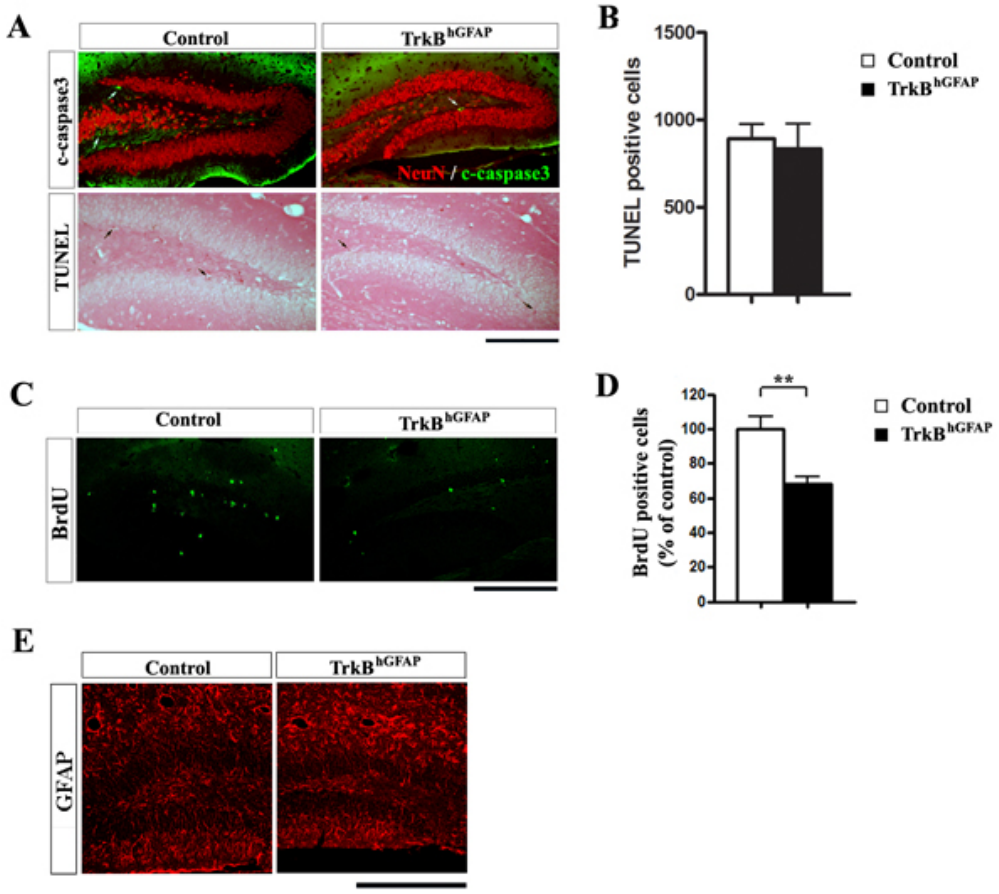

Figure 2.6. Lack of TrkB in NPCs did not promote apoptosis, but decreased long-term production of new cells.

(A-B) Low level of apoptosis was detected in the DG by immuno-staining for cleaved caspase 3 (green, top panels of A), and TUNEL assay (lower panels of A). Arrows point to positive cells. No significant increase in the number of TUNEL positive cells was observed in the $TrkB^{hGFAP}$ mice (B). $p>0.2$. Scale bar, 100um. C-caspase3, cleaved caspase 3.

(C-D) Immunohistochemical detection of BrdU (green) 30 days post injection showed fewer positive cells in the DG of $TrkB^{hGFAP}$ mice (C). Quantitative result of BrdU positive cells revealed a 30% reduction (D). Scale bar, 100um. $^{**}p<0.01$

(E) Immuno-staining for GFAP (red) in the DG of control and $TrkB^{hGFAP}$ mice did not reveal overt difference. Scale bar, 100um.

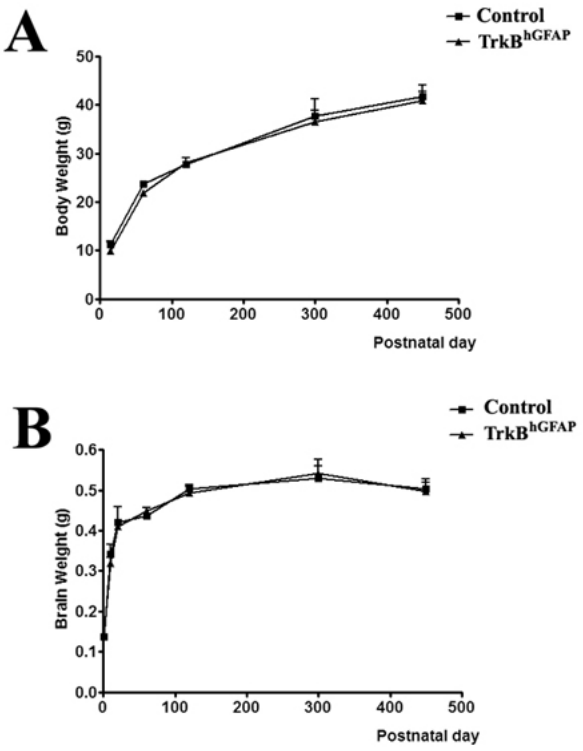

Figure 2.7. TrkB^{hGFAP} mice had normal body and brain weights.
(A-B) Quantitative analyses of the body weights (A) and brain weights (B) of TrkB^{hGFAP} mice compared to control mice. Note the absence of significant difference in either category. Data were represented as mean ± SEM.

2.3.4 Ablation of TrkB impairs proliferation and neurogenesis

Given the apparent reduction in the number of granule neurons in TrkB^{hGFAP} mice, but not TrkB^{Syn} mice, we examined whether lack of TrkB in the NPCs affected the neurogenic capacity of the SGZ. Control and TrkB mutant animals were evaluated at P15, during a period in which the DG undergoes dynamic morphogenesis (Altman and Bayer, 1990). The number of newly generated neurons, as visualized by immunohistochemistry using antibodies against NeuroD, was

drastically reduced in the $TrkB^{hGFAP}$ mice (Figure 2.8A). The $TrkB^{Syn}$ mice, however, had normal numbers of such newly generated neurons (Figure 2.8A). Thus TrkB ablation in the NPCs but not in differentiated neurons impaired hippocampal neurogenesis.

Reduced neurogenesis in the absence of TrkB could be caused by increased cell death, decreased proliferation, or a combination of both processes. We first examined programmed cell death using TdT-mediated dUTP nick end labeling (TUNEL) assay and immunohistochemistry for activated caspase 3. At all time points examined, the number of apoptotic cells detected with either method was uniformly low in all genotypes and no measurable increase was observed in the $TrkB^{hGFAP}$ mice, indicating that lack of TrkB did not appreciably affect survival *in vivo* (Figure 2.6; n=6 for each, $p>0.2$ for TUNEL quantification).

We next assessed proliferation by measuring the number of cells that incorporate the DNA synthesis marker 5-bromo-2'-deoxyuridine (BrdU). P15 mice were treated with multiple pulses of BrdU and sacrificed 24 hours after the first injection (n=7-9 for each genotype, see Experimental Procedures). Within the area encompassing the inner granular layer and SGZ, the number of BrdU positive cells in the $TrkB^{hGFAP}$ mice displayed a 48% reduction compared to control mice (Figure 2.8B

and 2.8C; $F_{2,21}$=78.39, p<0.0001; p<0.001 for *post hoc* test of control to $TrkB^{hGFAP}$ comparison). Similarly, the number of cells positive for Ki67, an endogenous marker for actively cycling cells, was decreased by 51% in the SGZ of the $TrkB^{hGFAP}$ mice (Figure 2.8B and 2.8C; n=7-9 for each; $F_{2,21}$=51.64, p<0.0001; p<0.001 for *post hoc* test of control to $TrkB^{hGFAP}$ comparison). Again, the numbers of BrdU or Ki67 positive cells were unaffected in the DG of the $TrkB^{Syn}$ mice (Figure 2.8B and 2.8C; p>0.2 for control to $TrkB^{Syn}$ comparisons).

To further investigate the cellular abnormality that leads to the significant decrease of proliferation in the $TrkB^{hGFAP}$ mice, we evaluated cell cycle exit of BrdU incorporating cells by examining their expression of Ki67 after a 2-hour chase period, at which point cells that were labeled with BrdU during the S-phase but have subsequently left the cycle would lose their Ki67 expression (BrdU+; Ki67-), whereas the ones that remained in active cell cycle would be double positive (BrdU+; Ki67+) (Chenn and Walsh, 2002). In the $TrkB^{hGFAP}$ mice 23.1 +/- 3.9 % of all BrdU+ cells were Ki67-, displaying a 208% increase in cell cycle exit over the control mice, where only 7.5 +/- 1.3 % are Ki67- (Figure 2.8D and 2.8E, numbers of BrdU+ cells examined were 1053 from 5 control mice, and 772 from 5 $TrkB^{hGFAP}$ mice, p<0.05). Collectively, these observations demonstrate that TrkB is required for normal precursor proliferation in the hippocampus.

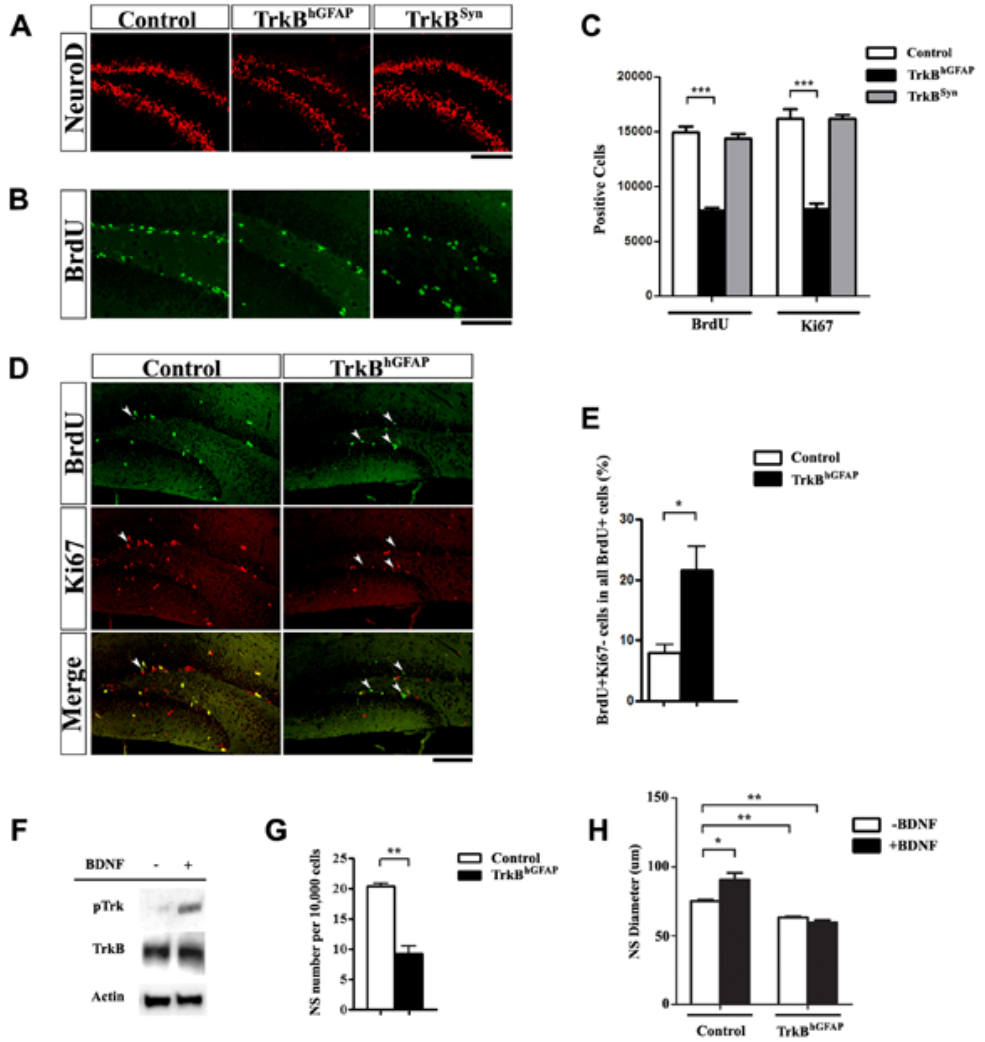

Figure 2.8. Lack of TrkB in NPCs impaired neurogenesis and proliferation *in vivo* and *in vitro*

(A) Representative confocal images of the DG immunostained for NeuroD (red). Note the reduction of NeuroD positive cells, representing immature neurons, in $TrkB^{hGFAP}$, but not $TrkB^{Syn}$ mice (P15). Scale bar, 100um.

(B-C) Proliferation in the DG was decreased in $TrkB^{hGFAP}$, but not $TrkB^{Syn}$ mice, evidence by a reduction in Ki67 positive (C), or BrdU positive cells (B and C). Scale bar, 100um. N=7-9 for each. $F_{2,21}=78.39$, $p<0.0001$ (BrdU); $F_{2,21}=51.64$, $p<0.0001$ (Ki67).

(D-E) Cell cycle analysis using BrdU pulsing and co-immunostaining for BrdU (green) and Ki67 (red) showed increase in the ratio of BrdU labeled cells that have exited the cell cycle (BrdU+Ki67-) in the DG of $TrkB^{hGFAP}$ mice. Arrowheads indicate BrdU+Ki67- cells. Scale bar, 100um. Data represents the ratio of (BrdU+Ki67-) / (All BrdU+).

(F) Western blots of lysates from DG derived neurospheres probed for phosphor-Trk490,

TrkB and actin, with and without BDNF stimulation. Note the abundance of TrkB expression and the increase of phospho-Trk in the presence of BDNF.
(G) Cells from the DG of adult mice were plated at equal density and allowed to proliferate in the presence of EGF and bFGF. The frequency of neurosphere formation was lower in the $TrkB^{hGFAP}$ mice, indicating a decrease in NPC population.
(H) Addition of BDNF facilitated the growth of primary neurospheres derived from the DG of control mice, but not the $TrkB^{hGFAP}$ mice. $TrkB^{hGFAP}$ neurospheres grown without BDNF were also smaller than control, indicated impaired proliferation. N=4 for each. ANOVA revealed significant effects of BDNF ($F_{1,12}$=6.994, p=0.0214), genotype ($F_{1,12}$=102.2, p<0.0001) and an interaction between the two ($F_{1,12}$=19.3, p=0.0009).
*p<0.05; **p<0.01; ***p<0.001.

2.3.5 Activation of TrkB in response to BDNF facilitates proliferation *in vitro*

Our finding that the $TrkB^{hGFAP}$ but not the $TrkB^{Syn}$ mice displayed impaired hippocampal neurogenesis suggested a cell autonomous requirement for TrkB in NPCs. To further examine their intrinsic properties, we cultured NPCs from the DG in serum-free conditions. In the presence of epidermal growth factor (EGF) and basic fibroblast growth factor (bFGF), DG NPCs cultured on an attachment-preventing surface form neurospheres, which expressed TrkB receptor that could be activated by exogenous BDNF (Figure 2.8F). Although maintaining adult DG-derived primary neurospheres in media containing BDNF (50 ng/ml) for 7-10 days did not increase the frequency of primary neurosphere formation (not shown), there was a significant increase in the size of the neurospheres, suggesting that activation of TrkB facilitates the expansion of neurosphere-forming cells (Figure 2.8H; n=4 for each group, p<0.05 for *post hoc* test of with to without BDNF

comparison in control cells). Primary neurospheres derived from the DG of adult $TrkB^{hGFAP}$ mice, when plated at equal density, displayed reduction in both the number (Figure 2.8G; n=4 for each group, $p<0.005$) and size (Figure 2.8H; $p<0.005$ for *post hoc* test of control to $TrkB^{hGFAP}$ (without BDNF) comparison; $F_{1,12}=102.2$, $p<0.0001$ for genotype; $F_{1,12}=6.994$, $p=0.0214$ for BDNF treatment). The ability of primary neurospheres to form secondary neurospheres was also impaired in the $TrkB^{hGFAP}$ mice (secondary-to-primary neurosphere ratio: 0.322 +/- 0.058 in $TrkB^{hGFAP}$ and 0.843 +/- 0.096 in control, n=4 for each, $p<0.005$). In addition, deletion of TrkB abolished neurosphere sensitivity to BDNF stimulation (Figure 2.8H, $p>0.2$). Using an Annexin V labeling assay, we examined the percentage of apoptotic cells in the neurosphere cultures. Similar to the *in vivo* results, we did not observe significant differences between control and $TrkB^{hGFAP}$ cells, with or without BDNF treatment (n=4 for each; with 50 ng/ml BDNF: 14.95 +/- 1.38% in controls, 16.25 +/- 2.65% in $TrkB^{hGFAP}$; without BDNF: 14.46 +/- 1.62% in controls, 17.69 +/- 2.56% in $TrkB^{hGFAP}$; $F_{1,8}=1.136$, $p=0.3177$ for genotype; $F_{1,8}=0.0498$, $p=0.8290$ for treatment), suggesting that the reduction in the size of neurosphere derived-from $TrkB^{hGFAP}$ mice was not due to survival deficits. Thus, BDNF facilitates proliferation by acting directly on NPCs and the activation of TrkB is solely responsible for this effect.

2.3.6 TrkB is required for induced proliferation and neurogenesis by

antidepressants and voluntary exercise.

Reduction in hippocampal volume has been observed in animal models of stress (Coe et al., 2003; Czeh et al., 2001; Isgor et al., 2004), which may be reversed or prevented by chronic AD treatment (Czeh et al., 2001; Sheline et al., 2003). Similarly, reduction of hippocampal volume has been reported in some studies of human patients with major depression (Bremner et al., 2000; MacQueen et al., 2003; Sheline et al., 1999) and post-traumatic stress disorder (Gilbertson et al., 2002; Karl et al., 2006; Smith, 2005). Although the cellular mechanism is unclear in humans, animal studies have demonstrated that chronic exposure to various types of ADs induces DG proliferation and neurogenesis (Malberg et al., 2000), thereby potentially contributing to the recovery of volume loss. In this context, we examined whether chronic AD treatment can restore neurogenesis in $TrkB^{hGFAP}$ mice. We thus treated control, $TrkB^{hGFAP}$ and $TrkB^{Syn}$ mice with daily injections of the serotonin reuptake inhibitor fluoxetine (10 μg/g) or the tricyclic imipramine (20 μg/g) for 21 days (Malberg et al., 2000) (n=7-29 for each group, Table 2.1). As previously established, compared with mice receiving daily saline injections, both drugs induced substantial Ki67 immuno-reactivity in the DG of control mice (Figure 2.9A and 2.9B; $F_{2,98}$=40.48, $p<0.0001$ for treatment; $p<0.001$ for *post hoc* test of both AD-to-saline comparisons). The induction of proliferation was echoed by an increase in the number of newly generated neurons expressing Doublecortin and NeuroD (Figure

Table 2.1. Number of control, TrkB^{hGFAP} and TrkB^{Syn} mice used for antidepressant associated behavioral and immunohistochemical analyses

Procedure[a]	Cohort	Control			TrkB^{hGFAP}			TrkB^{Syn}		
		Sal	Flx	Imi	Sal	Flx	Imi	Sal	Flx	Imi
Injection	I.	10	10		8	8				
	II.	11		10	7		8			
	III.	8	7	8				7	7	8
	Total	29	17	18	15	8	8	7	7	8
NSFT	I.	10	10		6[b]	6[b]				
	II.	11		10	5[b]		6[b]			
	III.	8	7	8				7	7	8
	Total	29	17	18	11	6	6	7	7	8
TST	I.	10	8[c]		6[c]	8				
	II.	10[c]		8[c]	6[c]		8			
	III.	8	7	8				7	7	8
	Total	28	15	16	12	8	8	7	7	8
Immuno analyses	I.	8[d]	8[d]		7[d]	8				
	II.	9[d]		8[d]	6[d]		8			
	III.	8	7	8				7	7	8
	Total	25	15	16	13	8	8	7	7	8

[a]Procedures were performed in the order as listed below;

[b-d]The numbers of mice listed in the "NSFT", "TST" and "immuno-analyses" sections represent the number of data points used in statistical evaluation; when such numbers are less than the numbers of mice listed in the "injection" section, the differences are explained as below:

[b]Data from mice that took longer than 10 min to feed in the novel environment were excluded;

[c]Data from mice that climbed up their tails during the 6 min video-recorded session were excluded;

[d]24 hours after the TST, fresh tissues of 1-2 mice from these group were collected for alternative experiments, therefore not used for immunohistochemical analyses;

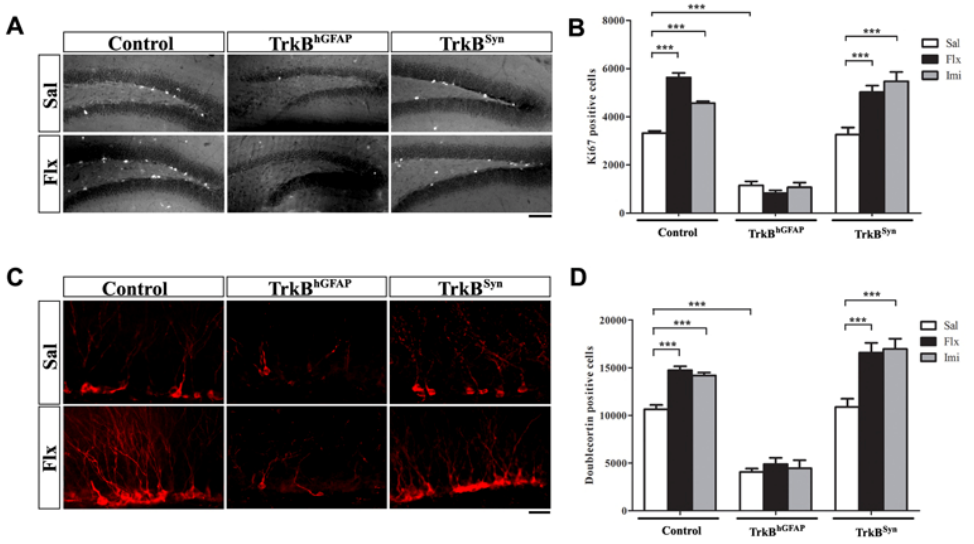

Figure 2.9. TrkB expression in NPCs was required for chronic ADs induced proliferation and neurogenesis

(A) Representative confocal images of immuno-staining for Ki67 in the DG of saline or fluoxetine treated mice. Chronic treatment with fluoxetine increased the number of proliferating cells (Ki67+) in the DG of control, $TrkB^{Syn}$, but not $TrkB^{hGFAP}$ mice. Scale bar, 100um. Sal, saline; Flx, fluoxetine.

(B) Quantitative analysis of Ki67 positive cells demonstrated lack of increases in the $TrkB^{hGFAP}$ mice after fluoxetine or imipramine treatment. Note the lower number of Ki67 positive cells in the $TrkB^{hGFAP}$ mice with either saline or AD, indicating impairment in proliferation at both basal and stimulated level. N=7-25 for each. ANOVA (GLM) found significant effects of AD treatment ($F_{2,98}$=40.48, p<0.0001), genotype ($F_{2,98}$=332.3, p<0.0001) and the interaction of both ($F_{2,98}$=19.64, p<0.0001). Imi, imipramine.

(C) Chronic fluoxetine treatment increased the number of Doublecortin positive cells (red) in the DG of control and $TrkB^{Syn}$ but not $TrkB^{hGFAP}$ mice. Scale bar, 10um.

(D) Fluoxetine and imipramine failed to elicit an increase in the number of immature neurons (Doublecortin+) in the $TrkB^{hGFAP}$ mice. N=7-25 for each. ANOVA (GLM) revealed significant effects of AD treatment ($F_{2,98}$=30.79, p<0.0001), genotype ($F_{2,98}$=211.6, p<0.0001) and interaction between the two ($F_{2,98}$=5.471, p=0.0005).

***p<0.001.

2.9C, 2.9D and data not shown; $F_{2,98}$=30.79, p<0.0001 for treatment; p<0.001 for *post hoc* test of both AD-to-saline comparisons). In contrast, $TrkB^{hGFAP}$ mice treated

with the same ADs did not show increase in the number of proliferating cells or immature neurons (Figure 2.9A to 2.9D; $F_{2,98}$=332.3, p<0.0001 for the effect of genotype on Ki67; $F_{2,98}$=211.6, p<0.0001 on Doublecortin). This treatment, or an extended six week treatment, also failed to restore the DG volume deficit in the $TrkB^{hGFAP}$ mice (not shown), consistent with the additional observation that long-term production of new-born neurons in the $TrkB^{hGFAP}$ mice was also impaired, both at baseline and with exposure to chronic AD (Figure 2.6 and not shown). The $TrkB^{Syn}$ mice responded normally to both ADs (Figure 2.9A to 2.9D; p<0.001 for *post hoc* test of both AD-to-saline comparisons).

In rodents, voluntary exercise, such as wheel-running behavior has been demonstrated to robustly induce neurogenesis, much in the same fashion as AD treatment (van Praag et al., 1999). Less is known, however, about the underlying mechanism of this AD-like effect of exercise. To determine whether TrkB was also required for this process, we subjected control and $TrkB^{hGFAP}$ mice to 6 weeks of wheel-running (n=8-16 for each group, Table 2.2). Both the number of Ki67 positive and Doublecortin positive cells increased in the control runners, compared to control sedentary animals (Figure 2.10C: $F_{1,36}$=13.64, p=0.0007 for exercise; Figure 2.10D: $F_{1,36}$=16.01, p=0.0003; p<0.001 for *post hoc* test of both comparisons). Also a significant increase in BDNF protein level in the hippocampus of runners was

Table 2.2. Number of control and TrkB^{hGFAP} mice used in the running experiment and subsequent behavioral and immunohistochemical analyses

Procedure[a]	Gender	Control		TrkB^{hGFAP}	
		Sed	Run	Sed	Run
Sed/Run	Female	3	7	3	6
	Male	5	9	5	7
	Total	8	16	8	13
NSFT	Female	3	7	3	6
	Male	5	9	5	7
	Total	8	16	8	13
TST	Female	3	7	3	6
	Male	5	9	5	7
	Total	8	16	8	13
Immuno analyses	Female	3	6[b]	3	6
	Male	3[b]	7[b]	5	7
	Total	6	13	8	13

[a]Procedures were performed in the order as listed below;
[b]24 hours after the TST, fresh tissues of 1-2 mice from these group were collected for alternative experiments, therefore not used for immunohistochemical analyses;

observed (66.44 +/- 3.65 pg/mg in runners; 45.83 +/- 2.99 pg/mg in sedentary controls; $p<0.05$). The TrkB^{hGFAP} mice, despite normal running distance (5.96 +/- 0.41 km/day in controls, 5.48 +/- 0.34 km/day in TrkB^{hGFAP}, $p>0.2$) as well as elevation of BDNF level in runners (60.33 +/- 4.43 pg/mg in runners; 40.94 +/- 1.37 pg/ml in sedentary controls; $p<0.05$; measured in a separate group of control and TrkB^{hGFAP} mice, n=3 for each genotype), did not show any increase in proliferation and neurogenesis (Figure 2.10C and 2.10D, $p>0.2$ for both). Since we tested male

and female mice in the voluntary exercise paradigm, we further separated the results into gender and genotype-specific groups and found no statistically significant difference between males and females of the same genotype (not shown).

Taken together, these experiments demonstrate an important role for TrkB in regulating basal proliferation and neurogenesis in the adult DG. Furthermore, ablation of TrkB in NPCs was sufficient to render them unresponsive to chronic AD treatment and voluntary exercise induced proliferation and neurogenesis. Given the similar beneficial aspects of these two stimulations, it is therefore likely that TrkB is a crucial component of a common antidepressive mechanism to regulate hippocampal NPCs in mice.

2.3.7 TrkB is required for behavioral improvement induced by ADs and exercise

To determine whether the lack of neurogenic response in the $TrkB^{hGFAP}$ mice was coupled with general insensitivity to chronic ADs and exercise, we compared the depression and anxiety-like behaviors in control and $TrkB^{hGFAP}$ mice. First, mice treated with fluoxetine, imipramine, or saline for 21 days were examined in the novelty-suppressed feeding test (NSFT), a conflict paradigm in which the latency to feed in a novel environment was used as an indicator of anxiety level

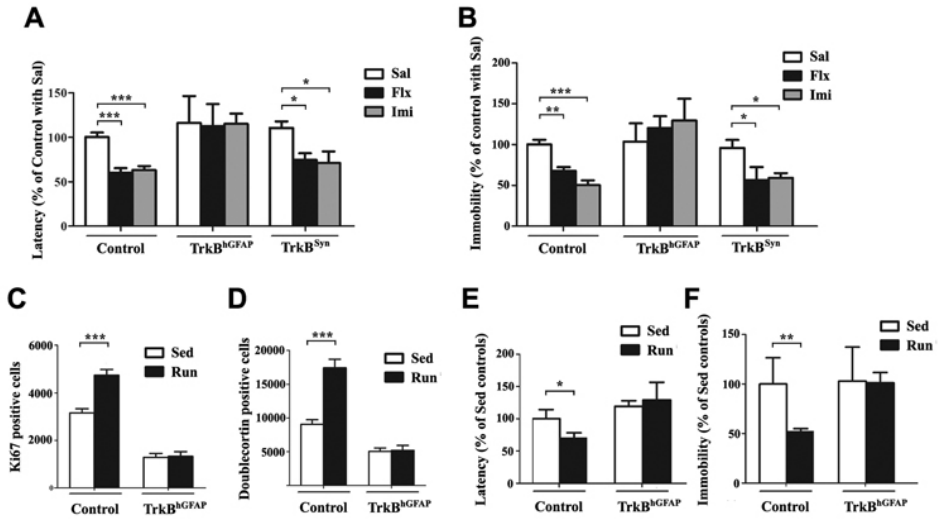

Figure 2.10. TrkB^{hGFAP} mice were insensitive to chronic AD and exercise induced improvement in depression and anxiety-like behaviors.

(A) In the novelty-suppressed feeding test (NSFT), chronic treatments with fluoxetine or imipramine shortened the latency to feed (indicating reduced anxiety) in control, TrkB^{Syn} but not TrkB^{hGFAP} mice. Data were shown as percentage of control with saline injection. N=6-29 for each group. ANOVA (GLM) found significant effects of AD treatment ($F_{2,100}$=8.022, p=0.0006) and genotype ($F_{2,100}$=10.49, p<0.0001).

(B) The tail-suspension test (TST) measured total duration of immobility ("behavior despair"), which could be reduced by chronic fluoxetine or imipramine in control, TrkB^{Syn} but not TrkB^{hGFAP} mice. Data were shown as percentage of control with saline injection. N=7-28 for each. ANOVA (GLM) revealed significant effects of AD treatment ($F_{2,100}$=4.233, p=0.0172), genotype ($F_{2,100}$=20.03, p<0.0001) and the interaction of both ($F_{2,100}$=5.085, p=0.0009).

(C-D) Running for 6 weeks failed to increase the number of Ki67 (C) or Doublecortin (D) positive cells in the DG of TrkB^{hGFAP} mice. N=6-13 for each. ANOVA (GLM) revealed significant effects of running ($F_{1,36}$=13.64, p=0.0007 for Ki67; $F_{1,36}$=16.01, p=0.0003 for Doublecortin), genotype ($F_{1,36}$=141.1, p<0.0001 for Ki67; $F_{1,36}$=58.46, p<0.0001 for Doublecortin) and the interaction of the two ($F_{1,36}$=12.66, p=0.0010 for Ki67; $F_{1,36}$=14.79, p=0.0005 for Doublecortin).

(E-F) TrkB^{hGFAP} mice did not display decrease in latency to feed (E, NSFT) or duration of immobility (F, TST) after 6 weeks of running, compared to sedentary controls. Data were shown as percentage of sedentary control. N=8-16 for each. NSFT ($F_{1,41}$=15.09, p=0.0004 for genotype), TST ($F_{1,41}$=9.082, p=0.0044 for genotype; $F_{1,41}$=8.273, p=0.0064 for exercise).

*p<0.05; **p<0.01; ***p<0.001.

(Santarelli et al., 2003). In agreement with the general capacity of chronic ADs to ease anxiety, 24 hours after the last dose, control mice receiving fluoxetine or imipramine displayed significantly shorter latency to feed compared to saline-treated control mice (Figure 2.10A; $F_{2,100}$=8.022, p=0.0006 for treatment; p<0.001 for *post hoc* test both AD-to-saline comparisons). The $TrkB^{hGFAP}$ mice, on the contrary, were insensitive to the effects of either AD (Figure 2.10A; $F_{2,100}$=10.49, p<0.0001 for genotype). Similarly, $TrkB^{hGFAP}$ mice exposed to 6 weeks of running showed no improvement in the NSFT, whereas the control runners displayed clear decrease in latency as compared to the sedentary animals (Figure 2.10E; $F_{1,41}$=15.09, p=0.0004 for genotype; p<0.05 for *post hoc* test of running effect in control mice). No difference in home cage consumption, or body weight loss was observed across genotypes (not shown).

Next we examined depression-like behavior in the control and $TrkB^{hGFAP}$ mice by using the tail-suspension test (TST), a paradigm of inescapable stress (Porsolt et al., 1987). All mice were tested 48 hours after the last dose of AD or saline to exclude the acute effects on behaviors that do not correlate with prior duration of drug treatment, or clinical responses. Control runners and AD treated control mice showed decreased immobility (a state of "behavioral despair"), compared to sedentary or saline treated control mice, respectively (Figure 2.10F:

$F_{1,41}$=9.082, p=0.0044 for exercise, *post hoc* p<0.01; Figure 2.10B: $F_{2,100}$=20.03, p<0.0001 for AD treatment, *post hoc* p<0.01 for fluoxetine, p<0.001 for imipramine). The $TrkB^{hGFAP}$ mice again failed to display any appreciable response to either treatment (Figure 2.10B: $F_{2,100}$=4.233, p=0.0172 for genotype; Figure 2.10F: $F_{1,41}$=9.082, p=0.0044 for genotype).

Despite the lack of response to ADs and exercise in the behavioral paradigms of NSFT and TST, the saline-treated $TrkB^{hGFAP}$ mice performed similarly compared to the control mice, suggesting relatively normal depression and anxiety-like behaviors at the basal level. To further investigate this finding, we examined a cohort of control and $TrkB^{hGFAP}$ mice in a series of behavioral measures (Figure 2.11; n=17-21 for each genotype). We observed no significant differences within these two groups in the dark-light test in both the length of time spent and activity in the light compartment. In the open field test, the $TrkB^{hGFAP}$ mice were equivalent to controls in the time spent in the center. In the elevated-plus maze test, the $TrkB^{hGFAP}$ mice spent more time in the open arm compared to littermate controls. Together these results suggest normal (and in some cases reduced) baseline anxiety-like behaviors in the $TrkB^{hGFAP}$ mice. Similarly, in the forced swim test, the $TrkB^{hGFAP}$ mice displayed normal latency to immobility, and a non-significant trend toward decreased total length of immobility, thereby supporting earlier observations

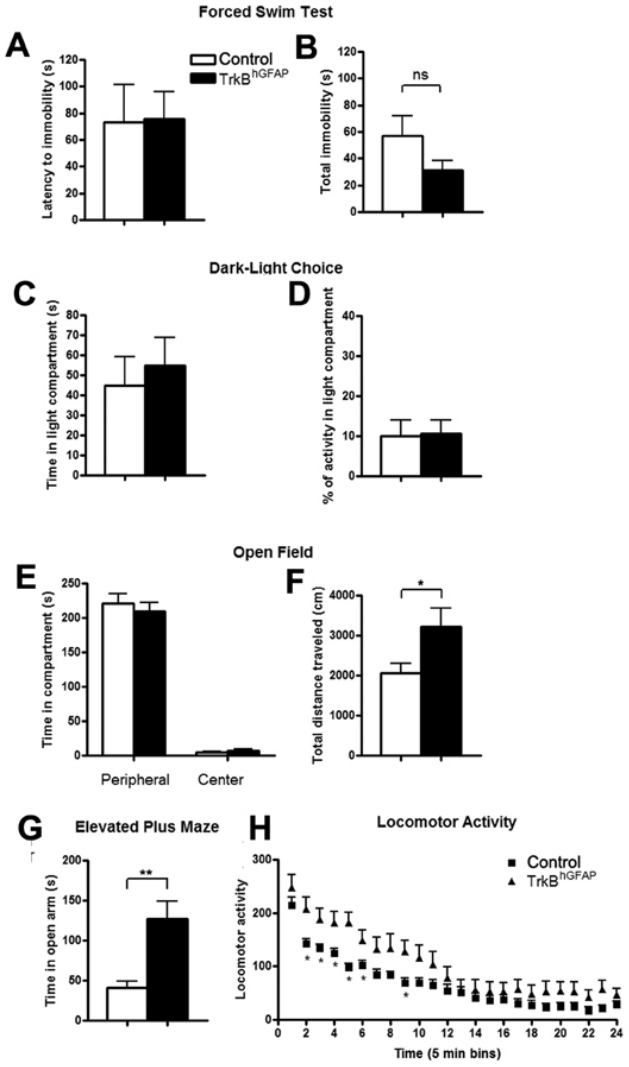

Figure 2.11. Examination of the TrkB^{hGFAP} mice in basal depression and anxiety-like behaviors.

(A-B) In the forced swim test, the TrkB^{hGFAP} mice did not show significant difference in the latency to become immobile (A), or the length of immobility (B). Legends in A are applied to B-G.

(C-D) In the dark-light test, the TrkB^{hGFAP} mice showed normal behaviors both in the length of time spent (C), and exploratory activity in the light compartment (D).

(E-F) In the open field test, the TrkB^{hGFAP} mice spent similar length of time in the center and the peripheral of the field as the control mice (E). The overall activity was increased in the TrkB^{hGFAP} mice as shown by total distance traveled (F).

(G) In the elevated plus maze test, the TrkB^{hGFAP} mice spent more time in the open arm than the control mice.

(H) In the locomotor activity test, the $TrkB^{hGFAP}$ mice were normal in the first 5 minutes, but displayed increased activity in the following 30 minutes. The $TrkB^{hGFAP}$ mice did habituate to a level comparable to control mice toward the second half of the test.
* $p<0.05$; ** $p<0.01$.

of normal baseline depression-like behavior. Based on the above observations, we conclude that the lack of responses to AD and exercise in the $TrkB^{hGFAP}$ mice could not be explained by alterations in baseline behaviors, but rather was a result of insensitivity to the molecular and cellular changes induced by chronic AD and exercise.

2.3.8 Normal sensitivity to chronic ADs in mice lacking TrkB in differentiated neurons

To explore whether the deficit in increased neurogenesis contributed to the abolished behavior sensitivity to chronic AD, we tested the $TrkB^{Syn}$ mice in the TST and the NSFT. Similar to control mice, upon chronic treatment with fluoxetine and imipramine, the $TrkB^{Syn}$ mice showed significant decreases in anxiety (Figure 2.10A; *post hoc* $p<0.05$ for both ADs) and depression-like behaviors (Figure 2.10B; *post hoc* $p<0.05$ for both ADs). This result, in conjunction with the observation that chronic AD treatment increases DG proliferation and neurogenesis in these mice (Figure 2.9), indicated that despite the lack of TrkB in differentiated neurons, the unaffected TrkB signaling in the NPCs was sufficient for the $TrkB^{Syn}$ mice to display a behavioral

response to chronic AD.

2.3.9 Specific ablation of TrkB in adult NPCs is sufficient to block sensitivity to AD

The preceding results were most consistent with the interpretation that TrkB loss in differentiated neurons alone is insufficient to mediate AD sensitivity, whereas ablation in both the neurogenic niche and the differentiated compartment did block the effect. To further delineate whether TrkB function in adult NPCs alone was required for AD induced neurogenic and behavioral responses, we utilized a tamoxifen-inducible form of Cre recombinase, $CreER^{T2}$, expressed under the regulatory element of the Nestin gene in which TrkB ablation could be confined to the adult neurogenic niches (Chen et al., 2008). When interbred with the R26 reporter mice ($R26^{Nestin}$), Cre activity in the Nestin-CreER mice could be visualized either in embryonic or in adult CNS, in a tamoxifen-dependent manner. Specifically, when 1 month old $R26^{Nestin}$ mice were injected with vehicle or tamoxifen (see Experimental Procedures) and analyzed 1 month afterwards, spontaneous recombination (vehicle treated) was minimal, while tamoxifen-induced recombination was restricted to the DG, sub-ventricular zone (SVZ), rostral migratory stream (RMS), olfactory bulb and cerebellum (Figure 2.12A and not shown). In the DG, recombination occurred specifically in the inner granular layer

and SGZ. To evaluate the efficiency of the Nestin-CreER to target NPCs, we analyzed tamoxifen-induced $R26^{Nestin}$ mice at 1 month post injection (2 months of age) and 6 months post injection (7 months of age). The number of X-gal stained cells was dramatically increased in the 6 months post-injection group, indicating effective recombination in the NPCs that were capable of proliferation and self-renewal (Figure 2.12B). Additional confirmation was obtained by double-immunostaining for β-gal and doublecortin in 3 month post-injection group (4 months of age), where the majority of doublecortin positive cells also co-expressed β-gal (Figure 2.12C).

As described above, hGFAP-Cre mediated ablation of TrkB resulted in a smaller DG (Figure 2.5) that we attributed to the lack of TrkB signaling in early postnatal NPCs to sustain rapid proliferation required for normal structural development. To bypass this essential phase of DG postnatal morphogenesis, we subjected $TrkB^{flox/flox}$; Nestin-CreER mice to tamoxifen ($TrkB^{Nestin}$) at 1 month of age. Littermate $TrkB^{flox/flox}$; Nestin-CreER mice injected with vehicle, and $TrkB^{flox/flox}$ mice injected with tamoxifen were also analyzed, and collectively presented as the control group. At the age of 6 weeks and 3 months, TrkB mRNA was virtually undetectable by RT-PCR in the DG NPCs of $TrkB^{Nestin}$ mice compared to vehicle treated control mice, using FACS sorted Nestin-GFP positive cells (Figure 2.12D). TrkB protein was also absent from the proliferating cells of the SGZ, while its level in the majority

of granular neurons was unaffected (Figure 2.12E). As expected, ablation of TrkB at 1 month of age did not lead to reduction in DG granular layer volume, when examined at 3 months of age (Figure 2.12F; n=6 for each; $p>0.2$). Basal proliferative activity in the SGZ at this age, measured by the number of Ki67 positive cells, was modestly decreased in the $TrkB^{Nestin}$ mice, whereas no aberrant cell death was observed (Figure 2.13). Upon exposure to fluoxetine (10ug/g) or imipramine (20ug/g) for 21 days (n=8-10 for each group), the $TrkB^{Nestin}$ mice did not display increased proliferation as measured by the numbers of Ki67 (Figure 2.12G; $F_{1,50}=176.7$, $p<0.0001$ for genotype; $F_{2,50}=12.45$, $p<0.0001$ for treatment; $F_{2,50}=13.57$, $p<0.0001$ for interaction) and phosphorylated histone-H3 positive cells (Figure 2.13; $F_{1,50}=131.9$, $p<0.0001$ for genotype; $F_{2,50}=17.46$, $p<0.0001$ for treatment; $F_{2,50}=17.34$, $p<0.0001$ for interaction). The number of newly generated neurons as labeled by Doublecortin also did not change in the $TrkB^{Nestin}$ mice (Figure 2.12H; $F_{1,50}=141.9$, $p<0.0001$ for genotype; $F_{2,50}=7.014$, $p=0.0021$ for treatment; $F_{2,50}=12.56$, $p<0.0001$ for interaction). The absence of neurogenic response in the $TrkB^{Nestin}$ mice coincided with a lack of behavioral improvements both in the NSFT (Figure 2.12I; $F_{1,50}=13.68$, $p=0.0005$ for genotype) and the TST (Figure 2.12J; $F_{1,50}=18.15$, $p<0.0001$ for genotype). These observations refine and confirm the preceding studies, indicating that ablation of TrkB from adult NPCs alone is sufficient to block sensitivity to chronic ADs.

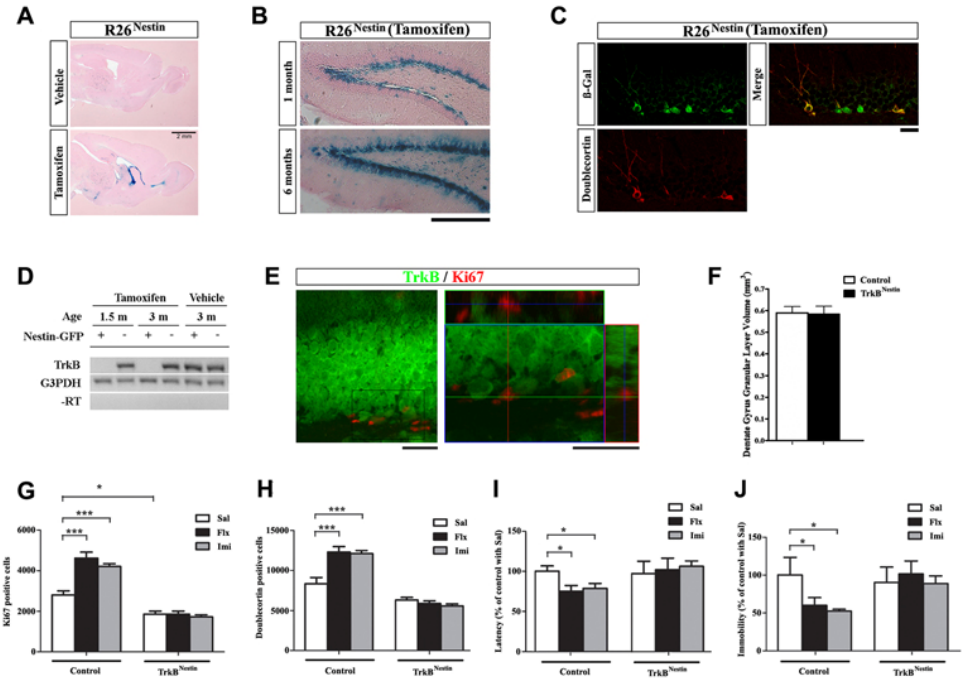

Figure 2.12. Specific ablation of TrkB in adult NPCs was sufficient to block AD sensitivity

(A) X-gal staining on sagittal brain sections of $R26^{Nestin}$ mice, treated with vehicle or tamoxifen at 1 month and analyzed at 2 months of age.

(B) X-gal staining on DG sections of $R26^{Nestin}$ mice, treated with tamoxifen at 1 month and analyzed 1 month or 6 months afterwards. Note the increase in X-gal stained cells 6 months after tamoxifen injection. Scale bar, 200um.

(C) Co-staining for β-gal (green) and Doublecortin (red) on DG sections from $R26^{Nestin}$ mice, treated with tamoxifen at 1 month and analyzed at 4 months of age. Scale bar, 10um.

(D) RT-PCR detection of TrkB and G3PDH transcripts in FACS sorted Nestin-GFP positive and negative cells from the DG of $TrkB^{flox/flox}$; Nestin-CreER mice treated with tamoxifen ($TrkB^{Nestin}$) or vehicle (control) at 1 month old.

(E) Co-staining for TrkB (green) and Ki67 (red) on DG sections from $TrkB^{Nestin}$ mice at the age of 3 months (2 months post-tamoxifen injection), note the lack of co-localization of TrkB and Ki67 in the SGZ. Scale bars, 10um and 5um.

(F) $TrkB^{Nestin}$ mice at the age of 3 months had normal DG volume.

(G-H) Quantitative analysis of Ki67 (G) and Doublecortin (H) positive cells demonstrated lack of increases in the $TrkB^{Nestin}$ mice after fluoxetine or imipramine treatments. N=8-10 for each. ANOVA (GLM) found significant effects of AD treatment ($F_{2,50}$=12.45, p<0.0001 for Ki67; $F_{2,50}$=7.014, p=0.0021 for Doublecortin), genotype ($F_{1,50}$=176.7, p<0.0001 for Ki67; $F_{1,50}$=141.9, p<0.0001 for Doublecortin) and an interaction of the two ($F_{2,50}$=13.57, p<0.0001 for Ki67; $F_{2,50}$=12.56, p<0.0001 for Doublecortin).

(I-J) $TrkB^{Nestin}$ mice did not display decrease in latency to feed (I, NSFT) or duration of immobility (J, TST) after chronic exposure to fluoxetine or imipramine, compared to control

mice. Data were shown as percentage of control treated with saline. N=8-10 for each. NSFT: $F_{1,50}$=13.68, p=0.0005 for genotype, $F_{2,50}$=4.206, p=0.0205 for the interaction of genotype and AD treatment. TST: $F_{1,50}$=18.15, p<0.0001 for genotype, $F_{2,50}$=6.848, p=0.0024 for AD and $F_{2,50}$=9.488, p=0.0003 for an interaction of the two.
*p<0.05. ***p<0.001.

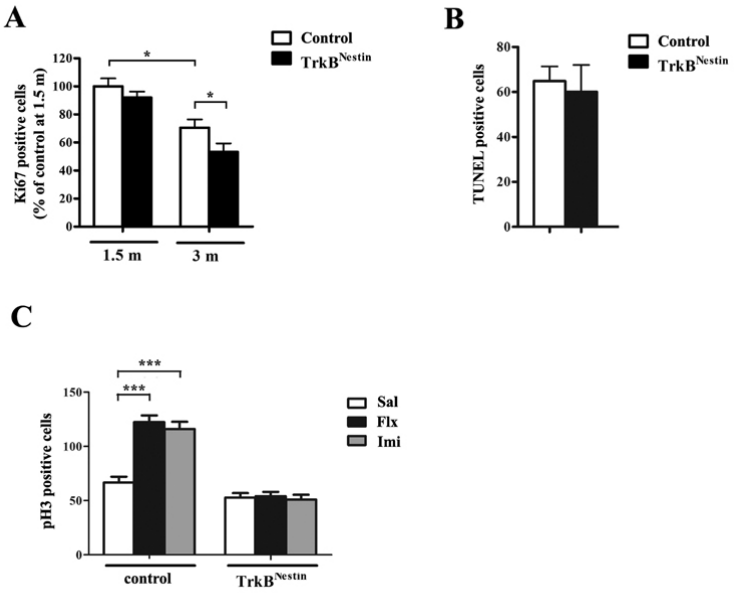

Figure 2.13. TrkB ablation in the $TrkB^{Nestin}$ mice impaired basal proliferation without promoting apoptosis.
(A) $TrkB^{Nestin}$ mice treated with tamoxifen at 1 month of age had normal level of Ki67+ cells at 1.5 month, but significantly lower level at 3 months.
(B) No increase in the number of TUNEL positive cells was detected in the $TrkB^{Nestin}$ mice at 3 months of age.
(C) Chronic treatment of fluoxetine or imipramine did not increase the number of phosphorylated histone H3 (pH3) positive cells in the $TrkB^{Nestin}$ mice. ANNOVA (GLM) found significant effects of AD treatment ($F_{2,50}$=17.46, p<0.0001), genotype ($F_{2,50}$=131.9, p<0.0001) and the interaction of the two ($F_{2,50}$=17.34, p<0.0001).
* p<0.05; ***p<0.001.

2.4 Discussions

2.4.1 Regulation of postnatal and adult neurogenesis in the dentate gyrus

The identification of NPCs in the largely post-mitotic adult brain has transformed the perspective on the development, physiology and pathogenesis of this organ. Benefiting substantially from prior knowledge of embryonic cortical neurogenesis, an array of factors and signaling pathways have been demonstrated to be involved in the regulation of postnatal and adult neurogenesis (Lledo et al., 2006; Ming and Song, 2005). Anatomically, NPCs in the postnatal and adult brain reside in the SVZ of the lateral ventricle and the SGZ of the DG, regions considered to be the residues of the embryonic germinal niche (Alvarez-Buylla and Lim, 2004). However, it is becoming increasingly clear that postnatal and adult NPCs bear characteristics distinctive from their embryonic counterparts. They have slower and less frequent division (Corti et al., 2005), increased susceptibility to telomere shortening (Ferron et al., 2004) and overall astrocyte-like morphology and gene expression (Doetsch et al., 1999; Imura et al., 2003; Seri et al., 2001). The deviation from the "embryonic properties" is more obvious in the DG NPCs, which have been noted to possess limited self-renewal, proliferation and migration capacities (Bull and Bartlett, 2005; Seaberg and van der Kooy, 2002). Paradoxically, DG NPCs gain a remarkable capacity to respond to various extrinsic and intrinsic stimuli, including environmental enrichment, exercise, learning, stress,

antidepressants, diet, hormone level, inflammation and drugs of abuse (Cameron and McKay, 1999; Eisch et al., 2000; Ekdahl et al., 2003; Gould et al., 1999; Gould et al., 1992; Kempermann et al., 1997; Lee et al., 2000; Malberg et al., 2000; Monje et al., 2003; van Praag et al., 1999). The signaling mechanisms that specify these unique properties of DG NPCs, both on the basal level and the induced state, remain unidentified.

Our study shows that TrkB-expressing NPCs in the postnatal and adult DG respond to BDNF. As demonstrated in the $TrkB^{hGFAP}$ mice, ablation of TrkB from the DG NPCs blocked BDNF-induced neurosphere formation *in vitro*, and impaired proliferation and neurogenesis *in vivo*. Although the Cre-mediated deletion of TrkB in the $TrkB^{hGFAP}$ mice was not restricted to DG NPCs, the requirement for TrkB in proliferation was cell-autonomous as evidenced by: (1) neurospheres generated from the DG of the $TrkB^{hGFAP}$ mice had impaired proliferation *in vitro*; (2) *In vivo*, the dividing cells in the DG of the $TrkB^{hGFAP}$ mice were more prone to prematurely exit the cell cycle; (3) Proliferation in the DG was unaffected in the $TrkB^{Syn}$ mice where Cre-mediated recombination occurs exclusively in differentiated neurons; (4) Temporal and spatial specific ablation of TrkB from young adult NPCs ($TrkB^{Nestin}$) also resulted in impaired proliferation and neurogenesis.

Neurotrophic factors, particularly BDNF, have been shown to promote proliferation of NPCs *in vitro* (Barnabe-Heider and Miller, 2003). Whether this effect resonates with a similar physiological requirement *in vivo* is less apparent. BDNF germline heterozygous mice have been reported to have decreased (Lee et al., 2000) or increased proliferation (Sairanen et al., 2005); as well as decreased (Sairanen et al., 2005) or normal long-term neurogenesis (Rossi et al., 2006). By directly ablating the BDNF receptor, TrkB, in NPCs, our data ascertain an unambiguous cell autonomous requirement for TrkB in maintaining proliferation and neurogenesis in the DG. It is worth noting that as TrkB is the high-affinity receptor for both BDNF and neurotrophin 4 (NT4), the phenotype observed in the $TrkB^{hGFAP}$ and $TrkB^{Nestin}$ mice could be a combinatory outcome of lacking signaling response to both ligands, although the expression level of NT4 in the postnatal brain is lower than BDNF. We have examined $BDNF^{hGFAP}$ conditional mutant mice and observed a similar degree of reduction in DG granular layer volume to that of the $TrkB^{hGFAP}$ mice. NT4 null mice are viable (Liebl et al., 2000) and appear to have normal DG volume (not shown).

The specific impairment of postnatal DG morphogenesis observed in the $TrkB^{hGFAP}$ mice appears to be a unique phenomenon. Although NPCs in the embryonic CNS express TrkB and have been shown to benefit from exogenous

BDNF *in vitro* (Barnabe-Heider and Miller, 2003), ablation of TrkB or BDNF *in vivo*, as demonstrated in TrkB and BDNF germline knockouts as well as the $TrkB^{hGFAP}$ mice, do not result in aberrant neurogenesis of the prenatal CNS. The $TrkB^{hGFAP}$ mice were born with, and continued to have normal brain size throughout adulthood. The reduction of the DG granular layer volume was absent at birth, and only became appreciable after P10. Absence of TrkB did not affect proliferation in the primary dentate neuroepithelium at E16.5, nor the migration and resettling of the secondary dentate matrix at P0 (not shown). These characteristics distinguish the $TrkB^{hGFAP}$ mice from other genetic mutants that exhibit abnormal adult neurogenesis, such as mice lacking NeuroD (Liu et al., 2000), FGFR1 (Ohkubo et al., 2004), NPAS3 (Pieper et al., 2005) or TLX (Shi et al., 2004), which have early and overall reduction of the hippocampus volume or brain size, indicating defects that may stem from abnormal embryogenesis. Therefore, we reveal here a regulatory mechanism that uncouples postnatal DG neurogenesis from embryonic development. Interestingly, while early ablation of TrkB ($TrkB^{hGFAP}$) dramatically reduced proliferation in adult DG, we also observed a more modest impairment in basal proliferation when TrkB was removed at the young adult age ($TrkB^{Nestin}$). This likely reflects the combined outcome of TrkB ablation in the early postnatal period on affecting individual cell division (by promoting cell cycle exiting), and diminishing the overall pool of progenitor cells available for proliferation. In contrast, late deletion of TrkB could

not significantly disturb the progenitor pool size and thus the phenotype in the $TrkB^{Nestin}$ mice likely represented the role of TrkB in regulating the behaviors of individual adult NPCs.

Our studies demonstrate that deletion of TrkB from DG NPCs ($TrkB^{hGFAP}$ and $TrkB^{Nestin}$) abolishes the proliferative and neurogenic effects of chronic AD treatments and voluntary exercise. This is consistent with earlier observations that both AD and running induce significant increases in BDNF level (Neeper et al., 1996; Nibuya et al., 1995). The inability of TrkB null NPCs to respond to AD and running was most likely due to the lack of sensitivity to BDNF, and not from developmental deficits that compromise cell division, as evidenced by their capacity to react to other exogenous factors, including EGF, bFGF and oxygen conditions *in vitro* (not shown). Conversely, when TrkB was ablated only from differentiated neurons ($TrkB^{Syn}$), both the proliferation and neurogenesis responses to chronic AD are maintained. It is intriguing that we observe a slightly more robust response to ADs in the $TrkB^{Syn}$ mice, suggesting that when surrounded by TrkB null neurons, NPCs and immature neurons with unaffected TrkB signaling may have a selective advantage in growth and/or survival.

2.4.2 TrkB and the behavioral efficacy of antidepressants

There has been considerable evidence that genetic ablation of BDNF or TrkB may interfere with the normal function of the adult brain, depending on the regions affected. Conditional knockout animals lacking TrkB in forebrain neurons (with broader recombination than $TrkB^{hGFAP}$ and $TrkB^{Syn}$) have impaired spatial learning behavior, but display normal anxiety level in the open field test (Minichiello et al., 1999). The latter is consistent with our observation that the $TrkB^{hGFAP}$ mice exhibit normal basal anxiety-like behavior in the NSFT (Figure 2.10), the open field test, and the dark-light preference test (Figure 2.11). Likewise, the $TrkB^{hGFAP}$ mice seem to have normal depression-like behavior at the basal level, as measured by the TST (Figure 2.10) and the forced-swim test (Figure 2.11). The $TrkB^{Nestin}$ mice only lack TrkB in a highly specific population of cells (adult NPCs), and are phenotypically indistinguishable from control mice at baseline. Previous studies with BDNF mutants regarding these anxiety and depression-like behaviors have yielded mixed results: some were normal (Adachi et al., 2008; Gorski et al., 2003; Monteggia et al., 2004; Saarelainen et al., 2003); while others were not (Chen et al., 2006; Monteggia et al., 2007; Rios et al., 2001). This discrepancy may be explained by the difference in the brain regions affected by the genetic ablation. BDNF is a secreted protein that can be transported and deposited across long distances both in retrograde and anterograde directions (Altar and DiStefano, 1998; DiStefano et al., 1992). Therefore local inactivation of the BDNF gene may well result in global

disturbance of BDNF protein level, thus confounding the interpretation of results. Recent discovery that BDNF in different regions of the brain may have opposing function in modulating stress response supports this notion (Berton et al., 2006).

Unlike control mice, the $TrkB^{hGFAP}$ (and $TrkB^{Nestin}$) mice were insensitive to chronic AD and exercise-induced improvement in depression and anxiety-like behaviors. This finding provides compelling evidence that TrkB is required for a shared molecular mechanism through which AD and exercise act. This process is likely to be BDNF-dependent, echoing previous studies showing elevated levels of BDNF with chronic AD (Miller et al., 2007; Nibuya et al., 1995) as well as blunted behavioral response to AD in BDNF mutant animals (Adachi et al., 2008; Chen et al., 2006; Monteggia et al., 2004; Saarelainen et al., 2003). Interestingly, $TrkB^{Syn}$ mice showed normal behavioral responses to chronic AD treatment, indicating neuronal expression of TrkB is not required for the behavioral efficacy of AD. Though the mechanism via which ADs (e.g. selective serotonin reuptake inhibitors and tricyclic antidepressants) elicit increase in hippocampal BDNF level remains undefined, this process only occurs after chronic exposure to ADs (Nibuya et al., 1995), implicating BDNF elevation and the subsequent TrkB activation as an indirect downstream event from the acute accumulation of monoamine, such as serotonin and noradrenaline. It has been suggested that chronic ADs promote the cAMP pathways and increase

CREB activity (Nibuya et al., 1996) – a transcription factor that activates the BDNF gene, among a multitude of other targets (Carlezon et al., 2005). While these observations provide important insight into the molecular underpinning of AD response, future work is needed to validate and further delineate the involvement of this pathway in regulating neurogenesis and mood (Conti et al., 2002; Gur et al., 2007; Nakagawa et al., 2002).

2.4.3 Functional link between neurogenesis and sensitivity to antidepressants

It has been debated whether neurogenesis in the adult hippocampus bears functional significance in the action of chronic AD, or the physiology of the hippocampus in general (Leuner et al., 2006; Scharfman and Hen, 2007; Zhao et al., 2008). In the current study, we selectively abolished the neurogenic sensitivity and a corresponding blockade of behavioral responses to chronic AD by ablating TrkB in adult NPCs ($TrkB^{Nestin}$), NPCs and neurons ($TrkB^{hGFAP}$), but not neurons alone ($TrkB^{Syn}$). While the hGFAP-Cre and the Syn-Cre studies cannot rule out the possibility that other differences in the recombination may contribute to the difference in behavioral responses between the $TrkB^{hGFAP}$ and $TrkB^{Syn}$ mice, the observation that specific deletion of TrkB in adult NPCs using the Nestin-CreER blocks the behavioral sensitivity to ADs provides a causal link between neurogenesis and AD response in the $TrkB^{Nestin}$ mice. Therefore we conclude that

TrkB-dependent increase in neurogenesis is required for the effects of chronic ADs in control and $TrkB^{Syn}$ mice in behavioral paradigms of NFST and TST. The hGFAP-Cre and Nestin-CreER transgenes elicit recombination in the neurogenic niches of SVZ as well as hippocampus. However, prior studies have excluded a possible link for SVZ neurogenesis and the behavioral effects of AD in rodents. Chronic AD administration does not affect proliferation in the SVZ and irradiation of the SVZ does not block behavioral responses to chronic ADs (Malberg et al., 2000; Santarelli et al., 2003). Thus our data provide genetic support and mechanistic insight to previous reports that irradiation-mediated ablation of dividing cells from the hippocampal region of rodents abolished their behavioral responses to ADs (Airan et al., 2007; Santarelli et al., 2003; Wang et al., 2008a). A recent study reports differential response to chronic AD in inbred strains of mice suggesting differing molecular and cellular mechanisms (Holick et al. 2008). Thus in contrast to the present findings and previous reports (Encinas et al., 2006; Miller et al., 2007; Santarelli et al., 2003; Wang et al., 2008a), chronic fluoxetine produces antidepressive behavioral effects in BALB/cJ mice by mechanisms independent of serotonin 1A receptor and DG neurogenesis. This marked strain difference highlights the existence of multiple mechanisms by which chronic AD changes anxiety and depression-like behaviors, and raises the intriguing possibility that genetic variations may be involved in determining the path of AD efficacy.

Our results also suggest that reduced levels of basal proliferation in the DG of $TrkB^{hGFAP}$ and $TrkB^{Nestin}$ mice do not directly lead to obvious affective impairment, an observation consistent with recent findings using irradiation-mediated NPC ablation method (Airan et al., 2007; Santarelli et al., 2003; Wang et al., 2008a). Rather, these animal studies suggest ADs and exercise-stimulated increase in DG neurogenesis may translate into enhanced synaptic plasticity in the pertinent neural circuits (Wang et al., 2008a), which subsequently manifests behavioral responsiveness to such treatments. One possible explanation for this dissociation between basal and induced neurogenesis may reside in functional differences between neurons generated at the constant state and stimulated state (Jakubs et al., 2006). The exact nature of these differences and the molecular mechanism that encodes them remain to be determined. Nonetheless, our data suggests that TrkB regulates DG NPCs in both states.

CHAPTER 3

ACTIVATION OF ADULT NEURAL PROGENITOR CELLS IS SUFFICIENT TO MODULATE DEPRESSION AND ANXIETY-LIKE BEHAVIORS

3.1 Summary

The production of new neurons in the rodent dentate gyrus (DG) occurs throughout adulthood but declines with age and stress. Neural progenitor cells (NPCs) residing in the sub-granular zone (SGZ) of the DG, regulated by an array of growth factors and receptors, can adjust their proliferation level to determine the rate of neurogenesis. Here we report that genetic ablation of NPCs in the adult brain led to insensitivity to chronic antidepressant (AD) induced behavioral effects, without affecting depression and anxiety-like behaviors on the basal state. Specific deletion of NF1, a tumor suppressor gene with RasGAP activity in adult NPCs reduced the decline of neurogenesis with age. This long-term activation of NPCs was accompanied by antidepressive-like behaviors. Furthermore, acute ablation of NF1 in adult NPCs enabled rapid proliferative and behavioral responses to sub-chronic AD, without altering neurogenesis and depression/anxiety-like behaviors on the basal level. Thus, our findings establish an important role for the Ras pathway in regulating adult NPCs, and demonstrate that activation of the adult NPCs is sufficient to modulate depression and anxiety-like behaviors.

3.2 Background

The production of new neurons in the dentate gyrus continues throughout adult life but declines drastically with age (Cameron and McKay, 1999). This decrease is further exacerbated by an array of innate and environmental influences, such as stress, social isolation and chronic inflammation (Czeh et al., 2001; Monje et al., 2003; Stranahan et al., 2006). Alternatively, activities that can be considered physiologically and psychologically "rewarding" such as learning, exercise and exploration of novel environment are associated with an increase in neurogenesis (Alvarez-Buylla, 1992; Kempermann et al., 1997). These phenomena invoke the fascinating possibility that augmenting DG neurogenesis may be directly beneficial for the maintenance and function of the CNS.

Our loss-of-function study on BDNF and TrkB has established a pivotal role for adult neurogenesis in mediating the behavioral effects of antidepressive treatments such as exercise and chronic AD. These findings reveal a critical dependence of adult NPCs on the availability of growth factors such as BDNF, and the cell-autonomous activation of growth factor receptors such as TrkB, in the context of chronic AD and exercise. These coincide with established standards to maintain the basal growth potential of adult NPCs *in vitro*, namely the usage of EGF and bFGF. Recent studies also suggest activations of the receptors for

platelet-derived growth factor (Jackson et al., 2006), insulin-like growth factor (Alcantara and Parada, unpublished results) and vascular endothelial growth factor (Warner-Schmidt and Duman, 2007) are important for maintaining the proliferation of adult NPCs. Together, these findings suggest a critical role for the activation of signaling cascades downstream from the growth factor receptors in regulating adult NPCs.

Molecular pathways such as MAPK, PI3K and PLCγ, are commonly stimulated by receptor tyrosine kinases (Huang and Reichardt, 2003), therefore are potentially involved in mediating growth factors-induced proliferation and neuronal differentiation in the adult neurogenic niches. The role of these pathways in the nervous system has been researched extensively in the context of neural development (Huang and Reichardt, 2001), as well as tumorigenesis (Zhu and Parada, 2002). Removal of inhibitors of these pathways bypasses the dependence on growth factors and results in constitutive activation (Le and Parada, 2007). Studies from this and others lab have utilized genetic manipulation of specific inhibitor genes to activate the respective signaling pathways, to achieve enhanced survival and growth capacity during embryonic development (Klesse and Parada, 1998; Vogel et al., 1995), adult spinal cord injury (Romero et al., 2007) and CNS/PNS tumor formation (Zhu et al., 2002; Zhu et al., 2005a).

The *Nf1* gene encodes a RasGAP protein that negatively regulates Ras, which lies downstream from receptor tyrosine kinases and upstream from Raf and PI3K (Klesse and Parada, 1998). In the present study, we specifically ablated *Nf1* in the adult NPCs to study the effects on their proliferation, self-renewal and production of new neurons. We demonstrated that while long-term ablation of N*f1* in the neurogenic niches of the adult brain did not result in signs of tumor formation, it promoted the proliferative potential of the dentate gyrus NPCs and subsequently enhanced neurogenesis. This increased basal neurogenesis was correlated with antidepressive-like behaviors. Furthermore, when N*f1* was acutely ablated from the adult NPCs, the animals displayed robust neurogenic and behavioral responses to sub-chronic administration of ADs. These findings demonstrated activation of tyrosine receptor kinase downstream pathways in NPCs promoted proliferation and neurogenesis, and was sufficient to modulate depression and anxiety-like behaviors.

3.3 Results

3.3.1 Genetic ablation of neurogenesis blocks chronic antidepressant induced behavioral changes

We have previously demonstrated that the tamoxifen-inducible form of Cre recombinase, $CreER^{T2}$, when expressed under the regulatory element of the *nestin* gene, enables temporally-controlled recombination specifically in the NPCs (Chen et al., 2008). By crossing the Nestin-CreER mice to the R26 reporter mice ($R26^{Nestin}$ mice), NPCs and their progeny that have undergone recombination could be labeled and lineage traced (Figure 2.13). To confirm these cells were capable of responding to chronic AD, we induced the $R26^{Nestin}$ mice with tamoxifen at the age of 2 months, and treated them with saline or imipramine (20ug/g) for 21 days starting from 2.5 months of age. X-gal staining revealed substantially more recombined cells in the SGZ of mice treated with imipramine, compared to saline controls (Figure 3.1A). This was consistent with prior observation that imipramine enhances the proliferation of amplifying NPCs (type 2 cells) in the SGZ, suggesting that the Nestin-CreER transgene could mediate recombination in these subset of NPCs.

To definitively evaluate the efficiency of Nestin-CreER transgene in targeting dentate gyrus NPCs that were required for the behavioral effects of chronic AD, we utilized a toxin-based cell-ablation approach that allowed selective and

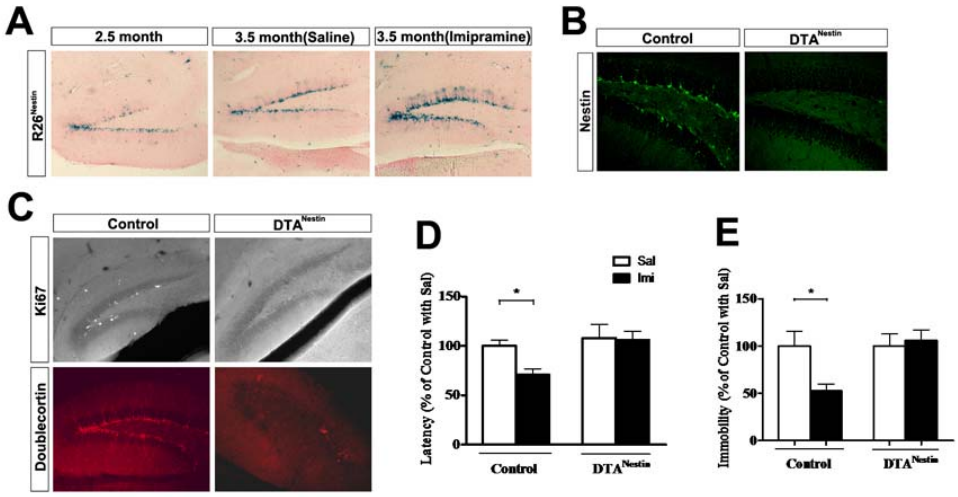

Figure 3.1. Genetic ablation of NPCs blocked chronic AD induced behavioral changes.
(A) X-gal staining on sagittal brain sections of the $R26^{Nestin}$ mice, induced with tamoxifen at 2 months and analyzed at 2.5 or 3.5 months of age. Imipramine treatment for 21 days increased the number and dendritic complexity of X-gal positive cells in the SGZ.
(B) Immuno-staining for Nestin in the DG of control and DTA^{Nestin} mice at 2.5 months (2 weeks after vehicle or tamoxifen exposure). Note the drastic reduction in the number of Nestin positive cells in the SGZ of the DTA^{Nestin} mice.
(C) Immuno-staining for Ki67 and Doublecortin in the DG of control and DTA^{Nestin} mice at 3.5 months (1.5 months after vehicle or tamoxifen exposure). Ablation of NPCs resulted in dramatically lower number of Ki67 and Doublecortin positive cells in the SGZ.
(D-E) DTA^{Nestin} mice did not display decrease in latency to feed (D, NSFT) or duration of immobility (E, TST) after chronic exposure to imipramine, compared to control mice. Data (mean +/- SEM) were shown as percentage of control treated with saline. *$p<0.05$.

near complete removal of NPCs from the adult brain. The Nestin-CreER mice were crossed with knockin mice carrying a conditional expression construct for diphtheria toxin subunit A (DTA) to generate the DTA^{Nestin} mice. The DTA flox allele allows cell ablation depending solely on the expression of Cre recombinase (Brockschnieder et al., 2006) Without tamoxifen induction, these mice were indistinguishable from

their littermate controls. When treated with tamoxifen at the age of 2 months and analyzed 2 weeks later, the DTA^{Nestin} mice had drastically fewer Nestin expressing cells in the SGZ (<5% compared to controls) and the SVZ (Figure 3.1B and not shown). This was echoed by a reduction in the number of proliferating cells (Ki67+), and immature neurons (Doublecortin+) at 3.5 month of age (Figure 3.1C). The morphology and number of the existing neurons and glia were unaffected by tamoxifen induction. These results demonstrate the capacity of the Nestin-CreER transgene to target the majority of NPCs in the SGZ and SVZ.

We have previously shown that deletion of *trkb* in adult NPCs with the Nestin-CreER transgene was sufficient to block the behavioral sensitivity to chronic AD, demonstrating a requirement of neurogenesis in chronic AD-induced behavioral changes. To test if complete ablation of adult NPCs altered depression and anxiety-like behaviors, we induced DTA^{Nestin} mice with vehicle or tamoxifen at 2 months of age, and treated them with saline or imipramine for 21 days. As expected, imipramine treated control mice showed significantly increased number of Ki67 and Doublecortin positive cells in the SGZ, compared to saline treated controls. Whereas tamoxifen induced DTA^{Nestin} mice treated with either saline or imipramine, showed near complete absence of these cells. When tested in the depression and anxiety-like behavioral paradigms (TST and NSFT respectively), imipramine

exposure produced no significant changes in the tamoxifen induced DTA^{Nestin} mice (Figure 3.1D and 3.1E). These results were consistent with findings in the $TrkB^{Nestin}$ mice, further confirming the requirement of neurogenesis for the behavioral effects of chronic AD. However, comparisons of saline treated control and DTA^{Nestin} mice yielded no significant difference in the TST and NSFT paradigms, indicating acute ablation of adult neurogenesis was not sufficient to perturb depression and anxiety-like behaviors (Figure 3.1D and 3.1E).

3.3.2 Temporally-regulated activation of neural progenitor cells via the deletion of NF1

Inactivating mutations in the *Nf1* gene cause neurofibromatosis type 1 (NF1), an autosomal dominant genetic disease that affects 1 in 3000 individuals. Aside from the various forms of benign and malignant tumors, NF1 patients exhibit high incidence of learning disabilities and mental retardation. In both tumor related and unrelated cases, affected individuals develop pathologies that involve neurons and glia, suggesting abnormalities in the stem/progenitor cells that give rise to progenies in these various lineages. Using the cre/loxp strategy, it has been shown that deletion of *Nf1* in embryonic NPCs (Dasgupta and Gutmann, 2005) and postnatal glia progenitors (Zhu et al., 2005b) led to hyper-proliferation. Concurrent deletion of *Nf1* and *P53* in NPCs was further demonstrated to be sufficient for brain tumor

formation (Zhu et al., 2005a). These findings strongly indicated a role for NF1-regulated signaling pathways in regulating the proliferation of NPCs.

To examine the function of NF1 in the adult DG neurogenesis, we utilized the Nestin-CreER transgene to specifically ablate the *Nf1* gene in the NPCs. $NF1^{flox/flox}$; Nestin-CreER mice at the age of 2 months were subjected to tamoxifen induction ($NF1^{Nestin}$ mice). Littermate $NF1^{flox/flox}$; Nestin-CreER mice treated with vehicle, and $NF1^{flox/flox}$ mice treated with tamoxifen were used as controls. These mice were analyzed at the age of 7 months for their status of DG neurogenesis by immuno-staining for Doublecortin. In 7-month-old control mice, the level of neurogenesis in the DG was dramatically lower compared to young adults. However, this decline in Doublecortin positive cells was significantly curtailed in the littermate $NF1^{Nestin}$ mice (Figure 3.2A). Therefore long-term deletion of *Nf1* from adult DG NPCs enhanced the capacity to continuously generate new neurons.

3.3.3 Ablation of NF1 in the NPCs modulates depression-like behaviors and responses to ADs

The increase in Doublecortin positive cells in the DG of $NF1^{Nestin}$ mice mimicked that observed with chronic AD treatments and exercise. To explore whether this increase in neurogenesis led to changes in depression and anxiety-like

behaviors, we subjected these 7-month-old mice (treated with vehicle or tamoxifen at 2 months) to the NSFT, TST and the FST. Compared to the control mice, the $NF1^{Nestin}$ mice showed decreased immobility in both the TST and the FST, indicating a lower basal depression level (Figure 3.2C and 3.2D). Interestingly, the $NF1^{Nestin}$ mice were comparable to the control mice in the NSFT, suggesting unchanged anxiety index (Figure 3.2B).

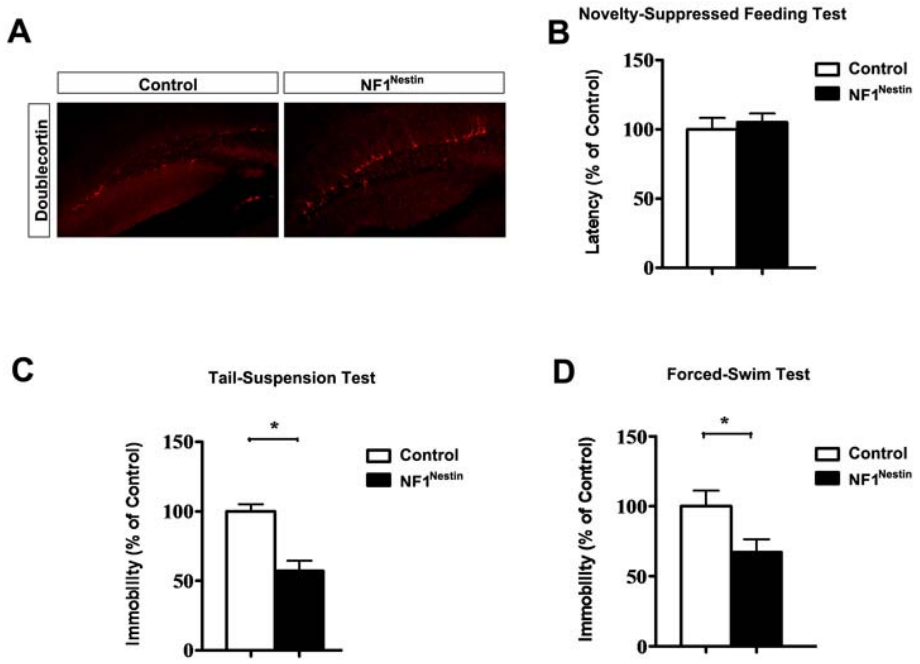

Figure 3.2. Specific ablation of NF1 from adult NPCs enhanced neurogenesis and led to antidepressive-like behaviors.

(A) Representative confocal images of immuno-staining for Doublecortin in the DG of 7 months old control and $NF1^{Nestin}$ mice (5 months after vehicle or tamoxifen treatment).

(B) $NF1^{Nestin}$ mice showed normal level of anxiety in the NSFT at 7 months. Latency to feed (mean + SEM) was shown as percentage of controls.

(C and D) $NF1^{Nestin}$ mice displayed decreased immobility in the TST (C) and the FST (D) at 7 months. Duration of immobility (mean + SEM) was shown as percentage of controls. *$p<0.05$.

The behavior changes seen in 7-month-old $NF1^{Nestin}$ mice were not observed when the ablation was more acute. Mice of the same genotype treated with tamoxifen at the age of 2 months were comparable to controls in the TST at 3 months (not shown). Therefore the antidepressive-like behaviors seen in older $NF1^{Nestin}$ mice might reflect the accumulative effects of enhanced NPC proliferation, generation of more new neurons, and the new synaptic connections formed by these cells. To further delineate the role of NF1 in undifferentiated NPCs, we examined the 3 months old control and $NF1^{Nestin}$ mice in their responses to sub-chronic administration of ADs. Mice were treated with saline, fluoxetine (18ug/g) or imipramine (20ug/g) for 7 days, analyzed in the NSFT and TST paradigms on day 8 and 9, and sacrificed on day 10. Mice were subjected to the TST on day 9 (48 hours after the last dose of fluoxetine or saline) to exclude the acute effects on behaviors that do not correlate with prior duration of drug treatment, or clinical responses. In the control group, mice treated with fluoxetine for 7 days performed similarly to the ones receiving saline injection, confirming previous reports that exposure to ADs for 1-14 days was insufficient to produce appreciable behavioral changes in rodents (Santarelli et al., 2003). The $NF1^{Nestin}$ mice, however, displayed significantly decreased latency to feed in the NSFT, and reduced immobility in the TST after fluoxetine injection for 7 days (Figure 3.3C and 3.3D). Since the $NF1^{Nestin}$ mice

were comparable to control mice on the basal level (saline treated group), these changes in behaviors likely represent more rapid responses to fluoxetine. These findings further coincided with immuno-staining results showing an increase in the number of Ki67 positive cells in the DG of $NF1^{Nestin}$ mice treated with fluoxetine for 7 days, whereas such increase in proliferation was completely absent in fluoxetine-treated control mice (Figure 3.3A and 3.3B).

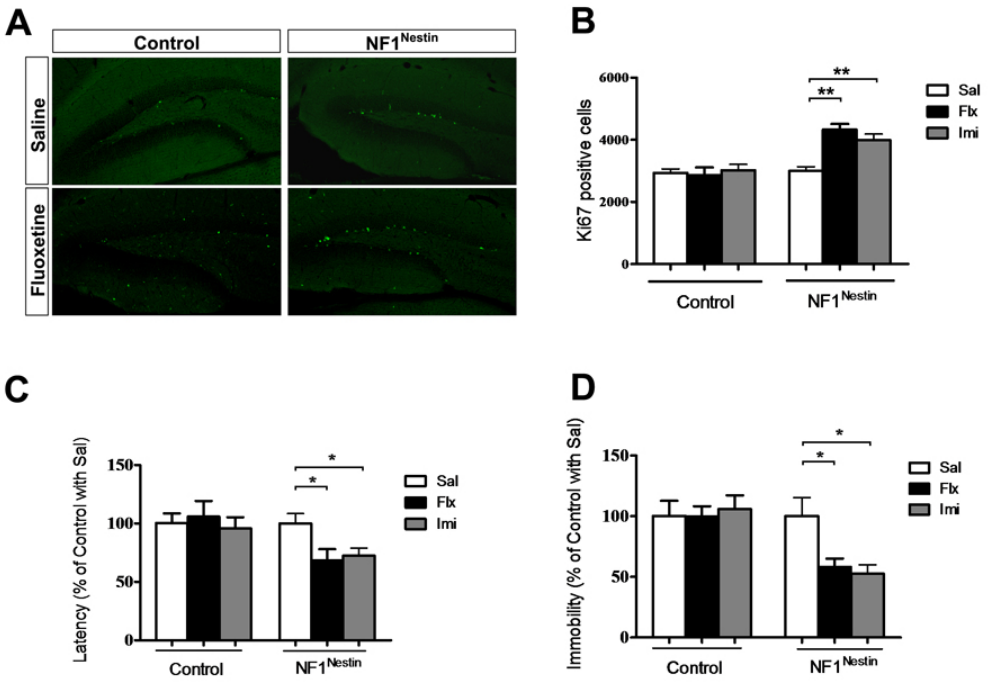

Figure 3.3. Acute ablation of NF1 from adult NPCs enabled rapid neurogenic and behavioral responses to sub-chronic AD treatments.

(A) Representative confocal images of immuno-staining for Ki67 in the DG of mice treated with saline or fluoxetine for 7 days. Control and $NF1^{Nestin}$ mice were exposed to vehicle or tamoxifen at 2 months of age, and treated with saline or fluoxetine at 3 months.

(B) Quantitative analysis of Ki67 positive cells demonstrated significant increases in the DG of $NF1^{Nestin}$ mice after 7-day fluoxetine or imipramine treatment. Flx, fluoxetine; Imi, imipramine. $^{**}p<0.01$.

(C-D) $NF1^{Nestin}$ mice displayed decrease in latency to feed (C, NSFT) and duration of immobility (D, TST) after 7-day AD treatments. $^{*}p<0.05$.

3.4 Discussions

3.4.1 Acute ablation of neurogenesis blocks AD sensitivity but not basal depression and anxiety-like behaviors

One intriguing observation arising from our studies on the $TrkB^{hGFAP}$ and $TrkB^{Nestin}$ mice is that inhibition of basal neurogenesis seems to be insufficient to produce an effect on the depression and anxiety-like behaviors. It indicates that basal neurogenesis does not contribute to the modulation of mood. This however contradicts human and animal studies reporting hippocampal volume reduction in depressed or chronically stressed subjects (Bremner et al., 2000; Coe et al., 2003; Czeh et al., 2001; MacQueen et al., 2003). Therefore it is possible that although ablation of TrkB in postnatal and adult NPCs ($TrkB^{hGFAP}$ and $TrkB^{Nestin}$, respectively) decreases the level of basal neurogenesis, the availability of other trophic factors such as bFGF, EGF and insulin-like growth factor is sufficient to maintain apparently normal hippocampal proliferation and neurogenesis. The observed partial loss of neurogenesis (in the $TrkB^{hGFAP}$ and $TrkB^{Nestin}$ mice) must remain above the critical threshold to maintain neuronal circuitry conductivity of the limbic system, thus no significant behavioral changes in the aforementioned depression and anxiety-like paradigms were observed. In the current study, we

examined this possibility by genetically ablating the majority of NPCs from the adult brain. Upon tamoxifen stimulation, the DTA^{Nestin} mice lose >95% Nestin positive cells from the DG SGZ. These mice were treated with AD for 21 days yet showed no behavioral changes in depression and anxiety-like paradigms. However, on the basal level, these mice performed similarly to their control littermates with intact neurogenic capacity. Therefore we conclude acute ablation of NPCs from the adult brain is not sufficient to perturb mood status in rodents.

3.4.2 Clinical implications of enhancing neurogenesis

Our finding that activation of the Ras pathway in adult NPCs directly contributes to changes in depression and anxiety-like behaviors suggests the intriguing possibility that reagents targeting these particular pathways and cell types could be used to modulating mood status. This could potentially open up a domain of options for the discovery of better treatments for depression/anxiety related mood disorders. Currently most ADs require chronic administration for weeks to months before clinically appreciable effects are achieved. Results from the $NF1^{Nestin}$ mice suggest pro-neurogenic reagents, when engineered to selectively activate DG NPCs, could not only serve as a putative AD, but also elicit more rapid behavioral improvements.

CHAPTER 4

THE ROLE OF BDNF AND TRKB IN REGULATING STRIATAL MEDIUM SPINY NEURON DEVELOPMENT AND DEGENERATION

4.1 Summary

Huntington's Disease (HD) is a neurodegenerative disorder caused by mutation in the *huntingtin* gene. Reduced BDNF protein level in the cortex and the striatum caused by such mutation has been implicated in the pathogenesis of the HD. Here we report that ablation of *bdnf* from the cortex and the substantia nigra led to depletion of BDNF in the striatum. Mice lacking BDNF-TrkB signaling in the corticostriatal and nigrostriatal circuits displayed severe motor deficits and striatal degeneration reminiscent of the HD. In contrast, specific ablation of TrkB from the striatal medium spiny neurons (MSNs) resulted in late-onset neuronal loss and spine degeneration, without causing obvious movement abnormalities. Thus, our results establish an essential cell-autonomous role for BDNF-TrkB signaling in regulating the normal maturation and maintenance of MSNs. Furthermore, our findings suggest disruption of BDNF-TrkB signaling in regions outside of the striatum may contribute to the behavioral aspects of the HD pathology.

4.2 Background

The striatum is a subcortical part of the telencephalon, and a major input component of the basal ganglia system. Composed mainly of dopaminoceptive medium spiny neurons (MSNs), the striatum plays a crucial role in regulating voluntary movements, as well as reward-associated learning and memory. The striatum can be further separated into the dorsal and ventral parts based on known anatomical and functional distinctions. In primates the dorsal striatum are composed of two observable subdivisions: caudate nucleus and putamen, however functionally the dorsal striatum form a single entity enclosed with a toric topology. This apparent homology of the dorsal striatum is also reflected by the observation that the rodent caudate and putamen are continuous and not structurally separated. The ventral striatum, including the olfactory tubercle and the nucleus accumbens, comprises distinct input and output stations and mainly regulates neurological functions associated with motivation, reward and emotion.

Similar to the other telencephalic regions, the striatum contains interneuronal populations that are generated from the medial ganglionic eminence. However, majority of the neurons are GABAergic MSNs that project outside of the striatum to neighboring structures such as the globus pallidus and the substantia nigra. The mechanism that regulates the generation of the MSNs involves combinatorial

codes of transcription factors, and seems to parallel development of other neural structures; however the molecular underpinning for the maturation and maintenance of these neurons remains largely unknown.

Abnormalities of the striatum lead to neurological and psychological disorders of the CNS, most notably the Huntington's disease (HD), where MSNs in the dorsal striatum undergo progressive degeneration. The sequential degeneration of MSNs involved in the indirect (inhibits movement) and direct (excites movement) pathways is responsible for the clinical representations of chorea (involuntary movement) at early stage and loss of mobility at late stage. These physical symptoms are often accompanied by psychiatric and cognitive deficits in mood regulation, attention, visuospatial recognition and short/long-term memory (Walker, 2007). Although the etiology of HD remains elusive on the molecular level, the genetic base of the disease is well understood. It has been shown that expansion of the polyglutamine repeat (CAG repeat) within the first exon of the *huntingtin* gene causes HD in a dominant fashion, with length of the repeat usually predicting the onset and the severity of the disease symptoms (1993). Mouse models of the HD engineered to carry mutant *huntingtin* gene with high copies of the polyglutamine repeat have been demonstrated to recapitulate the hallmarks of the disease (Mangiarini et al., 1996; Walker, 2007). Despite of these advances, our knowledge

of the molecular mechanisms that govern the initiation and progression of the disease remains limited. Therefore 15 years after the identification of the genetic cause of the disease, HD remains one of the most accurately predictable yet lethal diseases.

Due to the gradual degenerative nature of the disease progression, much effort has been devoted into the research on trophic factors that can potentially delay or reverse the cell-loss process. One of these factors is BDNF. MSNs don't express detectable level of BDNF mRNA, but rather receive exogenous BDNF protein transported anterogradely from areas such as the cortex, substantia nigra pas compacta and ventral tegmental area (VTA) (Altar et al., 1997). This process has been proven important for the development and functioning of the striatum (Baquet et al., 2004). In mouse models of HD, decrease in striatal BDNF level has been observed and has been implicated as an pathogenic factor, as further genetic reduction of BDNF accelerates disease progression (Pineda et al., 2005; Spires et al., 2004). Genetic ablation of BDNF from the cortex leads to dendrite deficits and neuronal loss in the striatum (Baquet et al., 2004).

In the present study, we conditionally ablated the gene encoding BDNF or TrkB in the corticostriatal and nigrostriatal neuronal circuits. We showed that deletion of *bdnf* from the cortex and substantia nigra led to depletion of BDNF in the

striatum. These mutant mice displayed dramatic neurological abnormalities and harbor cellular and molecular deficits in the striatum that were similar to HD. These HD related cellular phenotypes could be further recapitulated by deletion of the *trkB* gene in the MSNs, strongly suggesting that the BDNF-TrkB signaling plays a critical cell-autonomous role in the maturation and maintenance of the MSNs.

4.3 Results

4.3.1 BF1-Cre mediated depletion of BDNF in the striatum

Our laboratory has previously generated mutant mice with flox alleles of *Bdnf* (He et al., 2004; Monteggia et al., 2007). To acquire conditional knockout animals that lack BDNF in the striatum, the *Bdnf* flox mice were crossed to mice expressing cre recombinase under the endogenous *Bf1* promoter (Hebert and McConnell, 2000) ($BDNF^{BF1}$ mice). The *Bf1* gene encodes a transcription factor that has been shown to be expressed in the developing telencephalon, and regulates its structural formation (Xuan et al., 1995). The expression pattern of the BF1-Cre has been demonstrated to faithfully recapitulate the endogenous *Bf1* gene (Hebert and McConnell, 2000). By interbreeding the BF1-Cre with the R26 reporter mice, robust recombination could be observed in the developing striatum, resulting in almost complete ablations of the target gene in the adult striatum (caudate putamen and nucleus accumbens) (Figure 4.1A and 4.1B). Moreover, the broad range expression of the BF1-Cre enabled ablation of BDNF from the cortex and the substantia nigra (Figure 4.1A and 4.1C), the two main source of BDNF for the dorsal striatal MSNs. Since the cell-types that produce and transport BDNF in these brain regions are mostly neuronal, we further confirmed the occurrence of recombination in these cells by double immuno-staining for β-gal and NeuN in the cortex (Figure 4.1B), as well as β-gal and Tyrosine Hydroxylase (TH, dopaminergic marker) in the

substantia nigra (Figure 4.1C).

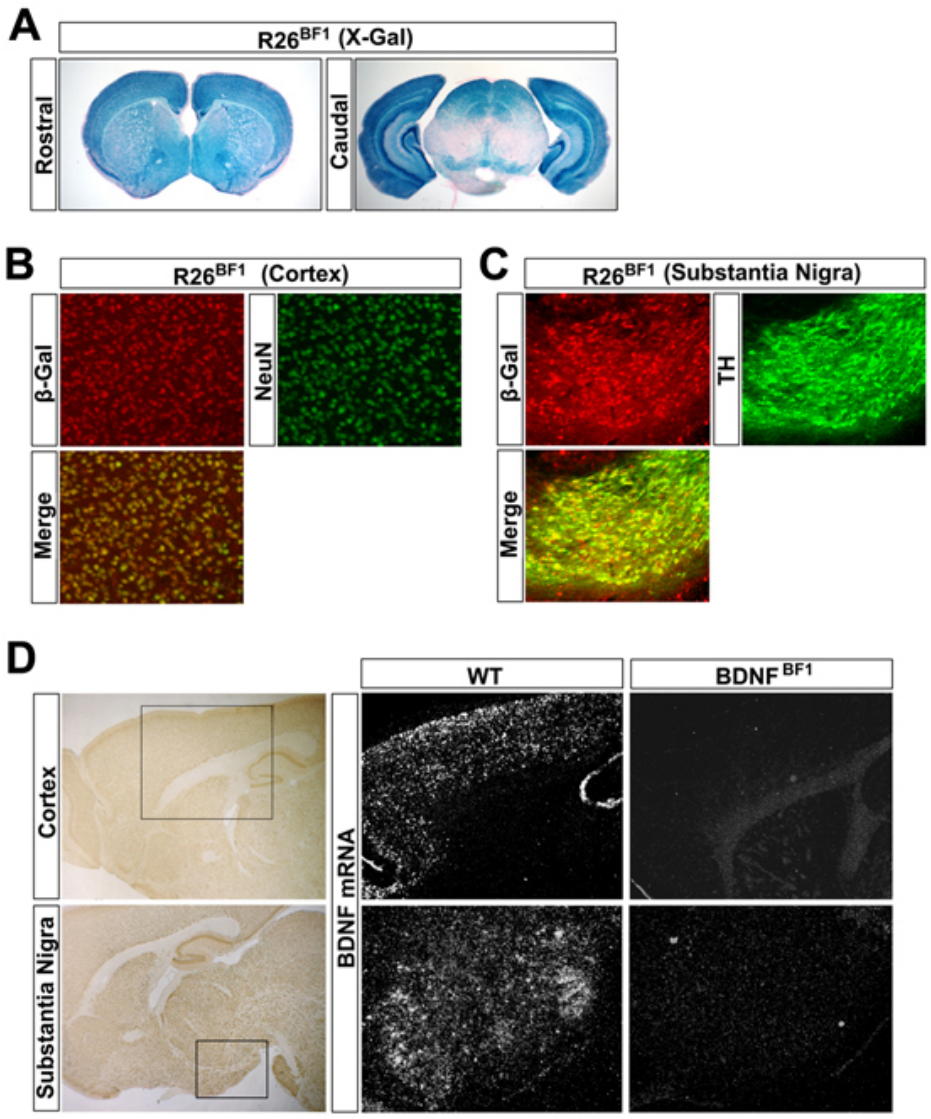

Figure 4.1. BF1-Cre mediated depletion of BDNF in the striatum

(A) X-gal staining on coronal sections of R26R^{BF1} and R26^{Syn} mice at P60.

(B-C) Co-staining for β-gal (red) and NeuN (B, green) or TH (C, green) on sections from adult R26^{BF1} mice. Note the co-localization of β-gal and these neuronal markers.

(D) *In situ* hybridization analysis of BDNF mRNA in the adult control and BDNF^{BF1} mice. Left panels depict the regions shown in the middle and right panels. Note the drastic reduction in BDNF mRNA level in the cortex, hippocampus, striatum and substantia nigra of the BDNF^{BF1} mice.

Finally, the effectiveness of this depletion approach was confirmed by *in situ* hybridization for BDNF mRNA in these two regions (Figure 4.1D), as well as ELISA assay that demonstrated 95% reduction of BDNF protein in the dorsal striatum.

4.3.2 Ablation of BDNF leads to motor dysfunction and deficits in MSN maturation

In contrast to BDNF germline knockout mice that are neonatal lethal, the $BDNF^{BF1}$ mice were viable at birth. However they were smaller and weaker as compared to littermate controls and were incapable of surviving past postnatal 8 weeks. In addition, the $BDNF^{BF1}$ mice displayed early-onset abnormal behaviors including hind-limb clasping, hyperactivity and circling, phenotypes indicative of neurological dysfunctions. Hind-limb clasping and mild hyperactive behaviors have been observed in other forebrain specific BDNF conditional knockout animals ($BDNF^{hGFAP}$ and $BDNF^{CaMKII}$ mice, data not shown), however the extreme hyperactivity and circling behaviors observed in the $BDNF^{BF1}$ mice were unique and thereby implyed the potential dysfunctioning of different neural circuits.

The overall development of the striatum in the $BDNF^{BF1}$ mice was normal, as evaluated by Nissl staining and immunostaining for NeuN (Figure 4.2A and not

shown). Quantitative volume analyses revealed significant volume reduction in multiple regions of the brain at postnatal ages, including the cortex, hippocampus and the striatum ($p<0.05$ for all comparisons), consistent with the observation that the brain and body weights of the $BDNF^{BF1}$ mice were reduced compared to their littermate controls. The degree of hippocampal volume reduction in the $BDNF^{BF1}$ mice was comparable to that observed in the $BDNF^{hGFAP}$ mice (Figure 2.5), therefore is most likely a direct result of the disruption of BDNF-TrkB signaling in DG NPCs. However, the significant reduction of the striatal volume (22.32 +/- 0.74 mm^3 in controls, 18.05 +/- 0.66 mm^3 in $BDNF^{BF1}$, n=3 for each, $p<0.05$) seen in the $BDNF^{BF1}$ mice was not observed in the other BDNF forebrain knockout mice ($BDNF^{hGFAP}$, $BDNF^{CaMKII}$ mice). This could be explained by the efficiency of BDNF depletion from the striatum in these different mutant mice. Indeed, we have previously reported that the hGFAP-Cre and the CaMKII-Cre elicit recombination in subsets of cortical neurons, but are mostly absent from the striatum, substantia nigra and the VTA, therefore only causing partial depletion of BDNF from the striatum (Luikart et al., 2005; Monteggia et al., 2007). To assess if the reduction of striatal volume was directly contributed by increase in cell death, we performed TUNEL staining and cleaved caspase-3 immuno-staining on p20 $BDNF^{BF1}$ mice. No increase in apoptosis was detected suggesting that lack of BDNF did not perturb the survival of striatal neurons (not shown).

It is known that MSNs are generated embryonically, but establish their morphology and synaptic connections during the early postnatal period. To exam whether lack of BDNF in the MSNs perturb their normal maturation and functionality, we examined the expression level and distribution of DARPP32 (dopamine- and cyclic AMP- regulated phosphoprotein, 32kDa), a major target of dopamine-activated adenylyl cyclase and the key mediator of dopamine signaling (Greengard et al., 1999). In control mice, the level of DARPP32 in the striatum increases significantly during the first three postnatal weeks and remains high throughout adulthood (Figure 4.3). In a subset of $BDNF^{BF1}$ mice at one month of age, we observed a dramatic reduction of DARPP32 intensity, suggesting abnormalities in dopamine signaling (Figure 4.2A). The degree of reduction varied in the individual $BDNF^{BF1}$ mice, however majority of them displayed visibly lower level of DARPP32 by immuno-staining. The definitive cause of this variation was unclear, but it could be related to differences in genetic composition.

Loss of DARPP32 expression has been associated with degeneration of MSNs and has been observed the striatum of HD mice (Bibb et al., 2000). To assess if the reduction of DARPP32 in the $BDNF^{BF1}$ mice was accompanied by other

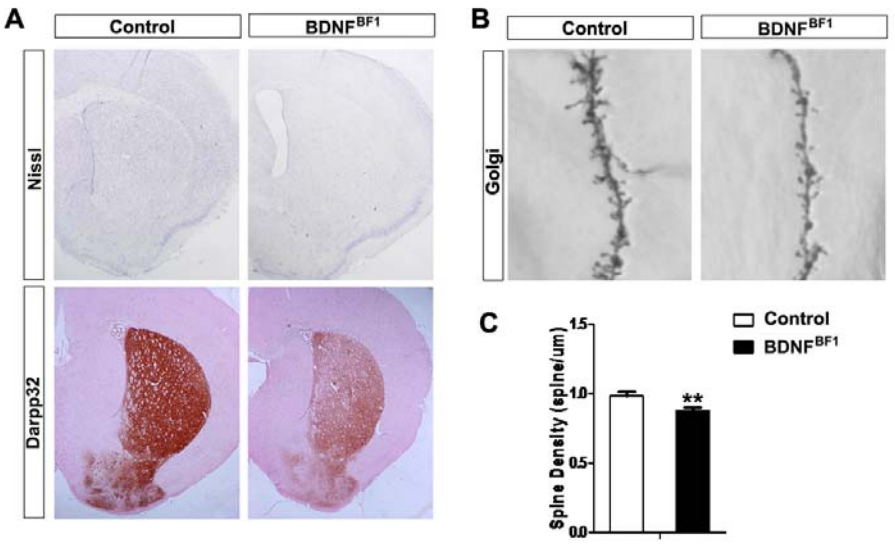

Figure 4.2. Depletion of BDNF in the striatum led to deficits in MSN maturation
(A) Nissl staining and DARPP32 immuno-staining on coronal sections of control and $BDNF^{BF1}$ mice. Note the reduction in DARPP32 level in the $BDNF^{BF1}$ mice.
(B-C) Golgi staining revealed a significant reduction in the spine density of MSNs from the $BDNF^{BF1}$ mice. **p<0.01.

degenerative traits, we examined the dendritic spines on the MSNs. Dendritic spines are the sites of synaptic contacts, their number and morphology are crucial criteria for cellular maturation. To examine whether lack of BDNF-TrkB altered spine formation on the striatal MSNs, spine density of secondary dendrites was measured on Golgi-stained brain sections. Quantitative analyses revealed a significant 10% reduction in spine density by the age of p20 (Figure 4.2B and 4.2C). Comparative study using a different BDNF conditional knockout ($BDNF^{hGFAP}$ mice) in which BDNF was only ablated in the cortex revealed no difference in MSN spine density (not shown). This coincided with earlier observation that hGFAP-Cre-

mediated ablation of *bdnf* from the cortex was not sufficient to completely deplete BDNF protein from the striatum, indicating a dosage requirement for BDNF in regulating MSNs spine formation.

4.3.3 Ablation of TrkB disturbs motor function and MSN maturation

TrkB, the high affinity receptor for BDNF, is highly expressed in the striatum (Figure 4.4A). However, the low affinity pan-TrkB receptor p75 has also been shown to be expressed in the basal ganglion cells during development (Batchelor et al., 1989). To ascertain the requirement of TrkB in mediating the effect of BDNF during striatal development, we examined germline TrkB knockout ($TrkB^{-/-}$ mice), as well as TrkB conditional knockout mice using the BF1-Cre ($TrkB^{BF1}$ mice).

We have previously reported that majority of the $TrkB^{-/-}$ mice die at birth (Luikart et al., 2003), however a small percent of them survive to the first postnatal week. These mice were growth retarded compared to littermate controls and had severe motor deficits. Upon examining the striatum of these mice at the age of P4 and P8, we observed a dramatic reduction in DARPP32 level (Figure 4.3A and 4.3B), strongly suggesting that complete ablation of BDNF-TrkB signaling impaired the

maturation of MSNs.

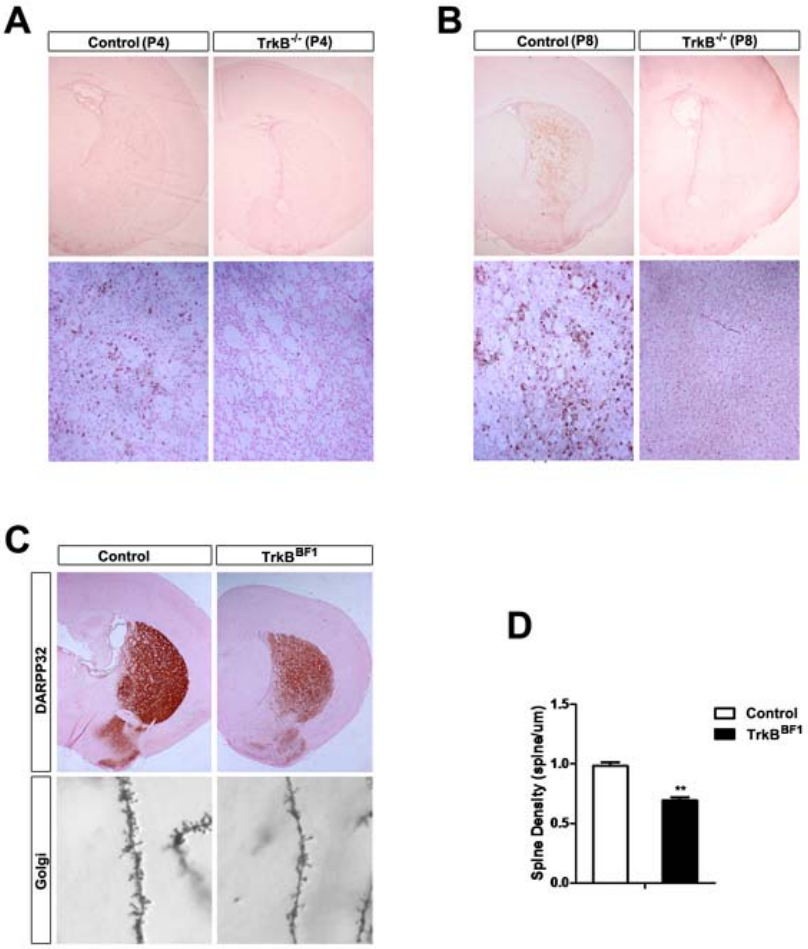

Figure 4.3. Ablation of TrkB in the striatum impaired MSN maturation

(A-B) DARPP32 immuno-staining on coronal sections of control and $TrkB^{-/-}$ mice at the age of P4 (A) and P8 (B). Lower panels are high-magnification view of the upper panels. Note the drastic reduction in DARPP32 level in the striatum of $TrkB^{-/-}$ mice.

(C-D) DARPP32 immuno-staining (C) and Golgi staining (C-D) revealed deficits in the MSNs from the $TrkB^{BF1}$ mice. **$p<0.01$.

To circumvent the neonatal lethality of the $TrkB^{-/-}$ mice, we generated TrkB conditional mice using the BF1-Cre ($TrkB^{BF1}$ mice). The BF1-Cre elicits robust and wide recombination in the nervous system and some non-neuronal tissues. As results of such wide-range of gene ablation, the $TrkB^{BF1}$ mice displayed an array of cellular and behavioral abnormalities that has been seen in other TrkB conditional mutant mice ($TrkB^{Syn}$, $TrkB^{hGFAP}$ mice) such as reduction in body weight, hind-limb clasping, hyperactivity and decrease in DG size. Strikingly, the $TrkB^{BF1}$ mice displayed circling behavior that has only been observed in the $BDNF^{BF1}$ mice, but no other TrkB mutants. Large percentage of the $TrkB^{BF1}$ mice was also ataxic. These observations provided ligand-receptor coincidence, strongly suggesting a role for BDNF-TrkB signaling in regulating motor functioning. The contrast of the $TrkB^{BF1}$ mice to the other TrkB mutant mice indicated abnormalities in neural circuits that were not impaired in the $TrkB^{Syn}$ or $TrkB^{hGFAP}$ mice.

Histological analyses of $TrkB^{BF1}$ mice revealed further similarities to the $BDNF^{BF1}$ mice, and often to a more severe extent. The $TrkB^{BF1}$ mice had reduced body and brain weights compared to littermate controls, and usually did not survive pass postnatal 1 month. They displayed circling behaviors during the first three postnatal weeks, and became hypoactive progressively. A similar degree of

reduction in DARPP32 immuno-staining was observed in the striatum of these mice at the age of P20 (Figure 4.3C). Golgi staining revealed a significant 27% reduction in the density of spines on secondary dendrites (Figure 4.3C and 4.3D). These results confirmed a critical role of TrkB in regulating the maturation of MSNs.

4.3.4 TrkB exerts a cell-autonomous role in regulating MSN maturation and maintenance

MSNs in the caudate-putamen and the nucleus accumbens receive glutamatergic inputs from the cortex and dopaminergic inputs from the substantia nigra and the VTA. Synaptic activities and trophic supports from these regions facilitate the maturation of the striatal MSNs. Given the known roles of BDNF-TrkB signaling in molding the development of some of these structures, it is possible that developmental deficits in regions outside of the striatum could contribute to the severe behavioral abnormalities observed in the $TrkB^{-/-}$ and $TrkB^{BF1}$ mice. Additionally, BDNF-TrkB plays important roles in the development and function of glia cells, therefore alterations in the neuronal conductivities secondary to changes in oligodendrocytes and astrocytes may exist in the $TrkB^{-/-}$ and $TrkB^{BF1}$ mice.

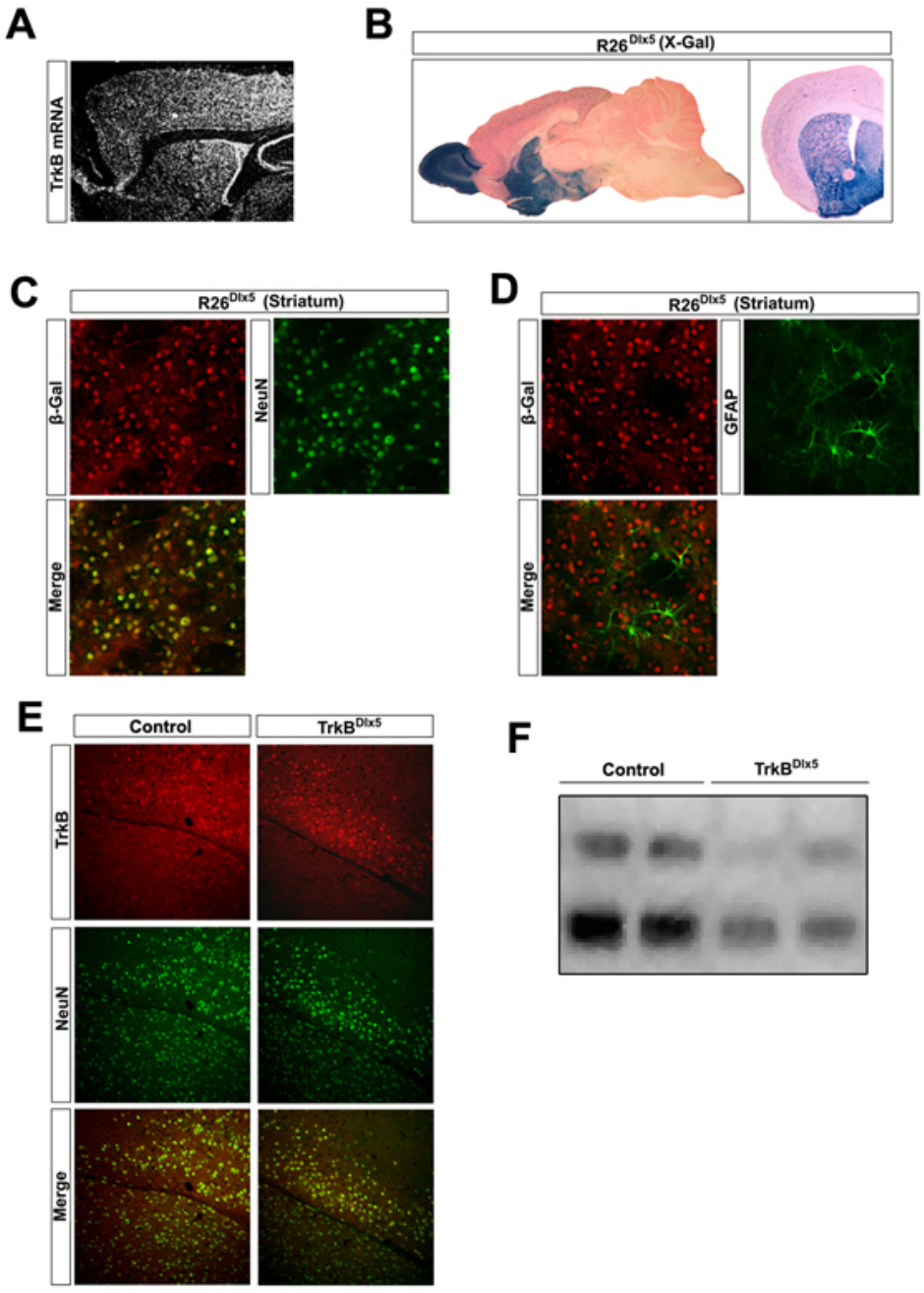

Figure 4.4. Dlx5-Cre mediated ablation of TrkB from the striatal MSNs.

(A) *In situ* hybridization analysis of TrkB mRNA distribution in the adult forebrain. TrkB is highly expressed in both the cortex and the striatum.

(B) X-gal staining on sagittal and coronal brain sections of $R26^{Dlx5}$ mice. Recombination was observed in the striatum, olfactory bulb and the cortex.

(C-D) Co-staining for β-gal (red) and NeuN (C, green) or GFAP (D, green) on the striatum of $R26^{Dlx5}$ mice. Note the co-localization of β-gal with neurons (NeuN+) but not astrocytes

(GFAP+).
(E) Co-staining for TrkB (red) and NeuN (green) on sections from adult control and $TrkB^{Dlx5}$ mice. Note the presence of TrkB protein in cortical, but not striatal neurons.
(F) Western blots of lysates from the striatum of control and $TrkB^{Dlx5}$ mice, probed for full-length and truncated TrkB.

To examine if BDNF-TrkB signaling was required cell-autonomously in the MSNs, we generated TrkB conditional knockout mice using the Dlx5-Cre transgenic line. The *dlx5* gene encodes a Distalless-related (DLX) homeobox protein that exists in neural lineage progenitors originates from the lateral and medial ganglionic eminence (Porteus et al., 1991). The recombination pattern of the Dlx5-Cre closely resembles the expression of the endogenous gene (Stenman et al., 2003). When crossed to the R26 reporter mice and examined at 2 months of age, robust β-gal activity was detected in the striatum and the olfactory bulb (Figure 4.4B). Limited recombination activity was also observed in the inhibitory neurons of the cortex. In the striatum, β-gal expressing cells expressed neuronal marker NeuN, but not astrocytic marker GFAP (Figure 4.4C and 4.4D). Dlx5-Cre mediated ablation of TrkB from striatal neurons was further confirmed by immuno-staining for TrkB protein (Figure 4.4E). NeuN positive neurons in the striatum lacked TrkB, while its expression in NeuN positive cortical neurons was mostly intact. Immuno-blotting revealed a more than 80% reduction in the levels of both full-length and truncated TrkB in the striatum (Figure 4.4F), the remaining TrkB protein was likely contributed

by glia cells that were not recombined by the Dlx5-Cre.

The $TrkB^{Dlx5}$ mice, intriguingly, did not display much obvious motor abnormalities. In contrast to $TrkB^{BF1}$ mice which only survived to postnatal 1 month, the $TrkB^{Dlx5}$ mice had normal life span, as well as body and brain weights comparable to their littermate controls. These results were unexpected, but also raised the intriguing possibility that the motor phenotypes observed in the $TrkB^{BF1}$ and $BDNF^{BF1}$ mice were not direct results of lacking BDNF-TrkB signaling in the striatum. Thereby the normal survival of the $TrkB^{Dlx5}$ mice provided us the opportunity to examine the consequence of MSN-specific ablation of TrkB in the context of long-term maintenance.

When examined at an advanced age (15 months), the $TrkB^{Dlx5}$ mice had normal cortical thickness and DG granular layer volume, indicating the absence of overt degeneration in the CNS. The number and morphology of TH positive dopaminergic neurons in the substantia nigra were also comparable to those seen in the littermate control mice (Figure 4.5A). However, Nissl staining revealed significant reduction in the volume of the striatum. Decrease in the intensity of DARPP32 immuno-staining was also observed (Figure 4.5B). Quantitative analyses

of Golgi-stained MSNs revealed a decrease in the density of spines to a degree comparable to that in the $TrkB^{BF1}$ mice. These results echoed findings in the $TrkB^{BF1}$ and $BDNF^{BF1}$ mice, strongly suggest TrkB was required cell-autonomously for the maintenance of MSNs.

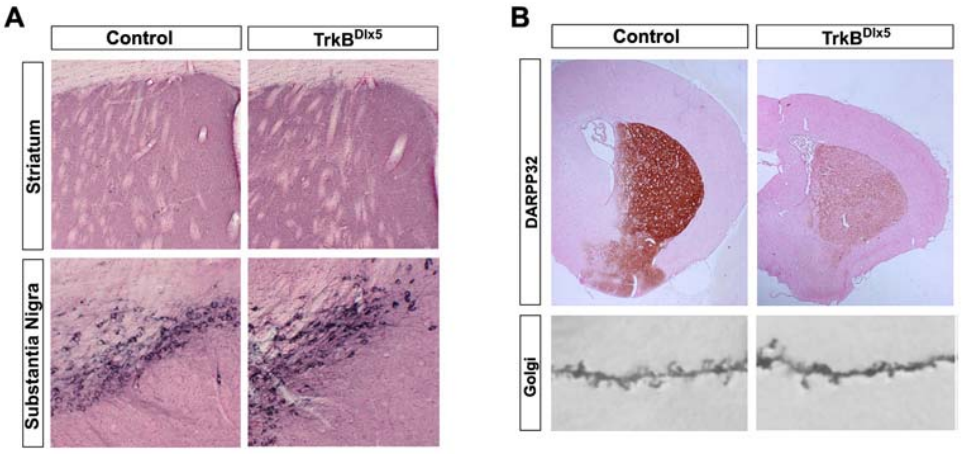

Figure 4.5. TrkB exerted a cell-autonomous role in MSN maintenance.
(A) TH immuno-staining on coronal sections of control and $TrkB^{Dlx5}$ mice. Note the normal number and morphology of TH positive dopaminergic neurons in the substantia nigra, as well as their innervations to the striatum in the $TrkB^{Dlx5}$ mice.
(B) DARPP32 immuno-staining and Golgi staining revealed deficits in the MSNs in the aged $TrkB^{Dlx5}$ mice.

4.4 Discussions

4.4.1 Anterograde transport of BDNF in the CNS

The basic tenet of the neurotrophic hypothesis is that limited production of neurotrophins in specific target tissues determines the survival of responsive neurons

that project to these regions. Axon terminals compete for the available neurotrophic molecules, which bind to their respective receptors and are retrogradely transported to neuronal cell bodies where they provide signals for survival and differentiation. It is now well established that neurotrophins, such as NGF, BDNF and NT3, can also be anterogradely transported by central and peripheral neurons (Altar and DiStefano, 1998; Ng et al., 2007). The neurotrophins supplied by afferents are released pre-synaptically and serve as trophic factors as well as neurotransmitters. This anterograde transport of neurotrophin is best depicted in the corticostriatal and nigrostriatal circuits, where BDNF protein produced in the cortex and the substantia nigra are transported into the striatum by projection neurons in these two regions (Zuccato et al., 2001). BDNF can be released from the glutamatergic terminals of the cortical neurons and the dopaminergic terminals of the nigral neurons in both activity-dependent and independent manner (Altar and DiStefano, 1998; Kohara et al., 2001). Therefore despite the apparent lack of BDNF mRNA, the striatum contains BDNF protein at level not far below that measured in the BDNF-rich hippocampus.

In the present study, we demonstrated that ablation of *bdnf* in the cortex and the substantia nigra led to near complete depletion of BDNF protein in the striatum. As results, the $BDNF^{BF1}$ mice displayed a multitude of neurological abnormalities and succumbed to early postnatal lethality. The apparent motor

deficits in these mice, such as hind-limb clasping and circling, have been observed in other mouse models of neurodegenerative disorders, but could not be definitively attributed to dysfunctioning of any particular neural circuitry. The circling behavior, for example, could be caused by abnormalities in the corticostriatal, nigrostriatal, vestibular system, or a combination of the above. Similarly, the hyperactivity and elevated anxiety-like behavior observed in these mice could be caused by deficits in multiple brain regions. The dramatic loss of BDNF protein in the striatum of the $BDNF^{BF1}$ mice also highlights the dynamic synthesis and distribution of BDNF in the brain, therefore local changes in BDNF level through methods such as region-specific gene ablation, over-expression and infusion, may well result in global disturbance of BDNF protein level. To further delineate the role of BDNF in the striatum, we used the Dlx5-Cre to delete TrkB in a region-specific manner. This approach confirmed the requirement of BDNF in maintaining spine density in the MSNs. Interestingly, mice lacking TrkB in the striatal neurons did not develop the severe motor deficits as observed in the $BDNF^{BF1}$ mice, suggesting disruption of BDNF-TrkB signaling in regions outside of the striatum is responsible for these phenotypes. Indeed, when TrkB was widely ablated in the nervous system with the BF1-Cre ($TrkB^{BF1}$ mice), these behavioral abnormalities were observed.

4.4.2 Clinical implications in HD

Reduction in BDNF protein level has been reported in human patients with HD and mouse models of HD (Zuccato and Cattaneo, 2007). This is likely caused by the loss of wild-type Huntingtin functions in regulating the transcription of BDNF mRNA and the anterograde transport of BDNF protein through the corticostriatal afferents (Gauthier et al., 2004; Zuccato et al., 2001; Zuccato et al., 2003). However, it remains unclear if such loss of BDNF is the cause or the symptom of HD pathogenesis. In the present study, we provided evidence that long-term depletion of BDNF-TrkB signaling in the MSN led to reduction in DARPP32 level and degeneration of spines. These cellular changes are hallmarks of striatal degeneration in the HD. Therefore by using the $TrkB^{Dlx5}$ mice we have modeled the degeneration of MSNs as seen in HD patients.

On a mechanistic level, however, the $BDNF^{BF1}$ and the $TrkB^{BF1}$ mice provided more resemblance to genetic models of HD, such as R6/1 and R6/2. Similar to human patients, these genetic models of HD carry mutant *huntingtin* genes with expansion of the polyglutamine repeat. The mutant *huntingtin* gene is ubiquitously expressed in the brain thereby conjures global disturbance in gene expression and vesicular transport. As a consequence, neuropathology in regions outside of the striatum, including the frontal cortex and the hippocampus, has been often observed in HD patients (Walker, 2007). This is also consistent with the

various cognitive and psychological symptoms displayed by HD patients, along with the more noticeable striatum-related motor deficits. In the $BDNF^{BF1}$ and the $TrkB^{BF1}$ mice, BDNF-TrkB signaling was disrupted in much of the forebrain and midbrain regions. As results these mice displayed more pronounced motor phenotypes, as well as elevated anxiety-like behaviors. Furthermore, similar to the HD mice, the $BDNF^{BF1}$ and the $TrkB^{BF1}$ mice also display early lethality.

CHAPTER 5

CONCLUSIONS AND PERSPECTIVES

The identification of NPCs capable of generating new neurons in the largely post-mitotic adult brain has been hailed as an extraordinary discovery that shattered the "central dogma" of neurobiology. Indeed, since the 1900s, it has been generally accepted that the mammalian CNS contains very limited capacity of regeneration. Santiago Ramón y Cajal, one of the most influential neuroscientist of all time, wrote of the brain and spinal cord in 1913:

> *"…once the development was ended, the founts of growth and regeneration of the axons and dendrites dried up irrevocably. In adult centers the nerve paths are something fixed, ended, immutable. Everything may die, nothing may be regenerated. It is for the science of the future to change, if possible, this harsh decree."*

This pessimism reigned for most of the last century, though pioneering work by Altman & Das in the mid-60s suggested the existence of continuing neurogenesis throughout adulthood (Altman and Das, 1965). In the past two decades, however, the "science of the future" began to emerge. It is now well accepted that new neurons are indeed born in restricted regions of the adult mammalian brain (Alvarez-Buylla et al., 2001; Gage, 2000). An ever-increasing body of work has demonstrated that this previously unknown structural plasticity is intricately involved in the development, physiology and pathology of the adult brain.

There has been accumulating evidence for neurogenic abnormalities in mood disorders such as depression and anxiety. However, whether the impairment of new neuron production observed in animal models of depression constitutes a pathogenic etiology remains controversial. In the current studies, we principally sought to address not the role of NPCs in the pathogenesis of mood disorders, but the mechanism by which antidepressive treatments ameliorate symptoms of the illness. In Chapters 2, we detailed the identification of a cell-autonomous role for BDNF-TrkB signaling in the regulation of adult hippocampal neurogenesis, and the behavioral effects of antidepressive regimen such as chronic ADs and exercise. These findings were further echoed by results from the toxin-based cell-ablation study (DTA^{Nestin}). Together these observations ascertain a pivotal role for the activation of adult NPCs in mediating AD-induced improvements in depression and anxiety-like behaviors.

Our finding that activation of TrkB by BDNF induces proliferation and neurogenesis coincided with studies showing NPCs sensitivity to a number of other growth factors that also activate receptor tyrosine kinases. Against this backdrop, we investigated the hypothesis that removal of inhibitor(s) for common signaling pathways downstream from receptor tyrosine kinases would augment proliferation

and neurogenesis (chapter 3). Indeed, ablation of NF1, a RasGAP protein known to antagonize the activation of MAPK and AKT pathways was sufficient to sensitize the adult NPCs to AD treatments, and stimulate neurogenesis in the long run. Furthermore, these changes in the intrinsic properties of NPCs were coupled with direct changes in depression and anxiety-like behaviors. These exciting results demonstrate the capacity to generate new neurons in the adult brain is regulated by distinct signaling mechanisms. But perhaps more intriguing is the realization that the adult brain contains such a population of multipotent progenitor cells that are amenable to manipulation and can serve as a module for complex physiological functions such as mood regulation.

The uneasy truth about the depression epidemic is that despite advances in our knowledge about the cause and treatment of this illness, much is still unknown. Depression is projected to be the second leading cause of death by the year 2020 (BBC), and currently AD is the most prescribed drug in the United States (CDC). Yet our understanding of the mechanism by which AD alleviates depression remains incomplete. This lack of knowledge further hampers the efforts to discover more fast-acting, effective treatments with fewer adverse effects. Findings from the current studies provide cellular and molecular insights into how AD exerts its behavioral effects, nevertheless the upstream and downstream components of the AD

mechanism remain to be elucidated. Further analyses are needed to: 1) examine the steps and kinetics of AD induced BDNF up-regulations; 2) investigate the intracellular events that relay the activation of TrkB signaling pathways to cell division and neuronal differentiation; 3) scrutinize synaptic properties of the newly generated neurons and the corresponding electrophysiological changes in response to AD treatment; 4) establish on the neural circuitry level the fundamentals of how connectivity and activity lead to alteration in depression and anxiety-like behaviors.

CHAPTER 6

MATERIALS AND METHODS

Animals

TrkB, BDNF, NF1 and PTEN conditional mutant mice were derived from interbreeding of flox/wt; cre/wt mice and flox/flox or flox/wt mice. The DTA^{Nestin} mice ($DTA^{flox/wt}$; Nestin-Cre/wt) were generated by crossing $DTA^{flox/wt}$ mice with Nestin-Cre/wt mice. PTEN flox, DTA flox, hGFAP-Cre, BF1-Cre, Dlx5-Cre mice were generously provided by Tak Mak (Toronto), Dieter Riethmacher (Southampton), Albee Messing (Wisconsin), Susan McConnell (Stanford) and Kenneth Campbell (Cincinnati). TrkB flox, BDNF flox, NF1 flox, Syn-Cre, and Nestin-GFP transgenic mice were generated in the laboratory of Luis Parada as previously described (Luikart et al., 2005; Monteggia et al., 2007; Yu et al., 2005; Zhu et al., 2001). The Nestin-CreER transgenic mice was generated and characterized by J.C., C.H.K. and L.F.P. (Chen et al., 2008). Rosa26R and R6/2 mice were from Jackson Lab. All animals were maintained on the 129/SvEv inbred background, except the $TrkB^{Nestin}$ mice which were on 129/SvEv and C57BL/6 mixed background. All mouse protocols were approved by the Institutional Animal Care and Research Advisory Committee at University of Texas Southwestern Medical Center.

Histology

Mice were intra-cardially perfused with PBS followed by 4% (w/v) paraformaldehyde (PFA) in PBS, and the dissected brains post-fixed in 4% PFA at 4

degree. X-gal staining and Nissl staining were performed using 50um thick vibratome sections or 7um thick paraffin sections, respectively (Lush et al., 2008). For X-gal staining, sections were washed in PBS and incubated in staining buffer (2mM $MgCl_2$, 1mg/ml X-gal, 5mM potassium ferrocyanide and 5mM potassium ferricyanide in PBS) for 3-8 hours at 37 degree in dark. Sections were then washed and mounted on slides, air-dried,counterstained with nuclear fast red, dehydrated through ethanol/xyelene, and coverslipped. TUNEL assay was performed using the NeuroApop kit as per manufacturer's instruction (Lei et al., 2005) (FD NeuroTechnologies).

Golgi Staining

Golgi staining was performed as described (Zhu et al., 2001). Briefly, adult mice were perfused with PBS. The brains were then dissected and incubated in Golgi-Cox staining solution for 12-14 days at room temperature, away from light. 100um vibratome sections of the brains were mounted on slides and briefly air-dried. The sections were then developed in the dark, dehydrated through ethanol/xyelene and coverslipped. Images of Golgi stained neurons were acquired using the MetaMorph software.

***In Situ* Hybridization**

In situ hybridization was done as previously described (Luikart et al., 2005), using 14um thick cryo-sections. Briefly, sections were digested for 15 minutes at 37 degree with 1mg/ml proteinase K, post-fixed in 4% PFA for 15 minutes, acetylated in 0.1M triethanolamine for 10 minutes, and dehydrated in ethanol. Radioactive [^{35}S] antisense cRNA probe was produced by *in vitro* transcription with T7, T3 or SP6 RNA polymerase from linearized clones for TrkB extracellular domain. Probes were denatured and added at 40000cpm/ul to the hybridization mix (0.3M NaCl, 0.02M Tris-HCl pH 8.0, 5mM EDTA, 10% Dextran sulfate, 1X Denhardt's, 0.5ug/ml yeast tRNA, 0.1M DTT and 50% formamide). The probes were allowed to hybridize for 16 hours at 60 degree. Sections were then washed for 30 minutes at 65 degree in stringent wash solution (0.15M NaCl, 0.02M Tris-HCl pH7.5, 5mM EDTA and 0.1M DTT), followed by RNase treatment for 15 minutes at 37 degree with 20ug/ml RNase A. Final washes were performed in 2X SSC for 15 minutes at 60 degree, then 0.1X SSC for 15 minutes at 60 degree. Sections were then dehydrated with ethanol, autoradiography was performed for 18 hours to estimate the strength of the signal. Slides were then dipped in Kodak emulsion (NTB2).and exposed in dark for 4-7 days, developed, counterstained with cresyl violet,dehydrated through ethanol/xyelene and coverslipped.

Immunohistochemistry

Sections used for immunohistochemistry were blocked in 3% donkey serum in PBS. Primary antibodies were against NeuN (1:500 Chemicon), NeuroD (1:500 Santa Cruz), GFP (1:500 Molecular Probe), BrdU (1:75 BD Bioscience), GFAP (1:300 DAKO), Ki67 (1:300 NeoMarker), Doublecortin (1:300 Santa Cruz), cleaved caspase 3 (1:100 Cell Signaling), Tyrosine Hydroxylase (1:5000 Chemicon), DARPP32 (1:3000 BD), LacZ (1:500 ICN), Serotonin (1:1000 Chemicon) and TrkB (1:500, Louis Reichardt). Microwave antigen retrieval method was used for all antibodies on paraffin sections. BrdU incorporation was examined 24 hours after the first injection (followed by three additional injections of 50 ug/g BrdU with 2 hours intervals), or 2 hours after single injection (200ug/g). For fluorescent immunohistochemistry, primary antibodies were visualized by secondary antibodies conjugated with Cy2, Cy3 or Cy5 (1:200, Jackson Immunoresearch) for 2 hours, followed by counterstaining with DAPI (Vector Labs). Alternatively, sections were incubated with secondary antibodies conjugated with biotin (1:200, Vector Lab) for 2 hours. Antibody staining was then visualized using the ABC kit (Vector Lab) with DAB substrate. Sections were then washed, mounted and coverslipped.

Western blotting

Western blotting was performed as described (Lush et al., 2008). Briefly, tissues or cells were collected and immediately frozen in liquid nitrogen, then

homogenized in PLC buffer [50mM HEPES pH7.5, 150mM NaCl, 10% glycerol, 0.1% Triton X-100, 1.5 mM MgCl2 and complete proteinase inhibitor (Roche)]. The extract was centrifuged, and protein concentration of the supernatant measured with the BCA kit following the manufacturer's instructions (Pierce). 10ug of total protein from the supernatant was separated on SDS-PAGE gels and transferred to PVDF membranes. Membranes were incubated in blocking solution containing in 5% non-fat milk or 5% BSA dissolved in 0.1% Tween-20 in TBS (TBST), then incubated in primary antibody solution. The following primary antibodies were used: TrkB (1:500, Louis Reichardt), phospho-Trk490 (1:1000, Cell Signaling) and actin (1:2000, Sigma). The membranes were then incubated in solution containing HRP conjugated secondary antibodies (1:10000, Santa Cruz) followed by ChemiGlow kit (Alpha Innotech) as per manufacturer's instructions. Membrane blotted for phospho-Trk was stripped (100mM β-mercaptoethanol, 2% SDS and 62.5mM Tris-HCl pH6.7) at 50 degree for 30 minutes then re-probed for total TrkB.

BDNF ELISA

The hippocampus was rapidly dissected, frozen in liquid nitrogen and stored at -80C. Total protein was extracted and measured using similar protocol as for western blotting (Luikart et al., 2005). BDNF level was measured using a BDNF ELISA kit (Promega) as per manufacturer's instructions. Following

chromogenic reaction, the absorbance was read at 450nm on a Fluostar Optima Microplate reader (BMG Labtech). Recombinant BDNF (Promega) was used as standards to quantify the absolute amount of BDNF. Standards and samples were performed in triplicates. 3 runners and 3 sedentary controls were used for each genotype. Runners were collected 24 hours after the last day of exercise.

Histological quantifications

To calculate the volume of the DG, 50um thick vibratome sections of the horizontal ($TrkB^{hGFAP}$ and $TrkB^{Syn}$ experiment; n>7 mice for each genotype at each time point) or coronal ($TrkB^{Nestin}$ experiment; n=6 for each genotype) brain were stained with DAPI, and the area of the granular layer from every second ($TrkB^{hGFAP}$ and $TrkB^{Syn}$) or fourth ($TrkB^{Nestin}$) section was measured using MetaMorph software (Universal Imaging Corporation), from which the total volume of granular layer in each hippocampus was calculated. To calculate the volume of the striatum, 50um thick coronal sections of the adult brain were Nissl-stained, and the area of the striatum from every fourth section was measured (n=6 for each genotype). The area of the striatum was manually outlined following defined morphological criteria. Briefly, the superior boundary of the striatum was defined by the corpus callosum, the lateral boundary by the external capsule, and the medial boundary by the lateral ventricle and the corpus callosum. Cell density, granular layer thickness and cell

size was measured using Nissl stained 7um thick coronal sections with the MetaMorph software (n=6 mice for each genotype). Immunohistochemistry for Ki67, BrdU, NeuroD, Doublecortin, cleaved-caspase3 and TUNEL positive cells were done using 7um-thick (P15) or 50um-thick (all adult ages) coronal sections through the hippocampus (bregma: -0.82mm to -4.24mm) of one hemisphere. The granular layer and SGZ of the dentate gyrus in every tenth (P15) or sixth (all adult ages) section was examined, from which the total number of positive cells in both hemispheres was calculated. Co-expression of TrkB and Ki67 or Doublecortin was examined on 50um coronal sections of equivalent anatomical regions. 30um-thick z-series of confocal images were collected using a Zeiss LSM-510 microscope, randomly selected Ki67+ or Doublecortin+ cells were assessed in individual planes for TrkB staining.

Neurosphere cultures

Neurosphere culture was established and maintained as described (Bull and Bartlett, 2005) with some modifications. Briefly, DG of adult mice were dissected (Seaberg and van der Kooy, 2002) and digested in 0.1% trypsin-EDTA (Sigma) followed by mechanical trituration until smooth. Cells were plated at a density of 20 cells/ul in complete growth medium, consisting of mouse NeuroCult NSC basal medium (StemCell Technologies), mouse NeuroCult NSC proliferation supplements

(StemCell Technologies), 2 ug/ml heparin (Sigma), EGF (20 ng/ml, Gibco) and bFGF (10 ng/ml, Sigma). Treatment with BDNF (50 ng/ml, R&D Systems) started from the first day, when indicated. Cells were fed every 2-3 days and passed every 8 to 10 days. For the measurement of secondary to primary neurosphere ratio, equal numbers of primary neurospheres were dissociated by trituration, replated and cultured for 10 days. For the measurement of neurosphere number and size, images of primary and secondary neurospheres (n=4 animals for each genotype) were taken 10 days after plating and processed by using the MetaMorph software. For X-gal staining, 0.1 M potassium ferricyanide, 0.1 M potassium ferrocyanide and 1mg/ml 5-bromo-4-chloro-3-indolyl-β-D-galactopyranoside in dimethylformamide (all from Sigma) were added to the complete growth medium and incubated for 5 h (n=3 animals for each genotype). For phospho-Trk490 western blotting, DG neurospheres (passage 3) generated from P7 mice were treated with BDNF (100 ng/ml) 30min before harvest (n=3 for each genotype and treatment). Apoptosis was quantified using an Annexin V-PE Apoptosis Detection Kit (BD Bioscienses) on single cells dissociated from primary neurospheres (10 days in vitro, n=3 animals for each genotype and treatment), and analyzed on a FACSAria (BD Bioscienses) as per manufacture's instructions.

FACS and RT-PCR

For FACS isolation of GFP positive or negative cells, primary cells were prepared from the DG of Nestin-GFP transgenic mice at the age of P2, P15 and 2 months following the procedure for establishing neurosphere culture (see above). Cells were resuspended in the solution containing L-15 (Gibco), 2% FBS, 2% B27 (Gibco) and 1 ug/ml propidium iodide (PI, Invitrogen). Cells from the DG of WT mice were used as GFP negative control. GFP positive and negative fractions of the live cells (PI negative) were analyzed and sorted on FACSAria. RT-PCR was performed using total RNA extracted from FACS sorted cells and adult DG neurospheres, with primer pairs against GAPDH, BDNF, TrkB kinase domain, Nestin, Musashi1, GFAP, NF-H and MAG.

Tamoxifen treatment

Tamoxifen (Sigma) was dissolved in a sunflower oil / ethanol mixture (9:1) at 6.7 mg/ml. Vehicle (9:1 sunflower oil / ethanol) or tamoxifen was injected intraperitoneally to 1 month old mice at 250 μl/20g (84.8mg/kg), twice a day for 5 consecutive days. All injected mice were observed daily for neurological related abnormality. $TrkB^{flox/flox}$; Nestin-CreER mice injected with vehicle, and $TrkB^{flox/flox}$ mice injected with tamoxifen were indistinguishable therefore pooled as the control group. Alternatively, tamoxifen was dissolved in sunflower oil at 20mg/ml. Vehicle (sunflower) or tamoxifen were delivered to 6-10 weeks old mice by gavage at

500ul/20g, once a day for 2 consecutive days.

Antidepressant treatment, voluntary exercise and behavioral tests

All animals used for AD treatment, running and subsequent behavioral tests are littermates. Since the same mice are later used for immunohistochemical analysis, age difference within each experimental group is no more than 1 week to eliminate any potential age-related influence on neurogenesis. Male control (n=10 and 10) and $TrkB^{hGFAP}$ (n=8 and 8) mice at the age of 2 months were injected with saline or fluoxetine (10 ng/ml) intraperitoneally for 21 days, respectively. A separate cohort of 2-month-old male control (n=11 and 10) and $TrkB^{hGFAP}$ mice (n=7 and 8) were treated with saline or imipramine (20 ng/ml) for the same length of time. Similarly, 2-month-old male control (n=8, 7 and 8) and $TrkB^{Syn}$ mice (n=7, 7 and 8) were treated with saline, fluoxetine and imipramine. Separate group of male control (n=9, 10 and 9) and $TrkB^{Nestin}$ mice (n=10, 10 and 8) at the age of 3 months were treated with saline, fluoxetine and imipramine. For voluntary exercise experiment, individual control (n=8 and 16) and $TrkB^{hGFAP}$ mice (n=8 and 13) at the age of 2 month were housed in standard cage or with access to running-wheel for 6 weeks. Wheel running activity was monitored continuously with a Dataquest Acquisition & Analysis System (Data Sciences International), and quantified by measuring wheel revolutions. Male and female animals were used, experimental results were

analyzed separately, and subsequently combined when no statistically significant gender difference within each group were observed. Immediately after the last dose of AD or saline, or last day of running, mice were deprived of food for 24 hours and then subjected to the NSFT. Individual mice were placed in a well-lit box (23 X 23 X 10 in) for up to 10 minutes where a food pellet was presented in the center. Mice were then returned to home cage, where food consumption in the next 5 minute was monitored. 24 hours afterwards, the same groups of mice were subjected to the TST, where individual mice were suspended from a horizontal bar using adhesive tape. Activity within a 6-minute session was video-recorded. Latency to feed in the NSFT and length of immobility in the TST were rated as previously described (Santarelli et al., 2003; Svenningsson et al., 2006), by investigators blind to genotypes. Mice were sacrificed 24 hours after the TST for tissue collection and subsequent analyses. For locomotor activity, open field, dark-light, elevated plus maze and forced swim test, separate cohorts of male control (n=17) and $TrkB^{hGFAP}$ mice (n=21) between the age of 12-15 weeks were tested.

Behavioral tests

Mice were tested in the following behavioral paradigms in the order of listing. Tests were performed on separate days with a minimum of 24 hours between tests. All mice were between the age of 3 months and 5 months, mutant

mice were studied along with littermate controls in two separate cohorts. Prior to behavioral examination, mice were acclimatized to vivarium conditions for a minimum of two weeks. Behavioral tests were conducted during the light cycle (7am to 19pm) under dim lighting conditions.

Locomotor Activity

Locomotor activity was measured as previously described (Monteggia et al., 2007). Mice were placed into a fresh home cage (18 cm x 28 cm) which was fitted into a dark plexiglass box. Movement was monitored by 5 photobeams (Photobeam Activity System, San Diego Instruments, San Diego, CA) for 2 hours, with the data collected in 5 min bins. Movement was classified in three ways: ambulatory (beam breaks in two consecutive photobeams), fine motor (repetitive beam breaks of one beam) and total movement (all beam breaks).

Open Field Test

Activity in a novel, open arena was measured to assess the general anxiety levels. As described previously (Kwon et al., 2006), mice were placed in the periphery of a brightly lit novel open field environment (44 cm x 44 cm, walls 30 cm high) and allowed to explore for 5 min. Mice were monitored from above by a video camera connected to a computer running video tracking software (Ethovision

3.0, Noldus, Leesburg, Virginia) to determine the time, distance moved and number of entries into two areas: the periphery (5 cm from the walls) and the center (14 cm x 14cm). In between mice, the open field arenas were wiped with 70% ethanol and allowed to dry to remove olfactory cues.

Elevated Plus Maze

The activity on an elevated plus maze was measured as previously reported (Powell et al., 2004). Mice were placed in the center of an elevated plus maze (each arm 30 cm long and 5 cm wide with two opposite arms closed by 25 cm high walls) elevated 31 cm from the ground in a dimly lit room and allowed to explore for 5 min. The animals were monitored from above by a video camera connected to a computer running video tracking software (Ethovision 3.0, Noldus, Leesburg, Virginia) to determine time spent in the open and closed arms, time spent in the middle, and the number of entries into the open and closed arm. The apparatus was wiped with 70% ethanol and allowed to dry between mice.

Dark-Light Test

The dark-light activity was measure in a two chamber apparatus (Med-PC IV, Med Associates, St. Albans, VT) similar to previously described (Powell et al., 2004). Mice were placed into a black plexiglas chamber (25 cm x 26 cm) and

allowed to explore for 2 min. Then a small door was opened allowing them to access the light side of the apparatus (25 cm x 26 cm lit to approximately 1700 lux). The animals were monitored by 8 photobeams (4 per compartment) connected to a computer which recorded the time spent in each compartment, latency to enter the light side and the number of entrances to each compartment. The dark-light apparatus was wiped with 70% ethanol and allowed to dry between mice.

Forced Swim Test

The forced swim test was conducted to measure acute swim-stress induced immobility behavior. Procedures were similar to previously described (Krishnan et al., 2007). Mice were placed in a 4L beaker (16.5 cm diameter) of water (21-25° C) to a depth of 17.8 cm. The mice remained in the water for 6 min and were then removed and allowed to dry in a clean dry cage before returning to their home cage. The water was changed between each subject. The mice were monitored from the side by a video camera and recorded video data were later scored by a trained observer blind to the genotypes. Only the last 4 min of the test were scored for latency to the first immobility and total time spent immobile. Immobility was defined as no volitional body or limb movement.

Statistical analyses

All data values are presented as mean +/- SEM. Student's t tests were applied to data with two groups of samples. ANOVA analyses were used for comparisons of data with greater than two groups. Generalized linear models (GLM) were used for unbalanced data. *Post hoc* group comparisons were performed with Bonferroni test. A value of $p<0.05$ was considered statistically significant.

BIBLIOGRAPHY

(1993). A novel gene containing a trinucleotide repeat that is expanded and unstable on Huntington's disease chromosomes. The Huntington's Disease Collaborative Research Group. Cell *72*, 971-983.

Adachi, M., Barrot, M., Autry, A.E., Theobald, D., and Monteggia, L.M. (2008). Selective loss of brain-derived neurotrophic factor in the dentate gyrus attenuates antidepressant efficacy. Biol Psychiatry *63*, 642-649.

Airan, R.D., Meltzer, L.A., Roy, M., Gong, Y., Chen, H., and Deisseroth, K. (2007). High-speed imaging reveals neurophysiological links to behavior in an animal model of depression. Science *317*, 819-823.

Altar, C.A., Cai, N., Bliven, T., Juhasz, M., Conner, J.M., Acheson, A.L., Lindsay, R.M., and Wiegand, S.J. (1997). Anterograde transport of brain-derived neurotrophic factor and its role in the brain. Nature *389*, 856-860.

Altar, C.A., and DiStefano, P.S. (1998). Neurotrophin trafficking by anterograde transport. Trends Neurosci *21*, 433-437.

Altman, J., and Bayer, S.A. (1990). Migration and distribution of two populations of hippocampal granule cell precursors during the perinatal and postnatal periods. J Comp Neurol *301*, 365-381.

Altman, J., and Das, G.D. (1965). Autoradiographic and histological evidence of postnatal hippocampal neurogenesis in rats. J Comp Neurol *124*, 319-335.

Alvarez-Buylla, A. (1992). Neurogenesis and plasticity in the CNS of adult birds. Exp Neurol *115*, 110-114.

Alvarez-Buylla, A., Garcia-Verdugo, J.M., and Tramontin, A.D. (2001). A unified hypothesis on the lineage of neural stem cells. Nat Rev Neurosci *2*, 287-293.

Alvarez-Buylla, A., and Lim, D.A. (2004). For the long run: maintaining germinal niches in the adult brain. Neuron *41*, 683-686.

Babyak, M., Blumenthal, J.A., Herman, S., Khatri, P., Doraiswamy, M., Moore, K., Craighead, W.E., Baldewicz, T.T., and Krishnan, K.R. (2000). Exercise treatment for major depression: maintenance of therapeutic benefit at 10 months. Psychosom Med *62*, 633-638.

Baquet, Z.C., Gorski, J.A., and Jones, K.R. (2004). Early striatal dendrite deficits followed by neuron loss with advanced age in the absence of anterograde cortical brain-derived neurotrophic factor. J Neurosci *24*, 4250-4258.

Barnabe-Heider, F., and Miller, F.D. (2003). Endogenously produced neurotrophins regulate survival and differentiation of cortical progenitors via distinct signaling pathways. J Neurosci *23*, 5149-5160.

Batchelor, P.E., Armstrong, D.M., Blaker, S.N., and Gage, F.H. (1989). Nerve growth factor receptor and choline acetyltransferase colocalization in neurons within the rat forebrain: response to fimbria-fornix transection. J Comp Neurol *284*, 187-204.

Berton, O., McClung, C.A., Dileone, R.J., Krishnan, V., Renthal, W., Russo, S.J., Graham, D.,

Tsankova, N.M., Bolanos, C.A., Rios, M., *et al.* (2006). Essential role of BDNF in the mesolimbic dopamine pathway in social defeat stress. Science *311*, 864-868.

Bibb, J.A., Yan, Z., Svenningsson, P., Snyder, G.L., Pieribone, V.A., Horiuchi, A., Nairn, A.C., Messer, A., and Greengard, P. (2000). Severe deficiencies in dopamine signaling in presymptomatic Huntington's disease mice. Proc Natl Acad Sci U S A *97*, 6809-6814.

Bremner, J.D., Narayan, M., Anderson, E.R., Staib, L.H., Miller, H.L., and Charney, D.S. (2000). Hippocampal volume reduction in major depression. Am J Psychiatry *157*, 115-118.

Brockschnieder, D., Pechmann, Y., Sonnenberg-Riethmacher, E., and Riethmacher, D. (2006). An improved mouse line for Cre-induced cell ablation due to diphtheria toxin A, expressed from the Rosa26 locus. Genesis *44*, 322-327.

Bull, N.D., and Bartlett, P.F. (2005). The adult mouse hippocampal progenitor is neurogenic but not a stem cell. J Neurosci *25*, 10815-10821.

Cameron, H.A., and McKay, R.D. (1999). Restoring production of hippocampal neurons in old age. Nat Neurosci *2*, 894-897.

Carlezon, W.A., Jr., Duman, R.S., and Nestler, E.J. (2005). The many faces of CREB. Trends Neurosci *28*, 436-445.

Chen, J., Kwon, C.H., Lin, L., Li, Y., and Parada, L.F. (2008). Inducible site-specific recombination in neural stem/progenitor cells. Submitted.

Chen, W.G., Chang, Q., Lin, Y., Meissner, A., West, A.E., Griffith, E.C., Jaenisch, R., and Greenberg, M.E. (2003). Derepression of BDNF transcription involves calcium-dependent phosphorylation of MeCP2. Science *302*, 885-889.

Chen, Z.Y., Jing, D., Bath, K.G., Ieraci, A., Khan, T., Siao, C.J., Herrera, D.G., Toth, M., Yang, C., McEwen, B.S., *et al.* (2006). Genetic variant BDNF (Val66Met) polymorphism alters anxiety-related behavior. Science *314*, 140-143.

Chenn, A., and Walsh, C.A. (2002). Regulation of cerebral cortical size by control of cell cycle exit in neural precursors. Science *297*, 365-369.

Choi, M.J., Kang, R.H., Lim, S.W., Oh, K.S., and Lee, M.S. (2006). Brain-derived neurotrophic factor gene polymorphism (Val66Met) and citalopram response in major depressive disorder. Brain Res *1118*, 176-182.

Coe, C.L., Kramer, M., Czeh, B., Gould, E., Reeves, A.J., Kirschbaum, C., and Fuchs, E. (2003). Prenatal stress diminishes neurogenesis in the dentate gyrus of juvenile rhesus monkeys. Biol Psychiatry *54*, 1025-1034.

Conti, A.C., Cryan, J.F., Dalvi, A., Lucki, I., and Blendy, J.A. (2002). cAMP response element-binding protein is essential for the upregulation of brain-derived neurotrophic factor transcription, but not the behavioral or endocrine responses to antidepressant drugs. J Neurosci *22*, 3262-3268.

Corti, S., Locatelli, F., Papadimitriou, D., Donadoni, C., Del Bo, R., Fortunato, F., Strazzer, S., Salani, S., Bresolin, N., and Comi, G.P. (2005). Multipotentiality, homing properties, and pyramidal neurogenesis of CNS-derived LeX(ssea-1)+/CXCR4+ stem cells. Faseb J *19*, 1860-1862.

Czeh, B., Michaelis, T., Watanabe, T., Frahm, J., de Biurrun, G., van Kampen, M., Bartolomucci, A., and Fuchs, E. (2001). Stress-induced changes in cerebral metabolites, hippocampal volume, and cell proliferation are prevented by antidepressant treatment with tianeptine. Proc Natl Acad Sci U S A *98*, 12796-12801.

Dasgupta, B., and Gutmann, D.H. (2005). Neurofibromin regulates neural stem cell proliferation, survival, and astroglial differentiation in vitro and in vivo. J Neurosci *25*, 5584-5594.

DiStefano, P.S., Friedman, B., Radziejewski, C., Alexander, C., Boland, P., Schick, C.M., Lindsay, R.M., and Wiegand, S.J. (1992). The neurotrophins BDNF, NT-3, and NGF display distinct patterns of retrograde axonal transport in peripheral and central neurons. Neuron *8*, 983-993.

Doetsch, F., Caille, I., Lim, D.A., Garcia-Verdugo, J.M., and Alvarez-Buylla, A. (1999). Subventricular zone astrocytes are neural stem cells in the adult mammalian brain. Cell *97*, 703-716.

Egan, M.F., Kojima, M., Callicott, J.H., Goldberg, T.E., Kolachana, B.S., Bertolino, A., Zaitsev, E., Gold, B., Goldman, D., Dean, M., *et al.* (2003). The BDNF val66met polymorphism affects activity-dependent secretion of BDNF and human memory and hippocampal function. Cell *112*, 257-269.

Eisch, A.J., Barrot, M., Schad, C.A., Self, D.W., and Nestler, E.J. (2000). Opiates inhibit neurogenesis in the adult rat hippocampus. Proc Natl Acad Sci U S A *97*, 7579-7584.

Ekdahl, C.T., Claasen, J.H., Bonde, S., Kokaia, Z., and Lindvall, O. (2003). Inflammation is detrimental for neurogenesis in adult brain. Proc Natl Acad Sci U S A *100*, 13632-13637.

Encinas, J.M., Vaahtokari, A., and Enikolopov, G. (2006). Fluoxetine targets early progenitor cells in the adult brain. Proc Natl Acad Sci U S A *103*, 8233-8238.

Fagiolini, A., and Kupfer, D.J. (2003). Is treatment-resistant depression a unique subtype of depression? Biol Psychiatry *53*, 640-648.

Ferron, S., Mira, H., Franco, S., Cano-Jaimez, M., Bellmunt, E., Ramirez, C., Farinas, I., and Blasco, M.A. (2004). Telomere shortening and chromosomal instability abrogates proliferation of adult but not embryonic neural stem cells. Development *131*, 4059-4070.

Frazer, A. (1997). Pharmacology of antidepressants. J Clin Psychopharmacol *17 Suppl 1*, 2S-18S.

Gage, F.H. (2000). Mammalian neural stem cells. Science *287*, 1433-1438.

Gauthier, L.R., Charrin, B.C., Borrell-Pages, M., Dompierre, J.P., Rangone, H., Cordelieres, F.P., De Mey, J., MacDonald, M.E., Lessmann, V., Humbert, S., and Saudou, F. (2004). Huntingtin controls neurotrophic support and survival of neurons by enhancing BDNF vesicular transport along microtubules. Cell *118*, 127-138.

Gilbertson, M.W., Shenton, M.E., Ciszewski, A., Kasai, K., Lasko, N.B., Orr, S.P., and Pitman, R.K. (2002). Smaller hippocampal volume predicts pathologic vulnerability to psychological trauma. Nat Neurosci *5*, 1242-1247.

Gorski, J.A., Balogh, S.A., Wehner, J.M., and Jones, K.R. (2003). Learning deficits in

forebrain-restricted brain-derived neurotrophic factor mutant mice. Neuroscience *121*, 341-354.

Gould, E., Beylin, A., Tanapat, P., Reeves, A., and Shors, T.J. (1999). Learning enhances adult neurogenesis in the hippocampal formation. Nat Neurosci *2*, 260-265.

Gould, E., Cameron, H.A., Daniels, D.C., Woolley, C.S., and McEwen, B.S. (1992). Adrenal hormones suppress cell division in the adult rat dentate gyrus. J Neurosci *12*, 3642-3650.

Gray, J., Yeo, G.S., Cox, J.J., Morton, J., Adlam, A.L., Keogh, J.M., Yanovski, J.A., El Gharbawy, A., Han, J.C., Tung, Y.C., *et al.* (2006). Hyperphagia, severe obesity, impaired cognitive function, and hyperactivity associated with functional loss of one copy of the brain-derived neurotrophic factor (BDNF) gene. Diabetes *55*, 3366-3371.

Greengard, P., Allen, P.B., and Nairn, A.C. (1999). Beyond the dopamine receptor: the DARPP-32/protein phosphatase-1 cascade. Neuron *23*, 435-447.

Gur, T.L., Conti, A.C., Holden, J., Bechtholt, A.J., Hill, T.E., Lucki, I., Malberg, J.E., and Blendy, J.A. (2007). cAMP response element-binding protein deficiency allows for increased neurogenesis and a rapid onset of antidepressant response. J Neurosci *27*, 7860-7868.

He, X.P., Kotloski, R., Nef, S., Luikart, B.W., Parada, L.F., and McNamara, J.O. (2004). Conditional deletion of TrkB but not BDNF prevents epileptogenesis in the kindling model. Neuron *43*, 31-42.

Hebert, J.M., and McConnell, S.K. (2000). Targeting of cre to the Foxg1 (BF-1) locus mediates loxP recombination in the telencephalon and other developing head structures. Dev Biol *222*, 296-306.

Holick, K.A., Lee, D.C., Hen, R., and Dulawa, S.C. (2008). Behavioral effects of chronic fluoxetine in BALB/cJ mice do not require adult hippocampal neurogenesis or the serotonin 1A receptor. Neuropsychopharmacology *33*, 406-417.

Huang, E.J., and Reichardt, L.F. (2001). Neurotrophins: roles in neuronal development and function. Annu Rev Neurosci *24*, 677-736.

Huang, E.J., and Reichardt, L.F. (2003). Trk receptors: roles in neuronal signal transduction. Annu Rev Biochem *72*, 609-642.

Imura, T., Kornblum, H.I., and Sofroniew, M.V. (2003). The predominant neural stem cell isolated from postnatal and adult forebrain but not early embryonic forebrain expresses GFAP. J Neurosci *23*, 2824-2832.

Isgor, C., Kabbaj, M., Akil, H., and Watson, S.J. (2004). Delayed effects of chronic variable stress during peripubertal-juvenile period on hippocampal morphology and on cognitive and stress axis functions in rats. Hippocampus *14*, 636-648.

Jackson, E.L., Garcia-Verdugo, J.M., Gil-Perotin, S., Roy, M., Quinones-Hinojosa, A., VandenBerg, S., and Alvarez-Buylla, A. (2006). PDGFR alpha-positive B cells are neural stem cells in the adult SVZ that form glioma-like growths in response to increased PDGF signaling. Neuron *51*, 187-199.

Jakubs, K., Nanobashvili, A., Bonde, S., Ekdahl, C.T., Kokaia, Z., Kokaia, M., and Lindvall, O. (2006). Environment matters: synaptic properties of neurons born in the epileptic adult

brain develop to reduce excitability. Neuron *52*, 1047-1059.

Jiang, X., Xu, K., Hoberman, J., Tian, F., Marko, A.J., Waheed, J.F., Harris, C.R., Marini, A.M., Enoch, M.A., and Lipsky, R.H. (2005). BDNF variation and mood disorders: a novel functional promoter polymorphism and Val66Met are associated with anxiety but have opposing effects. Neuropsychopharmacology *30*, 1353-1361.

Karl, A., Schaefer, M., Malta, L.S., Dorfel, D., Rohleder, N., and Werner, A. (2006). A meta-analysis of structural brain abnormalities in PTSD. Neurosci Biobehav Rev *30*, 1004-1031.

Kaufman, J., Yang, B.Z., Douglas-Palumberi, H., Grasso, D., Lipschitz, D., Houshyar, S., Krystal, J.H., and Gelernter, J. (2006). Brain-derived neurotrophic factor-5-HTTLPR gene interactions and environmental modifiers of depression in children. Biol Psychiatry *59*, 673-680.

Kempermann, G., Kuhn, H.G., and Gage, F.H. (1997). More hippocampal neurons in adult mice living in an enriched environment. Nature *386*, 493-495.

Kernie, S.G., Liebl, D.J., and Parada, L.F. (2000). BDNF regulates eating behavior and locomotor activity in mice. EMBO J *19*, 1290-1300.

Klein, R., Martin-Zanca, D., Barbacid, M., and Parada, L.F. (1990). Expression of the tyrosine kinase receptor gene trkB is confined to the murine embryonic and adult nervous system. Development *109*, 845-850.

Klesse, L.J., and Parada, L.F. (1998). p21 ras and phosphatidylinositol-3 kinase are required for survival of wild-type and NF1 mutant sensory neurons. J Neurosci *18*, 10420-10428.

Kohara, K., Kitamura, A., Morishima, M., and Tsumoto, T. (2001). Activity-dependent transfer of brain-derived neurotrophic factor to postsynaptic neurons. Science *291*, 2419-2423.

Korsching, S. (1993). The neurotrophic factor concept: a reexamination. J Neurosci *13*, 2739-2748.

Le, L.Q., and Parada, L.F. (2007). Tumor microenvironment and neurofibromatosis type I: connecting the GAPs. Oncogene *26*, 4609-4616.

Lee, J., Duan, W., Long, J.M., Ingram, D.K., and Mattson, M.P. (2000). Dietary restriction increases the number of newly generated neural cells, and induces BDNF expression, in the dentate gyrus of rats. J Mol Neurosci *15*, 99-108.

Lei, L., Laub, F., Lush, M., Romero, M., Zhou, J., Luikart, B., Klesse, L., Ramirez, F., and Parada, L.F. (2005). The zinc finger transcription factor Klf7 is required for TrkA gene expression and development of nociceptive sensory neurons. Genes Dev *19*, 1354-1364.

Leuner, B., Gould, E., and Shors, T.J. (2006). Is there a link between adult neurogenesis and learning? Hippocampus *16*, 216-224.

Levi-Montalcini, R. (1966). The nerve growth factor: its mode of action on sensory and sympathetic nerve cells. Harvey Lect *60*, 217-259.

Lewin, G.R., and Barde, Y.A. (1996). Physiology of the neurotrophins. Annu Rev Neurosci *19*, 289-317.

Liebl, D.J., Klesse, L.J., Tessarollo, L., Wohlman, T., and Parada, L.F. (2000). Loss of

brain-derived neurotrophic factor-dependent neural crest-derived sensory neurons in neurotrophin-4 mutant mice. Proc Natl Acad Sci U S A *97*, 2297-2302.

Liu, M., Pleasure, S.J., Collins, A.E., Noebels, J.L., Naya, F.J., Tsai, M.J., and Lowenstein, D.H. (2000). Loss of BETA2/NeuroD leads to malformation of the dentate gyrus and epilepsy. Proc Natl Acad Sci U S A *97*, 865-870.

Lledo, P.M., Alonso, M., and Grubb, M.S. (2006). Adult neurogenesis and functional plasticity in neuronal circuits. Nat Rev Neurosci *7*, 179-193.

Lu, B., Pang, P.T., and Woo, N.H. (2005). The yin and yang of neurotrophin action. Nat Rev Neurosci *6*, 603-614.

Luikart, B.W., Nef, S., Shipman, T., and Parada, L.F. (2003). In vivo role of truncated trkb receptors during sensory ganglion neurogenesis. Neuroscience *117*, 847-858.

Luikart, B.W., Nef, S., Virmani, T., Lush, M.E., Liu, Y., Kavalali, E.T., and Parada, L.F. (2005). TrkB has a cell-autonomous role in the establishment of hippocampal Schaffer collateral synapses. J Neurosci *25*, 3774-3786.

Lush, M.E., Li, Y., Kwon, C.H., Chen, J., and Parada, L.F. (2008). Neurofibromin is required for barrel formation in the mouse somatosensory cortex. J Neurosci *28*, 1580-1587.

MacQueen, G.M., Campbell, S., McEwen, B.S., Macdonald, K., Amano, S., Joffe, R.T., Nahmias, C., and Young, L.T. (2003). Course of illness, hippocampal function, and hippocampal volume in major depression. Proc Natl Acad Sci U S A *100*, 1387-1392.

Malberg, J.E., Eisch, A.J., Nestler, E.J., and Duman, R.S. (2000). Chronic antidepressant treatment increases neurogenesis in adult rat hippocampus. J Neurosci *20*, 9104-9110.

Mangiarini, L., Sathasivam, K., Seller, M., Cozens, B., Harper, A., Hetherington, C., Lawton, M., Trottier, Y., Lehrach, H., Davies, S.W., and Bates, G.P. (1996). Exon 1 of the HD gene with an expanded CAG repeat is sufficient to cause a progressive neurological phenotype in transgenic mice. Cell *87*, 493-506.

Manji, H.K., Drevets, W.C., and Charney, D.S. (2001). The cellular neurobiology of depression. Nat Med *7*, 541-547.

Matsumoto, T., Rauskolb, S., Polack, M., Klose, J., Kolbeck, R., Korte, M., and Barde, Y.A. (2008). Biosynthesis and processing of endogenous BDNF: CNS neurons store and secrete BDNF, not pro-BDNF. Nat Neurosci *11*, 131-133.

Miller, B.H., Schultz, L.E., Gulati, A., Cameron, M.D., and Pletcher, M.T. (2007). Genetic Regulation of Behavioral and Neuronal Responses to Fluoxetine. Neuropsychopharmacology.

Ming, G.L., and Song, H. (2005). Adult neurogenesis in the mammalian central nervous system. Annu Rev Neurosci *28*, 223-250.

Minichiello, L., Korte, M., Wolfer, D., Kuhn, R., Unsicker, K., Cestari, V., Rossi-Arnaud, C., Lipp, H.P., Bonhoeffer, T., and Klein, R. (1999). Essential role for TrkB receptors in hippocampus-mediated learning. Neuron *24*, 401-414.

Monje, M.L., Toda, H., and Palmer, T.D. (2003). Inflammatory blockade restores adult hippocampal neurogenesis. Science *302*, 1760-1765.

Monteggia, L.M., Barrot, M., Powell, C.M., Berton, O., Galanis, V., Gemelli, T., Meuth, S.,

Nagy, A., Greene, R.W., and Nestler, E.J. (2004). Essential role of brain-derived neurotrophic factor in adult hippocampal function. Proc Natl Acad Sci U S A *101*, 10827-10832.

Monteggia, L.M., Luikart, B., Barrot, M., Theobold, D., Malkovska, I., Nef, S., Parada, L.F., and Nestler, E.J. (2007). Brain-derived neurotrophic factor conditional knockouts show gender differences in depression-related behaviors. Biol Psychiatry *61*, 187-197.

Morilak, D.A., and Frazer, A. (2004). Antidepressants and brain monoaminergic systems: a dimensional approach to understanding their behavioural effects in depression and anxiety disorders. Int J Neuropsychopharmacol *7*, 193-218.

Nakagawa, S., Kim, J.E., Lee, R., Malberg, J.E., Chen, J., Steffen, C., Zhang, Y.J., Nestler, E.J., and Duman, R.S. (2002). Regulation of neurogenesis in adult mouse hippocampus by cAMP and the cAMP response element-binding protein. J Neurosci *22*, 3673-3682.

Neeper, S.A., Gomez-Pinilla, F., Choi, J., and Cotman, C.W. (1996). Physical activity increases mRNA for brain-derived neurotrophic factor and nerve growth factor in rat brain. Brain Res *726*, 49-56.

Nestler, E.J., Barrot, M., DiLeone, R.J., Eisch, A.J., Gold, S.J., and Monteggia, L.M. (2002). Neurobiology of depression. Neuron *34*, 13-25.

Ng, B.K., Chen, L., Mandemakers, W., Cosgaya, J.M., and Chan, J.R. (2007). Anterograde transport and secretion of brain-derived neurotrophic factor along sensory axons promote Schwann cell myelination. J Neurosci *27*, 7597-7603.

Nibuya, M., Morinobu, S., and Duman, R.S. (1995). Regulation of BDNF and trkB mRNA in rat brain by chronic electroconvulsive seizure and antidepressant drug treatments. J Neurosci *15*, 7539-7547.

Nibuya, M., Nestler, E.J., and Duman, R.S. (1996). Chronic antidepressant administration increases the expression of cAMP response element binding protein (CREB) in rat hippocampus. J Neurosci *16*, 2365-2372.

Ohkubo, Y., Uchida, A.O., Shin, D., Partanen, J., and Vaccarino, F.M. (2004). Fibroblast growth factor receptor 1 is required for the proliferation of hippocampal progenitor cells and for hippocampal growth in mouse. J Neurosci *24*, 6057-6069.

Pereira, A.C., Huddleston, D.E., Brickman, A.M., Sosunov, A.A., Hen, R., McKhann, G.M., Sloan, R., Gage, F.H., Brown, T.R., and Small, S.A. (2007). An in vivo correlate of exercise-induced neurogenesis in the adult dentate gyrus. Proc Natl Acad Sci U S A *104*, 5638-5643.

Perera, T.D., Coplan, J.D., Lisanby, S.H., Lipira, C.M., Arif, M., Carpio, C., Spitzer, G., Santarelli, L., Scharf, B., Hen, R., *et al.* (2007). Antidepressant-induced neurogenesis in the hippocampus of adult nonhuman primates. J Neurosci *27*, 4894-4901.

Pezawas, L., Verchinski, B.A., Mattay, V.S., Callicott, J.H., Kolachana, B.S., Straub, R.E., Egan, M.F., Meyer-Lindenberg, A., and Weinberger, D.R. (2004). The brain-derived neurotrophic factor val66met polymorphism and variation in human cortical morphology. J Neurosci *24*, 10099-10102.

Pieper, A.A., Wu, X., Han, T.W., Estill, S.J., Dang, Q., Wu, L.C., Reece-Fincanon, S., Dudley,

C.A., Richardson, J.A., Brat, D.J., and McKnight, S.L. (2005). The neuronal PAS domain protein 3 transcription factor controls FGF-mediated adult hippocampal neurogenesis in mice. Proc Natl Acad Sci U S A *102*, 14052-14057.

Pineda, J.R., Canals, J.M., Bosch, M., Adell, A., Mengod, G., Artigas, F., Ernfors, P., and Alberch, J. (2005). Brain-derived neurotrophic factor modulates dopaminergic deficits in a transgenic mouse model of Huntington's disease. J Neurochem *93*, 1057-1068.

Porsolt, R.D., Chermat, R., Lenegre, A., Avril, I., Janvier, S., and Steru, L. (1987). Use of the automated tail suspension test for the primary screening of psychotropic agents. Arch Int Pharmacodyn Ther *288*, 11-30.

Porteus, M.H., Bulfone, A., Ciaranello, R.D., and Rubenstein, J.L. (1991). Isolation and characterization of a novel cDNA clone encoding a homeodomain that is developmentally regulated in the ventral forebrain. Neuron *7*, 221-229.

Rios, M., Fan, G., Fekete, C., Kelly, J., Bates, B., Kuehn, R., Lechan, R.M., and Jaenisch, R. (2001). Conditional deletion of brain-derived neurotrophic factor in the postnatal brain leads to obesity and hyperactivity. Mol Endocrinol *15*, 1748-1757.

Romero, M.I., Lin, L., Lush, M.E., Lei, L., Parada, L.F., and Zhu, Y. (2007). Deletion of Nf1 in neurons induces increased axon collateral branching after dorsal root injury. J Neurosci *27*, 2124-2134.

Rossi, C., Angelucci, A., Costantin, L., Braschi, C., Mazzantini, M., Babbini, F., Fabbri, M.E., Tessarollo, L., Maffei, L., Berardi, N., and Caleo, M. (2006). Brain-derived neurotrophic factor (BDNF) is required for the enhancement of hippocampal neurogenesis following environmental enrichment. Eur J Neurosci *24*, 1850-1856.

Saarelainen, T., Hendolin, P., Lucas, G., Koponen, E., Sairanen, M., MacDonald, E., Agerman, K., Haapasalo, A., Nawa, H., Aloyz, R.*, et al.* (2003). Activation of the TrkB neurotrophin receptor is induced by antidepressant drugs and is required for antidepressant-induced behavioral effects. J Neurosci *23*, 349-357.

Sairanen, M., Lucas, G., Ernfors, P., Castren, M., and Castren, E. (2005). Brain-derived neurotrophic factor and antidepressant drugs have different but coordinated effects on neuronal turnover, proliferation, and survival in the adult dentate gyrus. J Neurosci *25*, 1089-1094.

Salmon, P. (2001). Effects of physical exercise on anxiety, depression, and sensitivity to stress: a unifying theory. Clin Psychol Rev *21*, 33-61.

Santarelli, L., Saxe, M., Gross, C., Surget, A., Battaglia, F., Dulawa, S., Weisstaub, N., Lee, J., Duman, R., Arancio, O.*, et al.* (2003). Requirement of hippocampal neurogenesis for the behavioral effects of antidepressants. Science *301*, 805-809.

Scharfman, H., Goodman, J., Macleod, A., Phani, S., Antonelli, C., and Croll, S. (2005). Increased neurogenesis and the ectopic granule cells after intrahippocampal BDNF infusion in adult rats. Exp Neurol *192*, 348-356.

Scharfman, H.E., and Hen, R. (2007). Neuroscience. Is more neurogenesis always better? Science *315*, 336-338.

Schule, C., Zill, P., Baghai, T.C., Eser, D., Zwanzger, P., Wenig, N., Rupprecht, R., and Bondy, B. (2006). Brain-derived neurotrophic factor Val66Met polymorphism and dexamethasone/CRH test results in depressed patients. Psychoneuroendocrinology *31*, 1019-1025.

Seaberg, R.M., and van der Kooy, D. (2002). Adult rodent neurogenic regions: the ventricular subependyma contains neural stem cells, but the dentate gyrus contains restricted progenitors. J Neurosci *22*, 1784-1793.

Seri, B., Garcia-Verdugo, J.M., McEwen, B.S., and Alvarez-Buylla, A. (2001). Astrocytes give rise to new neurons in the adult mammalian hippocampus. J Neurosci *21*, 7153-7160.

Sheline, Y.I., Gado, M.H., and Kraemer, H.C. (2003). Untreated depression and hippocampal volume loss. Am J Psychiatry *160*, 1516-1518.

Sheline, Y.I., Sanghavi, M., Mintun, M.A., and Gado, M.H. (1999). Depression duration but not age predicts hippocampal volume loss in medically healthy women with recurrent major depression. J Neurosci *19*, 5034-5043.

Shi, Y., Chichung Lie, D., Taupin, P., Nakashima, K., Ray, J., Yu, R.T., Gage, F.H., and Evans, R.M. (2004). Expression and function of orphan nuclear receptor TLX in adult neural stem cells. Nature *427*, 78-83.

Shirayama, Y., Chen, A.C., Nakagawa, S., Russell, D.S., and Duman, R.S. (2002). Brain-derived neurotrophic factor produces antidepressant effects in behavioral models of depression. J Neurosci *22*, 3251-3261.

Smith, M.E. (2005). Bilateral hippocampal volume reduction in adults with post-traumatic stress disorder: a meta-analysis of structural MRI studies. Hippocampus *15*, 798-807.

Snider, W.D. (1994). Functions of the neurotrophins during nervous system development: what the knockouts are teaching us. Cell *77*, 627-638.

Soriano, P. (1999). Generalized lacZ expression with the ROSA26 Cre reporter strain. Nat Genet *21*, 70-71.

Spires, T.L., Grote, H.E., Varshney, N.K., Cordery, P.M., van Dellen, A., Blakemore, C., and Hannan, A.J. (2004). Environmental enrichment rescues protein deficits in a mouse model of Huntington's disease, indicating a possible disease mechanism. J Neurosci *24*, 2270-2276.

Stenman, J., Toresson, H., and Campbell, K. (2003). Identification of two distinct progenitor populations in the lateral ganglionic eminence: implications for striatal and olfactory bulb neurogenesis. J Neurosci *23*, 167-174.

Stranahan, A.M., Khalil, D., and Gould, E. (2006). Social isolation delays the positive effects of running on adult neurogenesis. Nature neuroscience *9*, 526-533.

Svenningsson, P., Chergui, K., Rachleff, I., Flajolet, M., Zhang, X., El Yacoubi, M., Vaugeois, J.M., Nomikos, G.G., and Greengard, P. (2006). Alterations in 5-HT1B receptor function by p11 in depression-like states. Science *311*, 77-80.

Szeszko, P.R., Lipsky, R., Mentschel, C., Robinson, D., Gunduz-Bruce, H., Sevy, S., Ashtari, M., Napolitano, B., Bilder, R.M., Kane, J.M.*, et al.* (2005). Brain-derived neurotrophic factor val66met polymorphism and volume of the hippocampal formation. Mol Psychiatry *10*,

631-636.

Tao, X., Finkbeiner, S., Arnold, D.B., Shaywitz, A.J., and Greenberg, M.E. (1998). Ca2+ influx regulates BDNF transcription by a CREB family transcription factor-dependent mechanism. Neuron *20*, 709-726.

Tao, X., West, A.E., Chen, W.G., Corfas, G., and Greenberg, M.E. (2002). A calcium-responsive transcription factor, CaRF, that regulates neuronal activity-dependent expression of BDNF. Neuron *33*, 383-395.

Tardito, D., Perez, J., Tiraboschi, E., Musazzi, L., Racagni, G., and Popoli, M. (2006). Signaling pathways regulating gene expression, neuroplasticity, and neurotrophic mechanisms in the action of antidepressants: a critical overview. Pharmacol Rev *58*, 115-134.

Thase, M.E., and Rush, A.J. (1995). Treatment-resistant depression. In Psychopharmacology: The Fourth Generation of Progress, B. F.E., and K. D.J., eds. (New York: Raven Press), pp. 1081-1098.

van Praag, H., Kempermann, G., and Gage, F.H. (1999). Running increases cell proliferation and neurogenesis in the adult mouse dentate gyrus. Nat Neurosci *2*, 266-270.

Vogel, K.S., Brannan, C.I., Jenkins, N.A., Copeland, N.G., and Parada, L.F. (1995). Loss of neurofibromin results in neurotrophin-independent survival of embryonic sensory and sympathetic neurons. Cell *82*, 733-742.

Walker, F.O. (2007). Huntington's disease. Lancet *369*, 218-228.

Wang, J.W., David, D.J., Monckton, J.E., Battaglia, F., and Hen, R. (2008a). Chronic fluoxetine stimulates maturation and synaptic plasticity of adult-born hippocampal granule cells. J Neurosci *28*, 1374-1384.

Wang, J.W., Dranovsky, A., and Hen, R. (2008b). The when and where of BDNF and the antidepressant response. Biol Psychiatry *63*, 640-641.

Warner-Schmidt, J.L., and Duman, R.S. (2007). VEGF is an essential mediator of the neurogenic and behavioral actions of antidepressants. Proc Natl Acad Sci U S A *104*, 4647-4652.

Xuan, S., Baptista, C.A., Balas, G., Tao, W., Soares, V.C., and Lai, E. (1995). Winged helix transcription factor BF-1 is essential for the development of the cerebral hemispheres. Neuron *14*, 1141-1152.

Yeo, G.S., Connie Hung, C.C., Rochford, J., Keogh, J., Gray, J., Sivaramakrishnan, S., O'Rahilly, S., and Farooqi, I.S. (2004). A de novo mutation affecting human TrkB associated with severe obesity and developmental delay. Nat Neurosci *7*, 1187-1189.

Yu, T.S., Dandekar, M., Monteggia, L.M., Parada, L.F., and Kernie, S.G. (2005). Temporally regulated expression of Cre recombinase in neural stem cells. Genesis *41*, 147-153.

Zhao, C., Deng, W., and Gage, F.H. (2008). Mechanisms and functional implications of adult neurogenesis. Cell *132*, 645-660.

Zhou, X.F., Parada, L.F., Soppet, D., and Rush, R.A. (1993). Distribution of trkB tyrosine kinase immunoreactivity in the rat central nervous system. Brain Res *622*, 63-70.

Zhu, Y., Ghosh, P., Charnay, P., Burns, D.K., and Parada, L.F. (2002). Neurofibromas in NF1:

Schwann cell origin and role of tumor environment. Science *296*, 920-922.

Zhu, Y., Guignard, F., Zhao, D., Liu, L., Burns, D.K., Mason, R.P., Messing, A., and Parada, L.F. (2005a). Early inactivation of p53 tumor suppressor gene cooperating with NF1 loss induces malignant astrocytoma. Cancer Cell *8*, 119-130.

Zhu, Y., Harada, T., Liu, L., Lush, M.E., Guignard, F., Harada, C., Burns, D.K., Bajenaru, M.L., Gutmann, D.H., and Parada, L.F. (2005b). Inactivation of NF1 in CNS causes increased glial progenitor proliferation and optic glioma formation. Development *132*, 5577-5588.

Zhu, Y., and Parada, L.F. (2002). The molecular and genetic basis of neurological tumours. Nat Rev Cancer *2*, 616-626.

Zhu, Y., Romero, M.I., Ghosh, P., Ye, Z., Charnay, P., Rushing, E.J., Marth, J.D., and Parada, L.F. (2001). Ablation of NF1 function in neurons induces abnormal development of cerebral cortex and reactive gliosis in the brain. Genes Dev *15*, 859-876.

Zhuo, L., Theis, M., Alvarez-Maya, I., Brenner, M., Willecke, K., and Messing, A. (2001). hGFAP-cre transgenic mice for manipulation of glial and neuronal function in vivo. Genesis *31*, 85-94.

Zuccato, C., and Cattaneo, E. (2007). Role of brain-derived neurotrophic factor in Huntington's disease. Prog Neurobiol *81*, 294-330.

Zuccato, C., Ciammola, A., Rigamonti, D., Leavitt, B.R., Goffredo, D., Conti, L., MacDonald, M.E., Friedlander, R.M., Silani, V., Hayden, M.R.*, et al.* (2001). Loss of huntingtin-mediated BDNF gene transcription in Huntington's disease. Science *293*, 493-498.

Zuccato, C., Tartari, M., Crotti, A., Goffredo, D., Valenza, M., Conti, L., Cataudella, T., Leavitt, B.R., Hayden, M.R., Timmusk, T.*, et al.* (2003). Huntingtin interacts with REST/NRSF to modulate the transcription of NRSE-controlled neuronal genes. Nat Genet *35*, 76-83.

Zweifel, L.S., Kuruvilla, R., and Ginty, D.D. (2005). Functions and mechanisms of retrograde neurotrophin signalling. Nat Rev Neurosci *6*, 615-625.

Development/Plasticity/Repair

Neurofibromin Is Required for Barrel Formation in the Mouse Somatosensory Cortex

Mark E. Lush,* Yun Li,* Chang-Hyuk Kwon, Jian Chen, and Luis F. Parada

Department of Developmental Biology and Kent Waldrep Center for Basic Neuroscience Research on Nerve Growth and Regeneration, University of Texas Southwestern Medical Center, Dallas, Texas 75390-9133

The rodent barrel cortex is a useful system to study the role of genes and neuronal activity in the patterning of the nervous system. Several genes encoding either intracellular signaling molecules or neurotransmitter receptors are required for barrel formation. Neurofibromin is a tumor suppressor protein that has Ras GTPase activity, thus attenuating the MAPK (mitogen-activated protein kinase) and and PI-3 kinase (phosphatidylinositol 3-kinase) pathways, and is mutated in humans with the condition neurofibromatosis type 1 (NF1). Neurofibromin is widely expressed in the developing and adult nervous system, and a common feature of NF1 is deficits in intellectual development. In addition, NF1 is an uncommonly high disorder among individuals with autism. Thus, NF1 may have important roles in normal CNS development and function. To explore roles for neurofibromin in the development of the CNS, we took advantage of a mouse conditional allele. We show that mice that lack neurofibromin in the majority of cortical neurons and astrocytes fail to form cortical barrels in the somatosensory cortex, whereas segregation of thalamic axons within the somatosensory cortex appears unaffected.

Key words: **NF1; Ras-GAP; hGFAP-Cre; thalamocortical axons; development; conditional mutant**

Introduction

In the rodent CNS, the cortex is innervated by dorsal thalamic axons that segregate the cortex into different sensory regions such as visual, auditory, and somatosensory. Axons from the ventral posterior medial nucleus (VPM) of the thalamus innervate the somatosensory cortex where they segregate into discrete regions (Miller et al., 2001). Neurons within cortical layer IV form rings termed cortical barrels by arranging their cell bodies around and dendrites toward the incoming thalamic axons (Woolsey and Van der Loos, 1970; Woolsey et al., 1975).

Many studies have contributed to elucidation of factors required for barrel formation. Transplantation of visual cortex tissue in place of somatosensory cortex permitted barrel-like formation, suggesting that VPM thalamic axons specify barrel formation independent of the target (Schlaggar and O'Leary, 1991). Mouse knock-out studies have shown that barrel formation requires both ionotropic (NMDA) and metabotropic glutamate receptors, as well as various intracellular signaling molecules such as adenylyl cyclase type I, phospholipase C-β1 (PLC-β1), protein kinase A (PKA), and synaptic Ras GTPase activating protein (SynGAP) (Erzurumlu and Kind, 2001; Barnett et al., 2006; Inan et al., 2006; Watson et al., 2006).

The neurofibromatosis type 1 (*NF1*) gene encodes a large protein that contains a Ras GTPase-activating (GAP) domain that negatively regulates Ras activity. Inactivating mutations in *NF1* cause neurofibromatosis type 1 (Cawthon et al., 1990; Viskochil et al., 1990; Wallace et al., 1990), a common genetic disease that affects 1 in 3000 individuals (Cichowski and Jacks, 2001; Zhu and Parada, 2001). Aside from the more common tumor phenotypes, a significant number of individuals with NF1 display intellectual deficits (Costa and Silva, 2003). In addition, it has been estimated that as many as 1% of children with autism spectrum disorders are subsequently diagnosed with NF1 (Mbarek et al., 1999; Marui et al., 2004). Mouse models of neurofibromatosis have been generated, and complete loss of NF1 is lethal in mice because of defects in cardiac development (Brannan et al., 1994; Jacks et al., 1994). In the peripheral nervous system, loss of NF1 allows sensory neurons to survive in the absence of neurotrophin signaling (Vogel et al., 1995) because of increased Ras and phosphatidylinositol 3-kinase (PI-3 kinase) activity (Klesse and Parada, 1998).

Although a few NF1 patients show abnormalities in brain structure (Korf et al., 1999; Balestri et al., 2003), little is known about the basis for NF1-associated intellectual deficits and possible roles in development of the CNS. To circumvent the early embryonic lethality of *NF1* mutations, we have used cre/lox technology to generate a conditional allele of *NF1* (Zhu et al., 2001). Mice lacking NF1 in the majority of neurons displayed a thin cortex, while maintaining a normal number of neurons and normal dendritic arborization (Zhu et al., 2001). In the current study, we characterize a mouse line that has a deletion of *NF1* in the majority of cortical neurons and astrocytes. We find that these mice lack cortical barrels from early in development. Tha-

Received Sept. 22, 2006; accepted Dec. 26, 2007.

This work was supported by National Institute of Neurological Disorders and Stroke Grants R37NS33199 and NS34296 and the American Cancer Society to L.F.P. We thank Yanjiao Li, Linda McClellan, Alemji Taku, and Alvin Chandra for technical assistance and all members of the Parada laboratory for helpful ideas and discussions.

*M.E.L. and Y.L. contributed equally to this work.

Correspondence should be addressed to Dr. Luis F. Parada at the above address. E-mail: luis.parada@utsouthwestern.edu.

M. E. Lush's present address: Department of Neuroscience, University of Pennsylvania School of Medicine, Philadelphia, PA 19104.

DOI:10.1523/JNEUROSCI.5236-07.2008

 0270-6474/08/281580-08$15.00/0

lamic axons retain NF1 and segregate within cortical layer IV, although their appearance is not completely normal.

Materials and Methods

Animals. The generation and genotyping of NF1$^{flox/flox}$ animals have been described previously (Zhu et al., 2001). Mice expressing Cre under the control of the human GFAP promoter hGFAP-Cre were a gift from Dr. A. Messing (University of Wisconsin, Madison, WI) (Zhuo et al., 2001) and were used to generate NF1$^{flox/flox}$;hGFAP-Cre mice (Zhu et al., 2005b). No difference was seen in NF1$^{flox/flox}$, NF1$^{flox/+}$, and NF1$^{flox/+}$; hGFAP-Cre, so they are grouped together as controls. Rosa26R (R26) and Z/EG mice were obtained from The Jackson Laboratory (Bar Harbor, ME). All mice are on a mixed 129 and C57 background. All animal procedures conformed to National Institutes of Health and University of Texas Southwestern Medical Center Institutional guidelines for the care and use of animals.

5-Bromo-4-chloro-3-indolyl-β-D-galactopyranoside staining and Nissl staining. Adult mice were anesthetized and perfused transcardially with PBS followed by 4% paraformaldehyde (PFA). The dissected brains and skulls were postfixed in PFA at 4°C for 2–24 h. For the analysis of trigeminal ganglia neurons, skulls from postnatal day 0 (P0) mice were dissected and postfixed in PFA, followed by decalcification in CalRite (Richard-Allan Scientific, Kalamazoo, MI). We performed 5-bromo-4-chloro-3-indolyl-β-D-galactopyranoside (X-gal) staining on floating brain sections from adult R26;hGFAP-Cre and Z/EG;hGFAP-Cre mice as described previously (Kwon et al., 2006). Whole-mount X-gal staining was performed on the skulls, containing trigeminal ganglion, of adult R26;hGFAP-Cre mice. For Nissl staining, paraffin sections from P0 or adult mice were prepared as described previously (Kwon et al., 2006) and stained with 0.1% (w/v) toluidine blue (Poly Scientific, Bay Shore, NY) or cresyl violet for 5 min.

Cytochrome oxidase staining. Cytochrome oxidase staining was performed as described previously (Wong-Riley and Welt, 1980). The brains were removed and left intact or the cortex was flattened between glass slides for tangential sections and postfixed for 4 h in PFA at 4°C. Brains were sectioned at 40 μm with a vibratome or, alternatively, cryoprotected for 2 d at 4°C in 30% sucrose/PBS, imbedded in O.C.T. (optimal cutting temperature) compound (Tissue-Tek; Sakura Finetek, Torrance, CA), and sectioned at 40 μm with a cryostat (Leica, Wetzlar, Germany). Sections were washed in PBS, placed in staining solution (0.55 mg/ml DAB, 0.3 mg/ml cytochrome C, and 45 mg/ml sucrose; Sigma, St. Louis, MO), and incubated in the dark at 37°C until the staining gave strong signal (2–4 h). Sections were washed in PBS, mounted onto slides, dehydrated through ethanol and xylene, and coverslipped with *p*-xylene-bis-pyridinium bromide (DPX) (Sigma).

4,6-Diamidino-2-phenylindole staining. Intact or flattened cortices were sectioned at 40 μm and mounted onto slides to dry. Slides were washed in PBS-T (PBS/0.3% Triton X-100) and stained for 30 min in PBS-T plus 4′,6-diamidino-2-phenylindole (DAPI; 1 μg/ml; Sigma) to visualize cell nuclei. Slides were washed briefly in PBS and coverslipped with Immuno-mount (Thermo Shandon, Pittsburgh, PA) mounting medium. Images were taken with a Nikon (Tokyo, Japan) CCD camera using the MetaView program (Universal Imaging, West Chester, PA).

Immunohistochemistry. P4 or P8 pups were anesthetized and perfused with PBS followed by cold 4% PFA, and the brains were removed and postfixed overnight in PFA. Brains were sectioned at 50 μm with a Vibratome (Leica). Serotonin immunohistochemistry was performed as follows. Sections were washed in PBS-T, blocked for 1 h in PBS-T/6% goat serum (Sigma), and incubated overnight at room temperature in a blocking buffer with the addition of rabbit anti-serotonin antibody (1:10,000; Immunostar, Hudson, WI). Sections were washed in PBS and incubated with a biotinalyated secondary antibody (goat anti-rabbit, 1:400; Vector Laboratories, Burlingame, CA) for 45 min. Antibody staining was visualized using the ABC kit (Vector Laboratories) with DAB. Sections were mounted onto slides, dried, dehydrated through ethanol and xylene, and coverslipped with DPX. Fluorescent immunostaining for serotonin was performed as above, except the primary antibody was used at a dilution of 1:5000. Antibody staining was visualized with Cy3-conjugated goat anti-rabbit antibody (1:400; Jackson ImmunoResearch, West Grove, PA). To visualize cell nuclei, sections were counterstained with DAPI (1 μg/ml). Sections were mounted onto slides and coverslipped with Immuno-mount mounting medium.

Measuring barrel formation. To quantify the degree of barrel formation, a scoring system was used such that a score of 0 equaled no barrel segregation and a score of 3 equaled normal barrel segregation. Four consecutive DAPI-stained tangential sections were scored from each of four controls and three mutant animals from P30 to P35. An individual blind to the genotype determined scores. Statistical analysis was performed with a Student's *t* test.

Area measurements. All analyses were performed blind to genotype. Somatosensory (S1) and posterior medial barrel subfield (PMBSF) areas were measured on tangential sections stained with cytochrome oxidase or anti-serotonin antibody as described above. Digital images taken with a Nikon CCD camera were analyzed using the MetaView program (Universal Imaging). The size of individual patches and the width of septa were determined from B1–B3, C1–C3, and D1–D3 barrels.

Cell count. To quantify the number of neurons in the trigeminal ganglia, 5 μm continuous sagittal sections were collected from P0 mice and stained with cresyl violet. The images of every 10th section were used to count the number of neurons manually. The neuron number of the whole trigeminal ganglion was calculated by multiplying the sum of counts from individual sections by 10. To determine the density and wall/hollow distribution of nuclei within the barrel cortex, DAPI-stained tangential sections were viewed with a Leica confocal microscope. All sections were costained with anti-5-HT antibody to confirm the location within PMBSF. Three adjacent sections containing the barrel field were used for each animal. Seven micrometer optical images of B2, B3, C2, C3, D2, and D3 barrels were obtained, and each centered in a rectangle encompassing only the individual barrel. Cell counts were normalized to the area of the rectangle and presented as mean ± SEM. To determine the overall cell number in the barrel cortex, DAPI-stained tangential sections from P30–P35 animals were used. Five 50 μm sections were counted throughout the barrel cortex from six control and three mutant brains. Images were imported into NIH ImageJ software, and a particle count macro was used to determine the number of DAPI-positive puncta per section. Statistical analysis was performed with a Student's *t* test.

Immunoblotting. Control and mutant littermates were collected at P0 and P4 ($n = 3$ for each genotype and time point). The entire somatosensory cortex was dissected out and immediately frozen in liquid nitrogen. Tissues were homogenized in PLC buffer [50 mM HEPES, pH 7.5, 150 mM NaCl, 10% glycerol, 0.1% Triton X-100, 1.5 mM $MgCL_2$, and Complete proteinase inhibitor (Roche, Welwyn Garden City, UK)]. The extract was centrifuged, and protein concentration of the supernatant was quantified using the BCA method following the manufacturer's protocol (Pierce, Rockford, IL). Extracts (10 μg) were separated on SDS-PAGE gels and transferred to nitrocellulose. The following antibodies and concentrations were used: phospho-Erk (1:1000; Cell Signaling Technology, Danvers, MA), Erk (1:10,000; Santa Cruz Biotechnology, Santa Cruz, CA), phospho-Akt (1:1000; Cell Signaling Technology), Akt (1:1000; Cell Signaling Technology), phospho-PKA-RIIβ (1:1000; BD Transduction Laboratories, Lexington, KY), PKA-RIIβ (1:10,000; BD Transduction Laboratories), NMDA-R1 (1:500; Upstate Biotechnology, Lake Placid, NY), NF1GRD (1:500; Santa Cruz Biotechnology), SynGAP (1:2000; Affinity BioReagents, Golden, CO), PLC-β1 (1:4000; Santa Cruz Biotechnology), and actin (1:1000; Chemicon, Temecula, CA). Membranes were incubated in primary antibodies overnight at 4°C in blocking buffer (5% nonfat milk and 0.1% Tween 20 in TBS (TBS-T), or 5% BSA for phospho-antibodies). After washing in TBS-T, blots were incubated with appropriate secondary antibodies (1:10,000; Santa Cruz Biotechnology) for 1 h in TBS-T. Membranes were washed, developed using ChemiGlow West reagent (Alpha Innotech, San Leandro, CA), and exposed to film or imaged using Kodak Image Station 2000r (Eastman Kodak, Rochester, NY). As a loading control, blots were stripped and reprobed either with antibodies recognizing nonphosphorylated forms of the protein for the phosphor-specific antibodies and for total protein levels using actin antibody or Sypro Ruby (Invitrogen, Eugene, OR). Quantification of bands was performed essentially as described previously (Luikart et al., 2005). Briefly, the net band intensity for both the Western blots and the Sypro

Ruby staining was determined using Kodak 1D Image Analysis software. Values for the phosphorylated blots were normalized to the levels of unphosphorylated controls. Values for the other P4 data were normalized to the Sypro Ruby staining, and values for P0 data were normalized to actin. Data from control animals was set to 100%. Student's *t* test was used to determine statistical differences.

Results

To explore the role of NF1 in cortical development, we used a mouse line containing a conditional allele of *NF1* (Zhu et al., 2001) crossed to a transgenic line expressing Cre under control of the human GFAP promoter (Zhu et al., 2001; Luikart et al., 2005). In this line, Cre is expressed in cortical progenitors as early as embryonic day 12.5 (Zhuo et al., 2001; Malatesta et al., 2003; Zhu et al., 2005a) with continued expression in glia and neural progenitor cells in older animals. This early expression in cortical progenitors results in NF1 deletion in both neurons and glia (Zhu et al., 2005a). hGFAP-Cre mice were crossed to the Rosa26-LacZ (R26) reporter line (Soriano, 1999), and X-gal staining of adult brains revealed expression in the cortex but little staining in the thalamus (Fig. 1*a–c*). This observation was further confirmed when hGFAP-Cre mice were crossed to the Z/EG reporter line (Novak et al., 2000), demonstrating that the majority of cells in the cortex had undergone recombination, whereas Cre expression in the thalamus was minimal (Fig. 1*d–f*). Cortical neurons that remained unrecombined are thought to be interneurons (Malatesta et al., 2003). Additionally, Cre is also expressed in the spinal cord, cerebellum, and trigeminal ganglion (supplemental Fig. 1, available at www.jneurosci.org as supplemental material, and data not shown). NF1$^{flox/flox}$;hGFAP-Cre mice are born in normal numbers but become noticeably smaller than their littermates as they age (Fig. 1*j*), and most die by 4 months of age (Zhu et al., 2005b). Young adult NF1 mutant brains appear grossly normal (Fig. 1*g*,*h*).

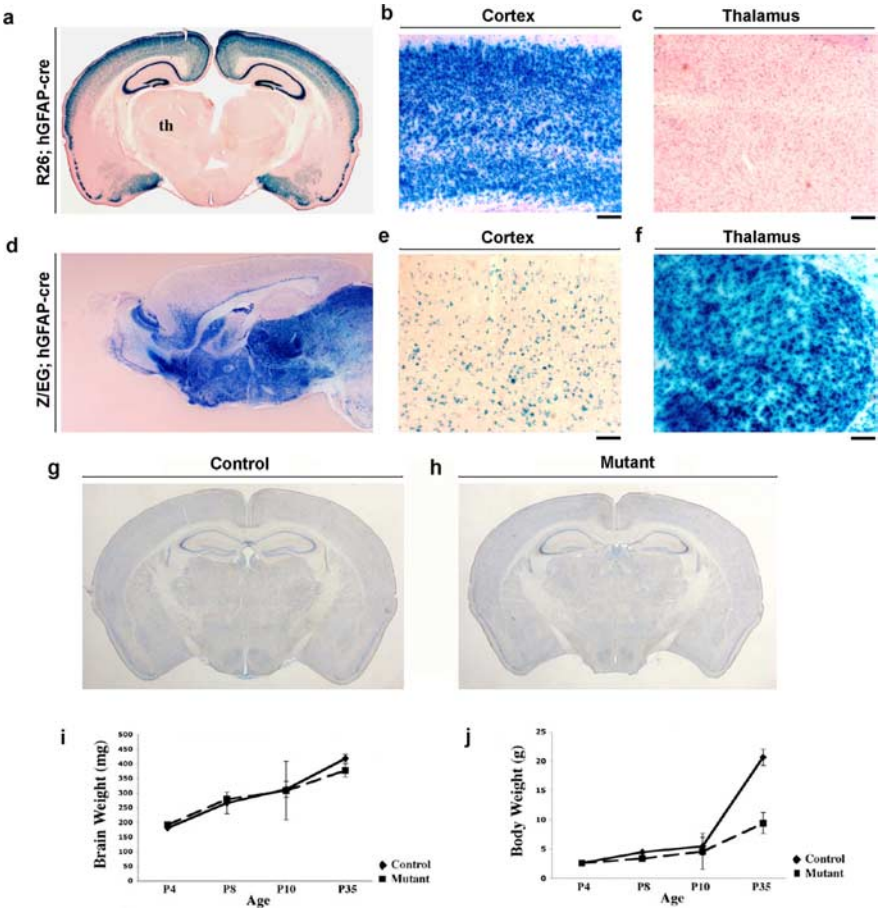

Figure 1. Cre-mediated recombination is restricted to the cortex in hGFAP-Cre mice. ***a–f***, X-gal staining of adult R26;hGFAP-Cre and Z/EG;hGFAP-Cre mice reveals recombination in the barrel cortex (***a***, ***b***, ***d***, ***e***) with little expression in the thalamus (th) (***c***, ***f***). ***g***, ***h***, Nissl staining of adult control (***g***) and NF1 conditional mutant (***h***) brains reveals no obvious differences in brain structure. ***i***, Total brain weight is normal from P4 to P35 in neurofibromin mutant animals. ***j***, Total body weight is normal until P35 in neurofibromin mutant animals. Scale bars, 100 μm. Error bars indicate SD.

To visualize the somatosensory cortex, we first performed cytochrome oxidase staining of brain sections in young adult mice (P35). Segregation of cytochrome oxidase staining in cortical layer IV throughout the barrel cortex is seen in coronal and tangential sections in both control ($n = 13$) and mutant ($n = 11$) mice (Fig. 2*a–d*). No differences were seen in the overall size of S1 (controls, 4.725 ± 0.201 mm^2; mutants, 4.673 ± 0.298 mm^2) or PMBSF (controls, 1.053 ± 0.042 mm^2; mutants, 1.011 ± 0.087 mm^2) areas. However, the morphology of the individual patches was slightly altered, reflected in a reduction in size (controls, 22341.51 ± 732.22 μm^2; mutants, 19803.49 ± 892.71 μm^2; $p < 0.05$) and an increase in the width of septa between patches (controls, 24.537 ± 0.791 μm; mutants, 32.732 ± 1.417 μm; $p < 0.01$).

To directly examine local organization of cortical barrels, we labeled cell nuclei using DAPI staining. In either coronal or tangential sections, segregation of cortical cells into barrels is clearly seen in the control brain (Fig. 2*e*, arrows, *g*,*i*) ($n = 16$). In the NF1 mutant mice, however, patterning of cortical cells into barrels is dramatically reduced or completely absent ($n = 12$) (Fig. 2*f*,*h*,*j*; and supplemental Fig. 3*a*, available at www.jneurosci.org as supplemental material) despite normal lamination of the six cortical layers (Fig. 2*f*). To determine the extent of cortical patterning deficit, we examined tangential sections throughout the entire cortex. We observed that loss of cortical NF1 resulted in reduced cellular aggregation throughout the entire somatosensory area (supplemental Fig. 2, available at www.jneurosci.org as supplemental material). Scoring for degree of barrel formation revealed a significant decrease in mutants compared with controls (supplemental Fig. 3*a*, available at www.jneurosci.org as supplemental material). These data indicate that loss of NF1 in cortical cells has little effect on wild-type thalamic axons but impairs the local cellular organization of cells in the cortex. No defects were observed in NF1$^{flox/+}$;hGFAP-Cre animals, so these were grouped together with controls (data not shown). The hGFAP-Cre transgene is expressed in trigeminal ganglion (supplemental Fig. 1*a*, available at www.jneurosci.org as supplemental material). To ascertain that unanticipated neuronal loss in trigeminal ganglion could contribute to the cortical barrel phenotype, we examined overall morphology and neuron number and found no difference in this ganglion in mutant animals (supplemental Fig. 1*b–d*, available at www.jneurosci.org as supplemental material). The

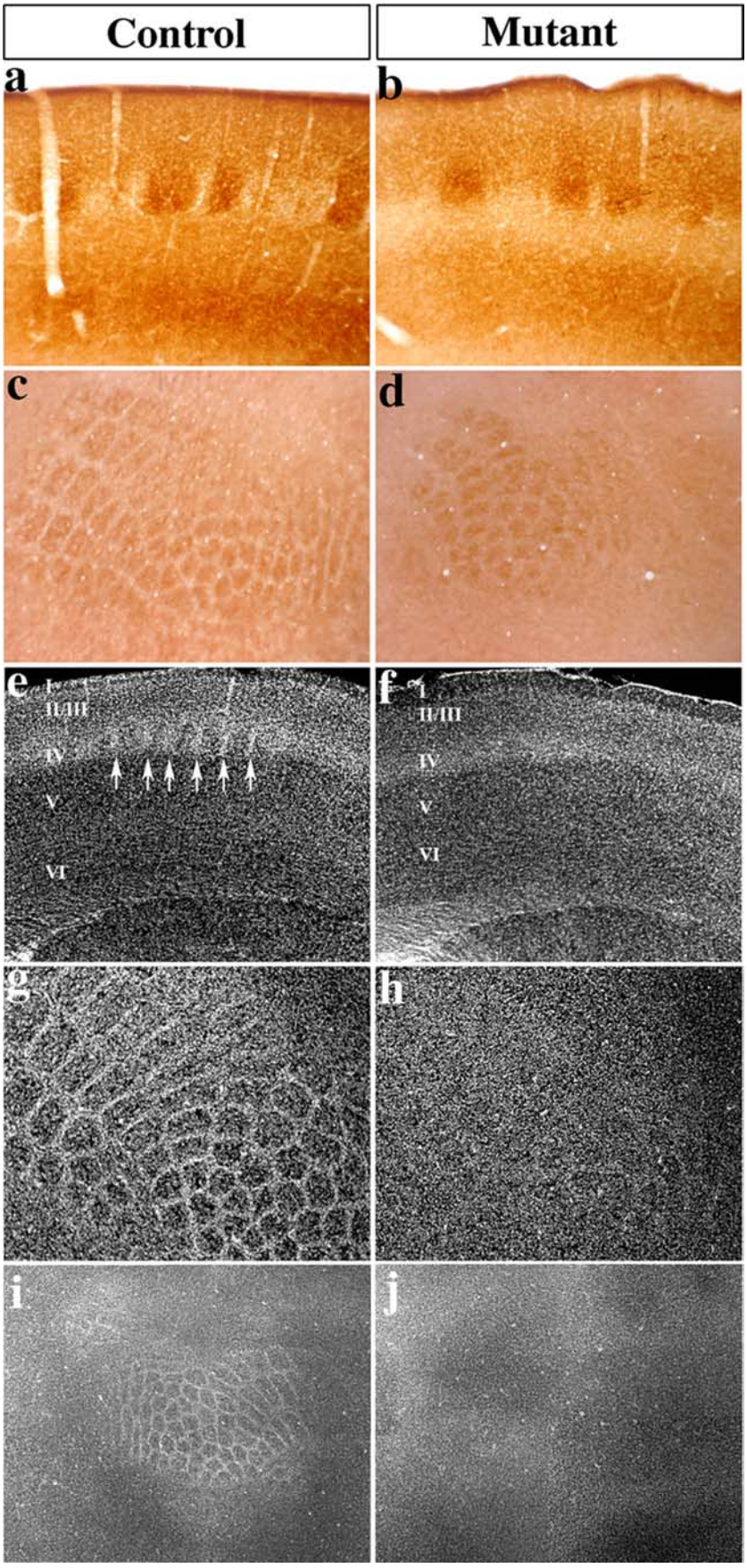

Figure 2. Adult neurofibromin conditional mutant mice lack cortical barrels. ***a–d***, Cytochrome oxidase staining of adult cortex in coronal (***a***, ***b***) and tangential (***c***, ***d***) orientation. Both control (***a***, ***c***) and mutant (***b***, ***d***) cortex show segregation of staining. ***e–j***, DAPI staining of adult cortex in coronal (***e***, ***f***) and tangential (***g–j***) orientation. Cortical barrels are seen in the control (***e***, arrows; ***g***) but absent in conditional (***f***, ***h***) knock-outs. Low-magnification images show no cortical segregation in any cortical region in mutants (***j***) compared with controls (***i***).

defects in barrel formation are unlikely to be the result of general ill health of mutant mice because no difference in brain weight is seen in NF1mutant animals from P4 to P35, although total body weight lags behind as the mutant ages (Fig. 1*i*). Consistent with this view, quantification of DAPI-positive puncta in tangential sections throughout the barrel cortex revealed no significant difference in numbers between controls and mutants (supplemental Fig. 3*b*, available at www.jneurosci.org as supplemental material). In addition, as described below, the deficit in mutant barrel cortex is evident at P8 when no differences in body weight are yet detectable.

To determine the timing of the defects in barrel cortex, we examined control and mutant littermates at P4, a time before cortical segregation has completed, and at P8 when cortical segregation is almost complete (Miller et al., 2001). Immunohistochemical staining for serotonin has been shown to label thalamic axons entering the barrel cortex in early postnatal mice (Cases et al., 1996). Thalamic axons, as visualized by serotonin immunohistochemistry, appear normal at P4 (Fig. 3*a*,*b*) ($n = 2$), and clear segregation is seen by P8 in the mutant cortex (Fig. 3*c*,*d*) ($n = 8$). In the P8 control brain, DAPI staining and immunohistochemistry for serotonin on tangential sections shows segregation of cortical barrels and thalamic axons, respectively (Fig. 3*e*,*g*,*i*) ($n = 8$). In comparison, segregation of thalamic axons is also present in the mutant cortex, but cortical barrels are not observed (Fig. 3*f*,*h*,*j*) ($n = 8$). Low-power micrographs of the serotonin immunostaining show segregation of multiple sensory regions (supplemental Fig. 4, available at www.jneurosci.org as supplemental material). Similar to observations from the adult mutant mice, the size of the S1 and PMBSF areas was unchanged, whereas the size of individual patches was reduced (significant differences between controls and mutants were found in the sizes of B1, B2, C1, and C3 patches). To quantify the change in segregation, DAPI-stained tangential sections across the PMBSF area were imaged as 7 μm optical slices. The density of DAPI-labeled nuclei in NF1 mutant mice was normal (controls, 55.68 $\pm$ 1.61; mutants, 55.94 $\pm$ 2.82), whereas the ring-like nuclei distribution was completely absent (wall-to-hollow ratios: controls, 1.81 $\pm$ 0.18; mutants, 1.03 $\pm$ 0.14; $p < 0.01$). Similar results were also seen at P10 with no barrel pattern of cortical cells seen in mutants (data not shown). Thus, cellular organization of cortical neurons re-

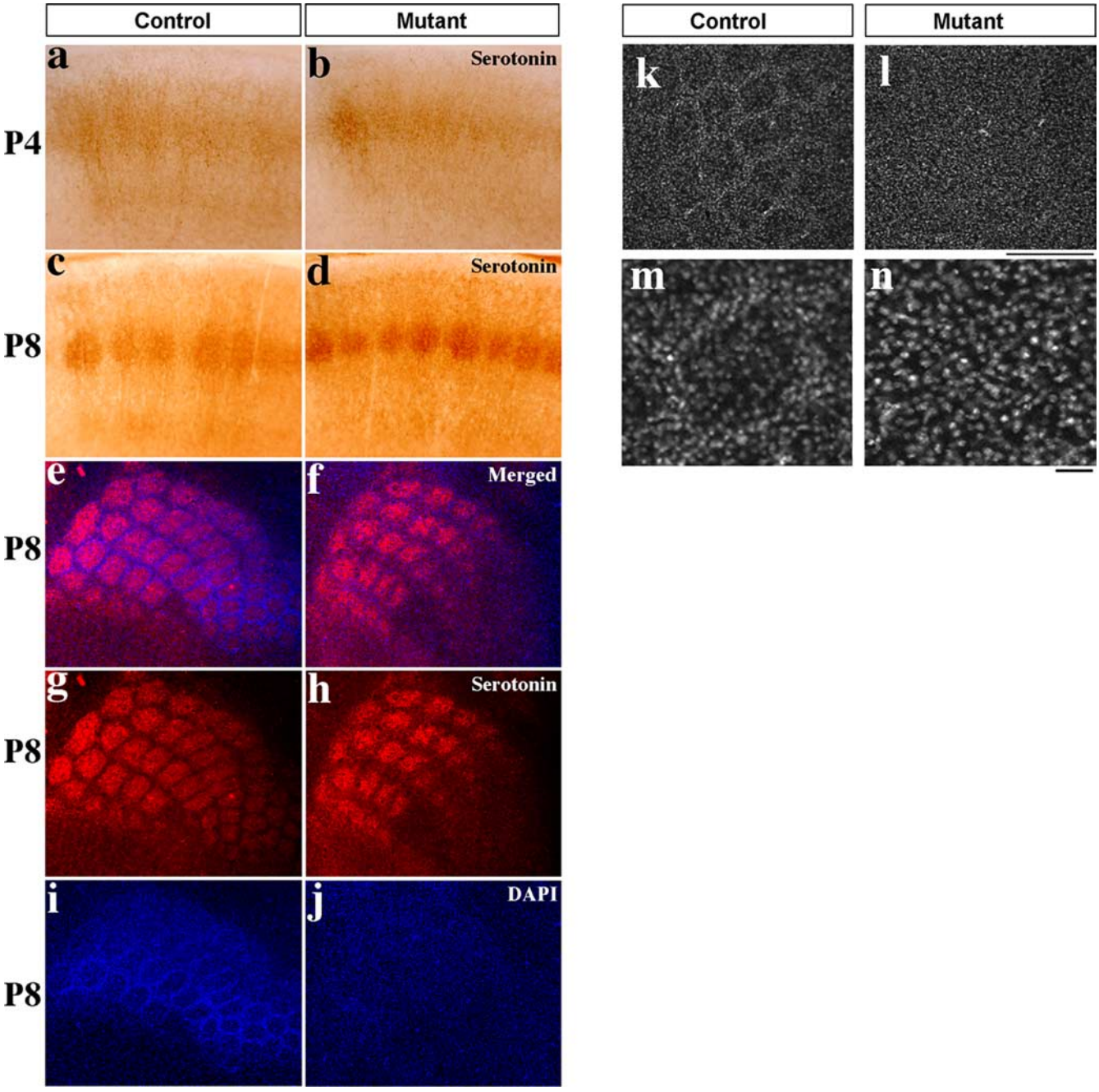

Figure 3. Thalamic axon development in neurofibromin conditional mutant mice. ***a–d***, Serotonin immunohistochemistry reveals both thalamic axon innervation and segregation into the cortex of mutant animals at P4 (***b***) and P8 (***d***) when compared with controls (***a***, ***c***). ***e–j***, Double-fluorescent staining for serotonin (red) and nuclei with DAPI (blue) of P8 tangential sections. There is clear thalamic axon segregation in the knock-out (***h***) similar to controls (***g***). DAPI staining shows cortical segregation into barrels in control animals (***i***) that is absent in NF1 mutant mice (***j***). ***k–n***, High-magnification view of individual patches shows normal nuclei density in the NF1 mutant mice (***l***, ***n***) compared with controls (***k***, ***m***). Scale bars: ***k***, ***l***, 100 μm; ***m***, ***n***, 10 μm.

quires NF1 function to respond appropriately to thalamocortical projection cues.

Several signaling molecules and neurotransmitters are required for barrel formation (Erzurumlu and Kind, 2001; Barnett et al., 2006). To explore the possible mechanism for the absence of cortical barrels in the NF1 mutants, we tested whether the expression of some of these proteins known to be required for barrel formation were affected by loss of NF1. Western blot analysis was performed on somatosensory cortex tissue extracts at P0 and P4, when cortical barrels are forming. No significant difference was found in the levels of NMDA receptor 1 (NR1), PLC-β1, SynGAP, or PKA-RIIβ at either age (Fig. 4*a–c*,*e*,*f*) ($n = 3$ for each genotype and time point). Western blot analysis for NF1 shows an 80% reduction in the NF1 mutant animals (Fig. 4*a*,*b*,*e*). The remaining NF1 expression likely comes from both interneurons and afferent axonal projections from non-Cre-expressing regions.

Both the Ras–mitogen-activated protein kinase (MAPK) pathway and the PI-3 kinase–Akt pathway are known to be elevated in the absence of NF1 (Klesse and Parada, 1998). We examined the levels of phosphorylated Erk and Akt in NF1 mutant cortex at P0 and P4. Phospho-Erk showed a significant increase in levels, whereas phospho-Akt levels were unchanged (Fig. 4*c*,*d*,*f*,*h*). We also examined the phosphorylation levels PKA-RIIβ subunit and found it to be unchanged (P0) (Fig. 4*f*,*h*) or slightly

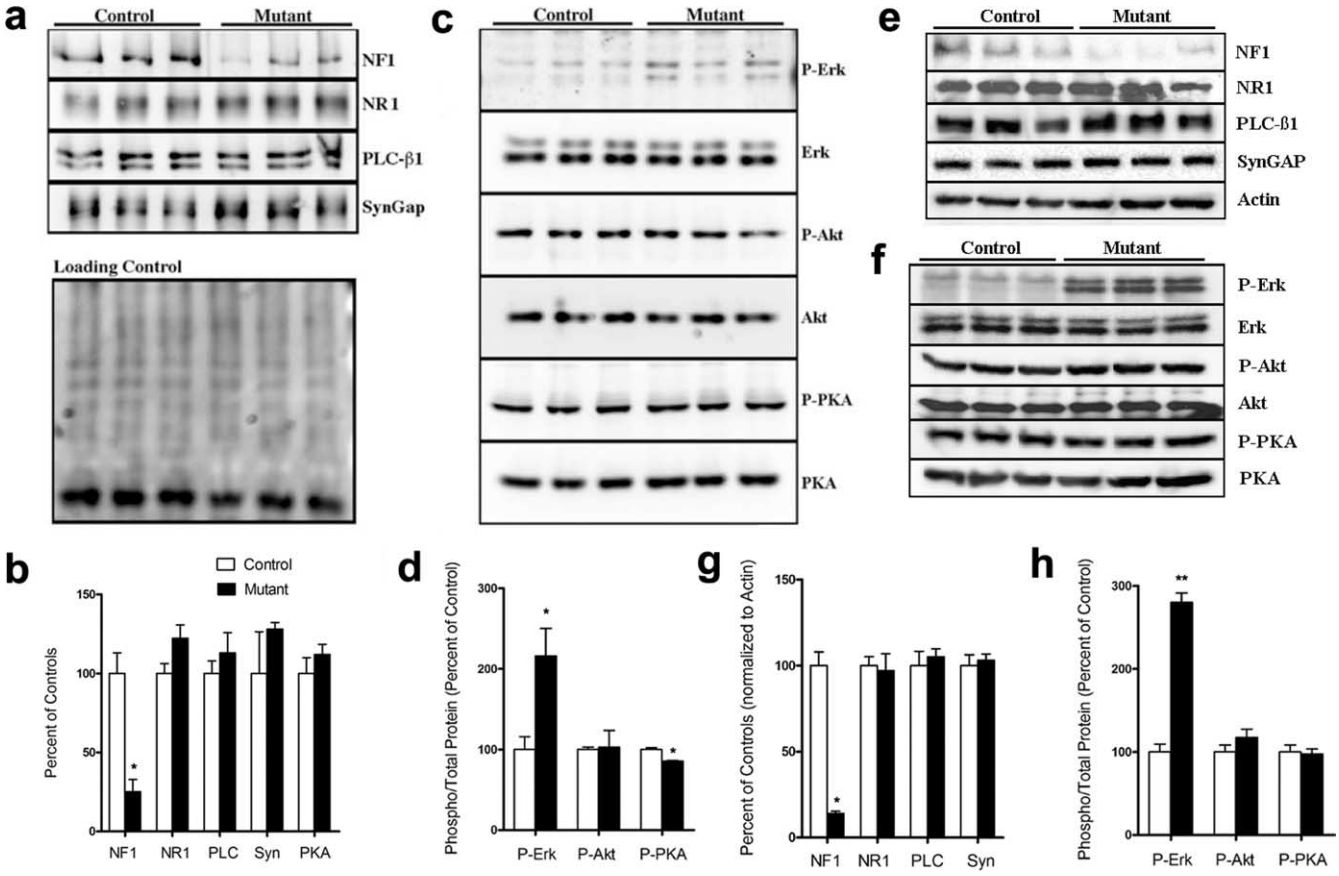

Figure 4. Western blot analysis of somatosensory cortex shows normal levels of protein expression for other proteins required for cortical barrel formation. In the somatosensory cortex of P4 (***a–d***) and P0 (***e–h***) NF1 mutant mice, immunoblots show ~80% reduction in NF1 (***a***, ***b***, ***e***, ***g***). No significant difference was found in NR1, PLC-β1 (PLC), SynGAP (Syn), or the PKA-RIIβ (PKA) subunit at P4 (***a***, ***b***) or P0 (***e–g***). Phospho-Erk levels are increased in mutant cortices at both ages (***c***, ***d***, ***f***, ***h***). $^*p < 0.05$; $^{**}p < 0.01$. Error bars indicate SE. P, Phosphorylated.

decreased (P4) (Fig. 4*c*,*d*) in the mutants, whereas the levels of total PKA-RIIβ were unaffected (Fig. 4*b*,*f*).

Discussion

NF1 regulates cortical barrel formation

Since its initial discovery by Woolsey and Van der Loos (1970), the rodent barrel cortex has been intensely studied as a well defined system that accommodates the interplay of developmental, physiological, and behavioral neuroscience. The precise one-to-one correspondence of the large whiskers with layer IV cortical neuron segregations ("barrels") provides an exquisite model for the studying of somatotopic mapping of sensory surfaces, as well as general mechanisms underlying the formation and functioning of the nervous system.

Development of the barrel cortex is regulated by an intricate network of genetic factors, many of which are only beginning to be unveiled (Erzurumlu and Kind, 2001; Petersen, 2007). In the present study, we demonstrate that the tumor suppressor neurofibromin 1 is also required for the proper formation of cortical barrels. Mice with a conditional deletion of NF1 in the cortex fail to form barrels postnatally (P8) and as adults. Thalamic neurons are devoid of Cre-mediated recombination, and their axonal segregation occurs with proper overall patterns. Mild morphological changes exist that are likely secondary effects of cortical NF1 ablation. This defect in cortical barrel segregation does not appear to be a result of gross brain development abnormality but rather a local consequence of NF1 deletion. Thus, the lack of cortical barrel formation can be attributed directly to NF1 loss in the cortex, supporting a cell-autonomous requirement of NF1 in this cellular compartment.

The bundling of thalamic axons into barrel-like patterns is thought to be instructive for cortical neurons to reposition their cell bodies and dendrites. This is best exemplified by transplantation studies demonstrating formation of barrels in visual cortex explants when they are placed in the somatosensory cortex and innervated by VPM thalamic axons (Schlaggar and O'Leary, 1991). Several lines of mouse genetic mutants have been generated that exhibit defects in the development of cortical barrels despite partial (Barnett et al., 2006; Hannan et al., 2001) or normal (Iwasato et al., 2000; Inan et al., 2006; Lu et al., 2006; Watson et al., 2006) thalamic axonal segregation. The phenotypes of the NF1 conditional knock-outs are similar to these mutants, further confirming the notion that signaling activities in the postsynaptic cortical neurons are critical in their rearrangement in response to thalamic cues.

Postsynaptic signaling and cortical mapping

Neurofibromin, the protein encoded by NF1, contains a Ras-GAP domain that serves as a checkpoint for Ras-mediated signaling events. Loss of NF1 leads to disinhibition of Ras and, consequently, increased activation of the MAPK and PI-3 kinase pathways when the specific cellular and environmental signaling capacity permits (Klesse and Parada, 1998). In the NF1 mutant cortex, we observed an upregulation of phospho-Erk, although the level of phospho-Akt remained unchanged. This finding, in conjunction with a recent report that germline mutant mice of

SynGAP, another Ras-GAP-containing protein, also lack cortical barrels (Barnett et al., 2006), strongly implicates an essential role of Ras signaling in barrel formation. The physiological substrates of NF1 and SynGAP in the barrel cortex, as well as the mechanism by which Ras signaling may mediates cortical neuron repositioning remains to be elucidated.

Our findings that Erk is constitutively activated in the barrel cortex of NF1 mutant mice suggest the precise on/off regulation of the Ras–MAPK pathway by NF1 is required for cortical neurons to react to signal inputs from the thalamic axon terminals. Although the exact nature of these upstream signaling molecules remains to be identified, previous studies have associated NF1 with a number of proteins and pathways that are involved in the thalamocortical synaptic communication. Both NF1 and SynGAP have been shown to interact with the NMDA receptor complex (Chen et al., 1998; Kim et al., 1998; Husi et al., 2000). This coincides with evidence showing lack of cortical barrels in cortex-specific conditional NR1 mutant mice (Iwasato et al., 2000), suggesting possible NMDA-related deficits in the NF1 mutant mice that contribute to the absence of barrel formation. Alternatively, there has been substantial evidence linking NF1 to adenylyl cyclase and PKA, both of which have been reported to be required for proper barrel formation (Welker et al., 1996; Abdel-Majid et al., 1998; Watson et al., 2006). In *Drosophila*, loss of NF1 leads to defects in body size as well as learning and memory, which are attributable to a decrease in adenylyl cyclase and PKA activities, not Ras and MAPK signaling (Guo et al., 1997, 2000; The et al., 1997). In mice, it has been demonstrated that loss of NF1 can also lead to decreases in adenylyl cyclase activation in the embryonic brain (Tong et al., 2002), but as yet no *in vivo* defects have been attributed to the impairments of this pathway. Together, further delineation of the NF1 signaling mechanism in the postsynaptic compartment will provide vital insights into the development of barrel cortex and patterning in the CNS in general.

Clinical implication in NF1

Aside from the various forms of benign and malignant tumors, NF1 patients exhibit high incidence of learning disabilities and mental retardation (North, 2000). In mouse mutants, it has been shown that the loss of Ras-GAP-dependent regulation constitutes a molecular basis for spatial learning deficits (Costa et al., 2002). This coincides with human genetic studies showing a missense mutation that specifically abolishes the Ras-GAP function of NF1 leads to cognitive disabilities, among groups of other symptoms (Klose et al., 1998). However, little is known about the cellular and circuitry abnormalities responsible for the wide range of mental impairments observed in NF1 patients. In the present study, we identified a significant neuronal patterning deficit in mutant mice lacking both alleles of NF1 in the cortex. Although the behavioral ramifications of such deficit in mutant animals do not immediately reflect clinical symptoms in NF1 patients, it suggests loss of NF1 in human likely disturbs pattern formation in neocortical columns and the CNS in general. It is also likely that differences in the timing and cell types that undergo loss of the remaining wild-type allele contribute greatly to the variability in the behavioral and neuroanatomical phenotypes seen in individuals with NF1. Future studies using more specific spatial and temporal knock-outs of NF1 should continue to uncover new roles for NF1 in neuronal development. Thus, our findings provide novel insights into the etiology of mental impairments associated with neurofibromatosis.

References

Abdel-Majid RM, Leong WL, Schalkwyk LC, Smallman DS, Wong ST, Storm DR, Fine A, Dobson MJ, Guernsey DL, Neumann PE (1998) Loss of adenylyl cyclase I activity disrupts patterning of mouse somatosensory cortex. Nat Genet 19:289–291.

Balestri P, Vivarelli R, Grosso S, Santori L, Farnetani MA, Galluzzi P, Vatti GP, Calabrese F, Morgese G (2003) Malformations of cortical development in neurofibromatosis type 1. Neurology 61:1799–1801.

Barnett MW, Watson RF, Vitalis T, Porter K, Komiyama NH, Stoney PN, Gillingwater TH, Grant SG, Kind PC (2006) Synaptic Ras GTPase activating protein regulates pattern formation in the trigeminal system of mice. J Neurosci 26:1355–1365.

Brannan CI, Perkins AS, Vogel KS, Ratner N, Nordlund ML, Reid SW, Buchberg AM, Jenkins NA, Parada LF, Copeland NG (1994) Targeted disruption of the neurofibromatosis type-1 gene leads to developmental abnormalities in heart and various neural crest-derived tissues. Genes Dev 8:1019–1029.

Cases O, Vitalis T, Seif I, De Maeyer E, Sotelo C, Gaspar P (1996) Lack of barrels in the somatosensory cortex of monoamine oxidase A-deficient mice: role of a serotonin excess during the critical period. Neuron 16:297–307.

Cawthon RM, Weiss R, Xu GF, Viskochil D, Culver M, Stevens J, Robertson M, Dunn D, Gesteland R, O'Connell P, White R (1990) A major segment of the neurofibromatosis type 1 gene: cDNA sequence, genomic structure, and point mutations. Cell 62:193–201.

Chen HJ, Rojas-Soto M, Oguni A, Kennedy MB (1998) A synaptic Ras-GTPase activating protein (p135 SynGAP) inhibited by CaM kinase II. Neuron 20:895–904.

Cichowski K, Jacks T (2001) NF1 tumor suppressor gene function: narrowing the GAP. Cell 104:593–604.

Costa RM, Silva AJ (2003) Mouse models of neurofibromatosis type I: bridging the GAP. Trends Mol Med 9:19–23.

Costa RM, Federov NB, Kogan JH, Murphy GG, Stern J, Ohno M, Kucherlapati R, Jacks T, Silva AJ (2002) Mechanism for the learning deficits in a mouse model of neurofibromatosis type 1. Nature 415:526–530.

Erzurumlu RS, Kind PC (2001) Neural activity: sculptor of "barrels" in the neocortex. Trends Neurosci 24:589–595.

Guo HF, The I, Hannan F, Bernards A, Zhong Y (1997) Requirement of *Drosophila* NF1 for activation of adenylyl cyclase by PACAP38-like neuropeptides. Science 276:795–798.

Guo HF, Tong J, Hannan F, Luo L, Zhong Y (2000) A neurofibromatosis-1-regulated pathway is required for learning in *Drosophila*. Nature 403:895–898.

Hannan AJ, Blakemore C, Katsnelson A, Vitalis T, Huber KM, Bear M, Roder J, Kim D, Shin HS, Kind PC (2001) PLC-beta1, activated via mGluRs, mediates activity-dependent differentiation in cerebral cortex. Nat Neurosci 4:282–288.

Husi H, Ward MA, Choudhary JS, Blackstock WP, Grant SG (2000) Proteomic analysis of NMDA receptor-adhesion protein signaling complexes. Nat Neurosci 3:661–669.

Inan M, Lu HC, Albright MJ, She WC, Crair MC (2006) Barrel map development relies on protein kinase A regulatory subunit II beta-mediated cAMP signaling. J Neurosci 26:4338–4349.

Iwasato T, Datwani A, Wolf AM, Nishiyama H, Taguchi Y, Tonegawa S, Knopfel T, Erzurumlu RS, Itohara S (2000) Cortex-restricted disruption of NMDAR1 impairs neuronal patterns in the barrel cortex. Nature 406:726–731.

Jacks T, Shih TS, Schmitt EM, Bronson RT, Bernards A, Weinberg RA (1994) Tumour predisposition in mice heterozygous for a targeted mutation in Nf1. Nat Genet 7:353–361.

Kim JH, Liao D, Lau LF, Huganir RL (1998) SynGAP: a synaptic RasGAP that associates with the PSD-95/SAP90 protein family. Neuron 20:683–691.

Klesse LJ, Parada LF (1998) p21 ras and phosphatidylinositol-3 kinase are required for survival of wild-type and NF1 mutant sensory neurons. J Neurosci 18:10420–10428.

Klose A, Ahmadian MR, Schuelke M, Scheffzek K, Hoffmeyer S, Gewies A, Schmitz F, Kaufmann D, Peters H, Wittinghofer A, Nurnberg P (1998) Selective disactivation of neurofibromin GAP activity in neurofibromatosis type 1. Hum Mol Genet 7:1261–1268.

Korf BR, Schneider G, Poussaint TY (1999) Structural anomalies revealed

by neuroimaging studies in the brains of patients with neurofibromatosis type 1 and large deletions. Genet Med 1:136–140.
Kwon CH, Zhou J, Li Y, Kim KW, Hensley LL, Baker SJ, Parada LF (2006) Neuron-specific enolase-cre mouse line with cre activity in specific neuronal populations. Genesis 44:130–135.
Lu HC, Butts DA, Kaeser PS, She WC, Janz R, Crair MC (2006) Role of efficient neurotransmitter release in barrel map development. J Neurosci 26:2692–2703.
Luikart BW, Nef S, Virmani T, Lush ME, Liu Y, Kavalali ET, Parada LF (2005) TrkB has a cell-autonomous role in the establishment of hippocampal Schaffer collateral synapses. J Neurosci 25:3774–3786.
Malatesta P, Hack MA, Hartfuss E, Kettenmann H, Klinkert W, Kirchhoff F, Gotz M (2003) Neuronal or glial progeny: regional differences in radial glia fate. Neuron 37:751–764.
Marui T, Hashimoto O, Nanba E, Kato C, Tochigi M, Umekage T, Ishijima M, Kohda K, Kato N, Sasaki T (2004) Association between the neurofibromatosis-1 (NF1) locus and autism in the Japanese population. Am J Med Genet B Neuropsychiatr Genet 131:43–47.
Mbarek O, Marouillat S, Martineau J, Barthelemy C, Muh JP, Andres C (1999) Association study of the NF1 gene and autistic disorder. Am J Med Genet 88:729–732.
Miller B, Blake NMJ, Woolsey TA (2001) Barrel cortex: structural organization, development, and early plasticity. In: Plasticity of adult barrel cortex (Kossut M, ed), pp 3–45. Johnson City, TN: Graham.
North K (2000) Neurofibromatosis type 1. Am J Med Genet 97:119–127.
Novak A, Guo C, Yang W, Nagy A, Lobe CG (2000) Z/EG, a double reporter mouse line that expresses enhanced green fluorescent protein upon Cre-mediated excision. Genesis 28:147–155.
Petersen CC (2007) The functional organization of the barrel cortex. Neuron 56:339–355.
Schlaggar BL, O'Leary DD (1991) Potential of visual cortex to develop an array of functional units unique to somatosensory cortex. Science 252:1556–1560.
Soriano P (1999) Generalized lacZ expression with the ROSA26 Cre reporter strain. Nat Genet 21:70–71.
The I, Hannigan GE, Cowley GS, Reginald S, Zhong Y, Gusella JF, Hariharan IK, Bernards A (1997) Rescue of a *Drosophila* NF1 mutant phenotype by protein kinase A. Science 276:791–794.
Tong J, Hannan F, Zhu Y, Bernards A, Zhong Y (2002) Neurofibromin regulates G protein-stimulated adenylyl cyclase activity. Nat Neurosci 5:95–96.
Viskochil D, Buchberg AM, Xu G, Cawthon RM, Stevens J, Wolff RK, Culver M, Carey JC, Copeland NG, Jenkins NA, White R, O'Connell P (1990) Deletions and a translocation interrupt a cloned gene at the neurofibromatosis type 1 locus. Cell 62:187–192.
Vogel KS, Brannan CI, Jenkins NA, Copeland NG, Parada LF (1995) Loss of neurofibromin results in neurotrophin-independent survival of embryonic sensory and sympathetic neurons. Cell 82:733–742.
Wallace MR, Marchuk DA, Andersen LB, Letcher R, Odeh HM, Saulino AM, Fountain JW, Brereton A, Nicholson J, Mitchell AL, Brownstein BH, Collins FS (1990) Type 1 neurofibromatosis gene: identification of a large transcript disrupted in three NF1 patients. Science 249:181–186.
Watson RF, Abdel-Majid RM, Barnett MW, Willis BS, Katsnelson A, Gillingwater TH, McKnight GS, Kind PC, Neumann PE (2006) Involvement of protein kinase A in patterning of the mouse somatosensory cortex. J Neurosci 26:5393–5401.
Welker E, Armstrong-James M, Bronchti G, Ourednik W, Gheorghita-Baechler F, Dubois R, Guernsey DL, Van der Loos H, Neumann PE (1996) Altered sensory processing in the somatosensory cortex of the mouse mutant barrelless. Science 271:1864–1867.
Wong-Riley MT, Welt C (1980) Histochemical changes in cytochrome oxidase of cortical barrels after vibrissal removal in neonatal and adult mice. Proc Natl Acad Sci USA 77:2333–2337.
Woolsey TA, Van der Loos H (1970) The structural organization of layer IV in the somatosensory region (SI) of mouse cerebral cortex. The description of a cortical field composed of discrete cytoarchitectonic units. Brain Res 17:205–242.
Woolsey TA, Dierker ML, Wann DF (1975) Mouse SmI cortex: qualitative and quantitative classification of golgi-impregnated barrel neurons. Proc Natl Acad Sci USA 72:2165–2169.
Zhu Y, Parada LF (2001) Neurofibromin, a tumor suppressor in the nervous system. Exp Cell Res 264:19–28.
Zhu Y, Romero MI, Ghosh P, Ye Z, Charnay P, Rushing EJ, Marth JD, Parada LF (2001) Ablation of NF1 function in neurons induces abnormal development of cerebral cortex and reactive gliosis in the brain. Genes Dev 15:859–876.
Zhu Y, Guignard F, Zhao D, Liu L, Burns DK, Mason RP, Messing A, Parada LF (2005a) Early inactivation of p53 tumor suppressor gene cooperating with NF1 loss induces malignant astrocytoma. Cancer Cell 8:119–130.
Zhu Y, Harada T, Liu L, Lush ME, Guignard F, Harada C, Burns DK, Bajenaru ML, Gutmann DH, Parada LF (2005b) Inactivation of NF1 in CNS causes increased glial progenitor proliferation and optic glioma formation. Development 132:5577–5588.
Zhuo L, Theis M, Alvarez-Maya I, Brenner M, Willecke K, Messing A (2001) hGFAP-cre transgenic mice for manipulation of glial and neuronal function in vivo. Genesis 31:85–94.